UNIVERSITÄT ZU LÜBECK

From the Institute of Experimental and Clinical Pharmacology and Toxicology
of the University of Lübeck

Interaction of adipokines with orexin signalling

Dissertation
for Fulfillment of Requirements
for the Doctoral Degree of the University of Lübeck

from the Department of Natural Sciences

Submitted by

Eva Frevel
From Recklinghausen

Lübeck 2018

First referee: Prof. Dr. rer. nat. Olaf Jöhren

Second referee: Prof. Dr. rer. nat. Jens Mittag

Date of oral examination: 19.06.2018

Approved for printing. Lübeck, 27.06.2018

Statement

I certify herewith that the dissertation included here was completed and written independently by me and without outside assistance. References to the work and theories of others have been cited and acknowledged completely and correctly. This work has never been submitted in this, or a similar form, at this or any other domestic or foreign institution of higher learning as a dissertation.

The abovementioned statement was made as a solemn declaration. I conscientiously believe and state it to be true and declare that it is of the same legal significance and value as if it were made under oath.

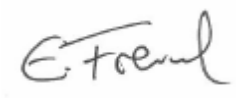

Lübeck, 23.02.2018

Content

I. List of figures

II. List of tables

III. Abbreviations

°C	degree Celsius
%	percent
µg	micro gram
µl	micro litre
µM	micro molar
µm	micro meter
ADH	antidiuretic hormone/vasopressin
AM	Acetoxymethyl
APS	Ammonium Persulfate
Arc	arcuate hypothalamic nucleus
ATP	adenosine triphosphate
ß-ME	beta mercaptoethanol
BMI	body mass index
bp	base pair
BSA	bovine Serum Albumin
Ca^{2+}	calcium
CA3	CA3 field of the ammon's horn
$CaCl_2$	calcium chloride
CAnaCore	Cell Analysis Core Facility
cDNA	complementary DNA
chp	choroid plexus
CLB	cell lysis buffer
cm^2	square centimetre
CNS	central nervous system
CO_2	carbon dioxide
Cre	cyclisation recombinase

CRH	Corticotropin-releasing Hormone
Ctrl	control
CVD	cardiovascular disease
Cy5	cyanine 5
DAG	diacylglycerol
DAPI	4',6-diamidino-2-phenylindole
db	*diabetes* gene
DEPC	diethylpyrocarbonate
DIG-UTP	Digoxigenin-11-Uridine triphosphate
DM/DMH	dorsomedial hypothalamic nucleus
DMEM	Eagle's minimal essential medium
DMSO	Dimethyl sulfoxide
DNA	deoxyribonucleotide acid
dNTP	nucleoside triphosphate
DTT	Dithiothreitol
E.coli	*Escherichia coli*
ec	external capsule
e.g.	exempli gratia
EDTA	Ethylenediaminetetraacetic acid
Elk-1	ETS domain-containing protein
EM	Emission
ERK1/2	extracellular signal–regulated kinases 1/2
EtOH	Ethanol
EtBr	Ethidium bromide
EX	Excitation
fa	*fatty* gene
FACS	Fluorescent activated cell sorting
FCS	Fetal calve serum

FISH	Fluorescent *in situ* hybridisation
fLuc	Firefly luciferase
g	Gram
GB	Gallbladder
GFP	Green fluorescent protein
GPCR	G-protein coupled receptor
GOI	Gene of interest
GrDG	Granular layer of the dentate gyrus
h	Hour
HRP	Horseradish peroxidase
Hz	Hertz
IBMX	isobotylmethylxanthin
ICV	Intracerebroventricular
IP	Intraperitoneal
IP_3	Inositol trisphosphate
IRES	Internal ribosome entry site
IRS	insulin receptor substrate
JACoP	Just Another Colocalization Plugin
Kb	kilo base
KCL	potassium chloride
Kg	kilogram
LB	Lysogeny broth
LepR/ObR	leptin receptor
LepRb/ObRb	leptin receptor version b
LH/LHA	lateral hypothalamic area
M	Menders coefficient
MAPK	mitogen-activated protein
MD	mediodorsal thalamic nucleus

mDM	adipocyte differentiation medium
ME	median eminence
MeOH	Methanol
MePV	medial amygdaloid nucleus, posteroventral part
mHypoA	mouse hypothalamic adult
mHypoE	mouse hypothalamic embryonic
MeOH	Methanol
min	minute
ml	millilitre
mm	millimetre
mM	millimolar
mRNA	messenger ribonucleotide acid
mTORC1	mechanistic Target of Rapamycin complex 1
n	number
Na_2CO_3	Sodium carbonate
NaCl	sodium chloride
NAFLD	Non-alcoholic fatty liver disease
ng	nanogram
nm	nanometre
NaOH	Sodium hydroxide
NPY	neuropeptide Y
OA	orexin A
OB	orexin B
ob	*obese* gene
ObRb	Leptin receptor version b
ORF	open reading frame
OX_1R	orexin receptor type 1
OX_2R	orexin receptor type 2

PAGE	Polyacrylamide gel electrophoresis
PBS	Phosphate-buffered saline
PCR	polymerase chain reaction
Pen/strep	penicillin/streptomycin
PFA	paraformaldehyde
PFH	perifornical hypothalamus
PH	posterior hypothalamic nucleus
pH	potential of hydrogen
PI3K	phosphatidylinositol-3-kinases
PIP_2	Phosphatidylinositol 4,5-bisphosphate
Pit	pituitary gland
PLC	phospholipase C
PLD	phospholipase D
Pmol	pico mol
PMSF	phenylmethane sulfonyl fluoride
POMC	pro-opiomelanocortin
PPO	prepro-orexin
PVN	paraventricular nucleus
qPCR	quantitative polymerase chain reaction
Re	nucleus of reuniens
rLuc	renilla luciferase
RNA	ribonucleotide acid
Rpm	Revolutions per minute
RSG	retrosplenial granular cortex
RT	room temperature
s	second
SEM	Standard error of the mean
SCh	suprachiasmatic nucleus

SDS	sodium dodecyl sulfate
SHP2	src homology region 2 domain-containing phosphatase-2
SNA	sympathetic nervous system activity
SNS	Sympathetic nervous systematic
S.O.C.	Super Optimal Broth with glucose
SSC	saline-sodium citrate
STAT3	signal transducer and activator of transcription 3
STAT5	signal transducer and activator of transcription 5
T	temperature
TBS	Tris-buffered saline
TK	thymidine kinase
TNB	Tris-NaCl-blocking
TNT	Tris-NaCl-Tween buffer
Thr	threonine
TSA	Tyramide Signal Amplification
Tyr	tyrosine
UV	ultra violet
V	volt
VMH	ventromedial hypothalamic area
W	watt
WAT	white adipose tissue
WHO	world health organisation
WT	wild type
ZsGreen	tetrameric *Zoanthus sp*. green fluorescent protein

IV. Abstract

The neuropeptides orexin A and orexin B are expressed by neurons located in the lateral hypothalamus. Although the population of orexin expressing neurons is relatively small, they project to numerous brain regions, which play a role in regulating arousal, energy homoeostasis and reward-motivated behaviour. Their corresponding G-protein coupled receptor subtypes OX_1R and OX_2R are widely expressed in brain and peripheral tissues. Orexin induced activation of both orexin receptor subtypes efficiently couple to PLC-related calcium influx and furthermore activates the MAP kinase pathway leading to phosphorylation of the extracellular signal-regulated kinase (ERK1/2).

Already shortly after the discovery of orexins, the interaction of orexin neurons and leptin signalling in the brain was postulated. Initially, it was found that leptin receptors (LepRb) are expressed on orexin neurons. Leptin was also capable to inhibit the activity of isolated orexin neurons indicating a direct effect of leptin on orexin neurons. However, recent results questioned these early data showing that orexin neurons are rather indirectly regulated by leptin. In this thesis, anatomical identification of a possible direct effect of leptin on orexin neurons by co-localisation studies for LepRb and the mRNA expression of prepro-orexin, the precursor of orexins, in LebRb-ZsGreen mice indicate LepRb expression in cells proximate to orexin neurons but not in orexin neurons themselves, demonstrating, that a leptin effect on orexin neurons is only indirect.

In addition, former complementary results indicated that terminals of orexin neurons innervate LepRb expressing neurons in the arcuate nucleus. According to the literature these neurons are NPY and/or POMC expressing neurons, which were shown to be immuno-positive for orexin receptors, innervated by orexin fibres and activated by orexins. However, the molecular mechanisms and neuronal circuits mediating this central leptin - orexin interaction remain unclear. One possible interaction of orexin and leptin signalling may occur at the MAPK/ERK pathway that is activated by LepRb but also orexin receptor activity. This study utilised LepRb-ZsGreen mice and murine immortalised hypothalamic cell lines as models for anatomical and functional identification and characterization of cooperative intracellular leptin - orexin signalling in mutual target neurons.

It was shown via fluorescent *in situ* hypridisation (FISH) in LepRb-ZsGreen mice, that orexin neurons do not express the LepRb, which excludes the possibility of a direct leptin effect on orexin neurons. Cooperative intracellular leptin - orexin signalling in mutual target neurons was investigated in the commercialy available immortalized cell lines mHypoE N41, mHypoE N25/2 and mHypoA 2/23. However, these cell lines turned out to be not suitable for conclusive orexin signalling studies. When mHypoE N41 cell were stably transfected with human OX_1R or OX_2R though, the cell lines show MAPK phosphorylation, calcium responses and reporter gene activation typical for orexin A and B signalling. Furthermore, immortalized hypothalamic cell lines show a strong activation of the ERK1/2 pathway as a response to medium that was previously primed by cultured epididymal adipocytes. This response is independent of orexin signalling and SHP-2.

Identification of common target neurons of leptin and orexin in LepRb-ZsGreen mice as *in vivo* model was problematic due to experimental limitations in receptor FISH and RNA recovery after fluorescent activated cell sorting (FACS). The respective protocols need to be further evolved in future experiments.

V. Zusammenfassung

Die Neuropeptide Orexin A und Orexin B werden von Neuronen im lateralen Hypothalamus exprimiert. Obwohl die Population von Orexin exprimierenden Neuronen relativ klein ist, projizieren diese in zahlreiche Regionen des Gehirns, die eine Rolle in der Regulation von Erregung, Energie Homöostase und Belohnungsmotiviertem Verhalten. Die entsprechenden G-Protein gekoppelten Rezeptorsubtypen OX_1R und OX_2R, sind weitreichend im Gehirn und peripheren Geweben exprimiert. Orexin induzierte Aktivierung beider Orexin Rezeptorsubtypen ist mit hoher Effizienz sowohl an einen PLC -vermittelten Kalzium Einstrom, als auch der Aktivierung des MAP Kinase Signalwegs, der zur Phosphorylierung der Extracellular-signal Regulated Kinase /ERK1/2) führt, gekoppelt.

Bereits kurz nach der Entdeckung von Orexinen, wurde eine Interaktion zwischen der Orexin und Leptin Signaltransduktion postuliert. Ursprüngliche Ergebnisse fanden, dass Leptin Rezeptoren (LepRb) in Orexin Neuronen exprimiert werden. Außerdem wurde gezeigt, dass Leptin die Aktivität von isolierten Orexin Neuronen inhibiert, was auf einen direkten Effekt von Leptin auf Orexin Neuronen hindeutet. Neuere Studien allerdings stellen diese früheren Ergebnisse in Frage, indem sie zeigen, dass Orexin Neuronen eher indirekt als direkt von Leptin reguliert werden. In dieser Arbeit zeigte die anatomische Identifikation eines möglichen direkten Effekts von Leptin auf Orexin Neuronen, anhand von Co-Lokalisationsstudien von LepRb und der mRNA von Präpro-Orexin, der Vorstufe der Orexine, in LepRb-ZsGreen Mäusen, dass LepRb zwar in zu Orexin-Neuronen benachbarten, nicht aber in Orexin Neuronen selber exprimiert wird und somit ein Effekt von Leptin auf Orexin Neuronen nur indirekt sein kann.

Darüber hinaus zeigen frühere, ergänzende Ergebnisse, dass Axone von Orexin Neuronen LepRb exprimierende Neuronen im Nucleus arcuatus innervieren. Bei diesen Neuronen handelt es sich, der Literatur zu Folge, um NPY und/oder POMC exprimierende Neuronen, die außerdem Immunoreaktivität für Orexin-Rezeptoren aufweisen und von Orexin aktiviert werden. Die molekularbiologischen Mechanismen und neuronalen Schaltkreise, die diese zentrale Leptin – Orexin Interaktion vermitteln sind allerdings weiter unklar. Der MAPK/ERK Signaltransduktionsweg wird sowohl durch die Aktivität des LepRb als auch der Orexin Rezeptorsubtypen angeregt und könnte daher als mögliche Interaktionsstelle dienen. Diese Studie nutzt LepRb-ZsGreen Mäuse und murine, immortalisierte, hypothalamische Zelllinien als Modell zur

anatomischen und funktionalen Untersuchung einer zusammenwirkenden, intrazellulären Leptin – Orexin Signaltransduktion in gemeinsamen Zielneuronen.

Mittels Fluoreszenz *in situ* Hybridisierung (FISH) in LepRb-ZsGreen Mäusen wurde gezeigt, dass Orexin Neuronen den LepRb nicht exprimieren, wodurch ein direkter Effekt von Leptin auf Orexin Neuronen ausgeschlossen werden kann. Zusammenwirkende, intrazelluläre Leptin – Orexin Signaltransduktion wurde an den kommerziell erwerblichen immortalisierten Zelllinien mHypoE N41, mHypoE N25/2 und mHypoA 2/23 untersucht, welche sich jedoch als ungeeignet für schlüssige Orexin Signaltransduktionsstudien erwiesen. Wurden mHypoE N41 Zellen allerdings stabil mit dem humanen OX_1R oder OX_2R transfiziert, zeigten die Zelllinien MAPK Phosphorylierung, Kalzium antworten und Reportergen Aktivierung, die der typischen Orexin A und B Signaltransduktion entsprechen. Außerdem zeigen immortalisierte hypothalamische Zelllinien eine starke Aktivierung des ERK1/2 Signaltransduktionswegs als Antwort auf Medium, dass zuvor durch kultivierte, epididymale Adipocyten angereichert wurde. Diese Reaktion scheint unabhängig von Orexin Signaltransduktion und SHP-2 Aktivierung zu sein.

Die Identifikation von gemeinsamen Zielneuronen von Leptin und Orexin in LepRb-ZsGreen Mäusen als *in vivo* Modell gestaltete sich durch experimentelle Limitierungen der Rezeptor FISH und der RNA Gewinnung nach Fluoreszenz-aktivierter Zell Sortierung (FACS) als problematisch. Die entsprechenden Protokolle müssen in zukünftigen Experimenten weiterentwickelt werden.

1 Introduction

1.1 Obesity

According to the world health organisation (WHO), overweight and obesity are best defined by the quotient of bodyweight in kg and the square of height in m, called body mass index (BMI). In adults overweight starts at a BMI of 25, whereas everything greater than 30 is categorised as obese (WHO, 2017). With increase in BMI the risk to develop comorbidities, such as cardiovascular disease, stroke, metabolic syndrome, type-2 diabetes, sleep apnoea, osteoarthritis and several cancers significantly increases as well (Bray, 2004; Haslam and James, 2005; Williams et al., 2015; WHO, 2017). In most countries the number of overweight related deaths exceeds the one of deaths resulting from underweight (WHO, 2017). The fast and global increase of obesity lead to the classification of obesity as a global epidemic in 1997 by the WHO (Caballero, 2007; WHO, 2017).

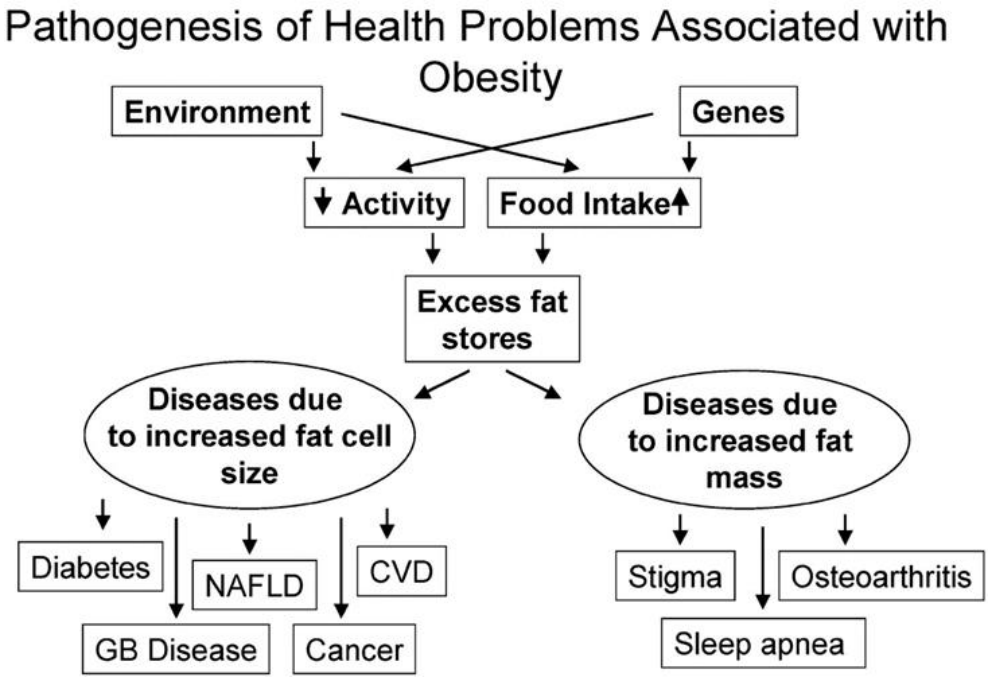

Figure 1.1.1.: Pathogenesis of health problems associated with obesity. NAFLD: Non-alcoholic fatty liver disease, CVD: cardiovascular disease, GB Disease: Gallbladder disease (Bray, 2004).

A sustained imbalance in energy intake and expenditure of the body leads to weight gain and subsequently to overweight and obesity (Stunkard, 1996; Martinez, 2007). In many

cases this impaired energy homeostasis is caused by a genetic predisposition in combination with other factors like modern life style, consisting of changed dietary compositions and food availability (Gonzalez-Muniesa et al., 2017) as well as an overall decrease of physical activity (Martinez-Gonzalez et al., 1999). The highest prevalence for overweight and obesity is therefore found in 'upper-middle-income countries', because of their lifestyle, such as decrease in physical labour, industrial food production and overall food abundance, although developing and 'lower-middle-income countries' show high prevalence as well (Williams et al., 2015; WHO, 2017). In the adult population of the world, 39 % are overweight and 18 % are even obese (WHO, 2017).

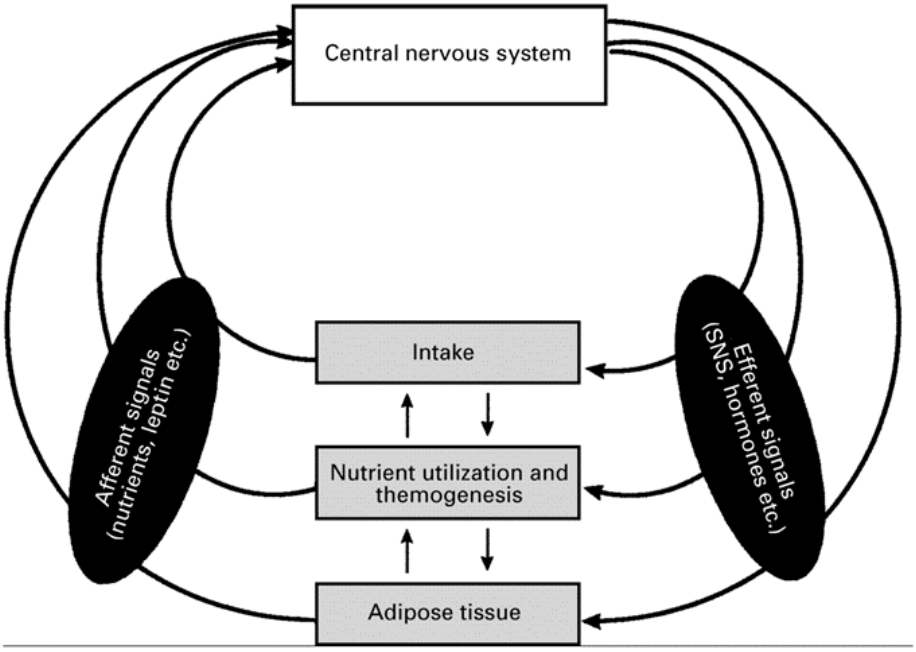

Figure 1.1.2.: Regulation circuit of energy homeostasis. Sympathetic nervous systematic (SNS) and hormonal efferent signals from the central nervous system (CNS) influence energy intake, nutrient utilisation and thermogenesis, as well as the adipose tissue, which also regulate each other and in turn send afferent signals to the CNS (Martinez, 2007).

Energy homeostasis is regulated by the central nervous system involving afferent signals from food intake, nutrient utilisation and thermogenesis and fat storage to the CNS as well as efferent signals from the CNS (Bray, 1991; Horn et al., 1999; Martinez, 2007) (Figure 1.1.2). The central integrator of all afferent into efferent signals is the hypothalamus (Buckingham, 1977).

1.2 The hypothalamus

The hypothalamus is part of the diencephalon and located around the lower part of the third ventricle, building its bottom and parts of its site and front wall (Trepel, 2015). It is the region of the brain coordinating respiration, circulation, the circadian clock (Zucker, 1972), sleep wake behaviour, body temperature, fluid and food intake, appetite and reproductive behaviour (Trepel, 2015). The hypothalamus responds to circulating stimuli and afferent signals from the body, from other brain regions as well as from the hypothalamus itself by releasing neuropeptides that in turn activate or inhibit the production of hormones in the anterior pituitary gland or are release to the blood stream via the posterior pituitary, thus linking the brain to the endocrine system and keeping the body's homeostasis (Buckingham, 1977; Trepel, 2015). The most prominent afferent signal regarding energy storage in form of fat and energy balance is provided by leptin, a hormone released by adipocytes into the blood and transported to the brain where it inhibits hunger (Zhang et al., 1994).

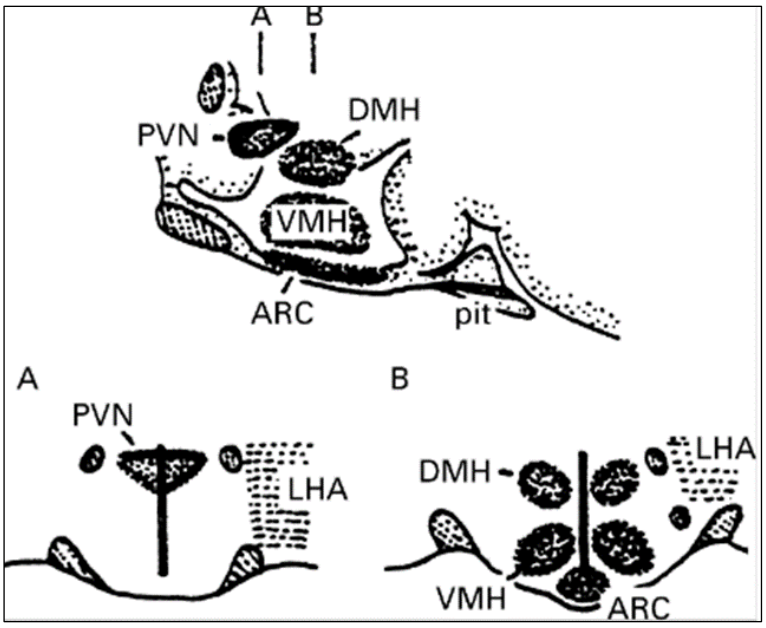

Figure 1.2.1.: Overview of the hypothalamic nuclei. A scheme showing the distribution of nuclei within the hypothalamus from a sagittal point of view, indicating the paraventricular hypothalamic nucleus (PVN), the dorsomedial hypothalamic nucleus (DMH), ventromedial hypothalamic nucleus (VMH), arcuate nucleus (ARC) and pituitary gland (pit) and frontally in a rather posterior position (**A**) at the level of the PVN and lateral hypothalamic area (LHA) and anterior level (**B**) with the DMH, VMH, ARC and also the LHA. (Williams et al., 2000)

The hypothalamus is further divided into areas, like the supraoptic nucleus releasing vasopressin (ADH from antidiuretic hormone) responsible for hydration, the paraventricular nucleus responsible for thermo-regulation, blood pressure and releasing corticotropin-releasing hormone (CRH) and oxytocin, and the suprachiasmatic nucleus with the circadian clock and the preoptic nucleus regulating body temperature (Trepel, 2015).

The most important hypothalamic nuclei regarding the regulation of bodyweight, appetite and energy balance are the arcuate nucleus (feeding), the ventromedial (appetite, body weight, insulin regulation) nucleus as well as the lateral hypothalamic area (appetite and body weight control) (Trepel, 2015). The arcuate nucleus is highly responsive to the adipokine leptin and expresses the respective leptin receptor in a high concentration (Rahmouni, 2012). Furthermore, lesions in the arcuate nucleus lead to the loss of leptin induced feeding behaviour and satiety (Balthasar et al., 2004; van de Wall et al., 2008; Rahmouni, 2012). Opposed to leptin induced satiety stands the lateral hypothalamus, known to express orexins/Hypocretins, that promote hunger (de Lecea et al., 1998; Sakurai et al., 1998).

1.3 The orexin system

1.3.1 Orexins

The neuropeptides orexin A (OA) and orexin B (OB), also known as hypocretin 1 and hypocretin 2, are expressed by a specific population of neurons in the lateral hypothalamus (de Lecea et al., 1998; Sakurai et al., 1998). They were discovered in 1998 independently by two groups by either screening for endogenous ligands of an orphan G-protein coupled receptors (GPCRs) (Sakurai et al., 1998) or by identifying mRNA transcripts selectively located within the hypothalamus (Gautvik et al., 1996; de Lecea et al., 1998).

Orexins derive from a common 130 amino acid long precursor protein called prepro-orexin (PPO), that is alternatively proteolyzed into either orexin A or orexin B. They share about 50 % homology but differ in size (orexin A 33 and orexin B 28 amino acids) and structure, with orexin A being stabilised by two disulphide bridges between the cysteine molecules at position 7 and 12 and 7 and 14 (Jöhren et al., 2004).

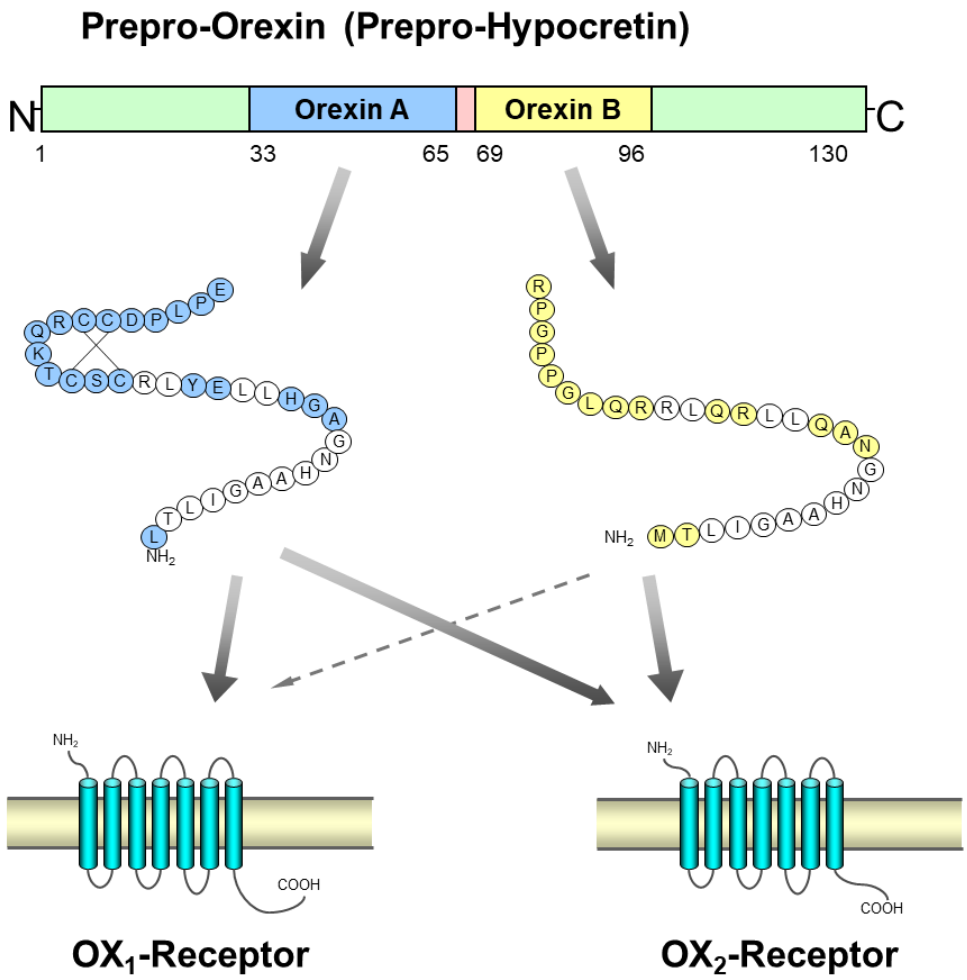

Figure 1.3.1.: The orexin system. The precursor protein prepro-orexin is processed to orexin A or orexin B, which then bind to the orexin receptor type 1 (OX_1-Receptor) and type 2 (OX_2-Receptor). OX_1R has a higher affinity for orexin A, whereas OX_2R has similar affinities for orexin A and B, which is indicated by the grey arrows (modified after (Jöhren et al., 2004)).

Orexins were initially reported to be involved in the regulation of appetite and feeding behaviour (Sakurai et al., 1998; Akiyama et al., 2004). Fasting rats showed increased expression of *prepro-orexin* mRNA and intracerebroventricular (ICV) injection of orexin A or orexin B increased food intake in a dose dependent manner (Sakurai et al., 1998). Later findings showed that orexinergic neurons project to many brain regions where they are also involved in influencing neuroendocrine systems and the autonomic nervous system, arousal, emotion, stress response and the reward system/addiction (Peyron et al., 1998; Date et al., 1999; Yamanaka et al., 2003b; Boutrel et al., 2005; Harris et al., 2005; Narita et al., 2006). Furthermore and very prominently several studies on narcolepsy have shown orexins to be mediators of sleep-wake behaviour (Chemelli et al., 1999; Lin et al., 1999;

Peyron et al., 2000; Thannickal et al., 2000; Arias-Carrión et al., 2015). Narcoleptic patients exhibited low concentrations of orexin in cerebrospinal fluid, a reduced number or orexin expressing neurons or even general absence of orexin in the brain (Peyron et al., 2000; Thannickal et al., 2000; Nishino et al., 2001).

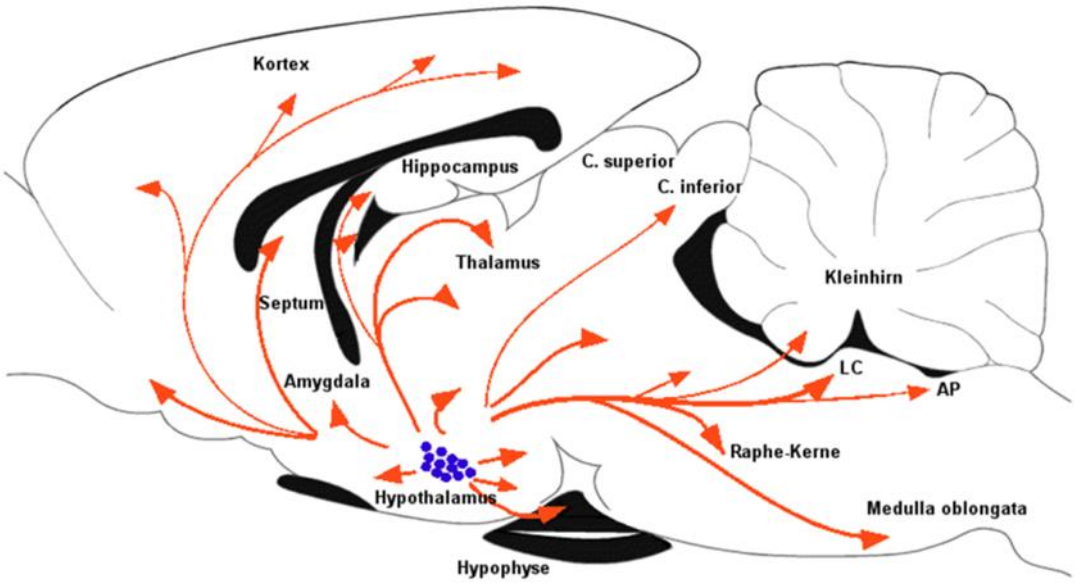

Figure 1.3.2.: Schematic overview of the neuronal orexin system. Orexin expressing neurons in the lateral hypothalamus are marked in blue, whereas red arrows show efferent signals originating from orexinergic neurons to different brain areas, where they influence various physiological processes. (Nambu et al., 1999)

The high activity of orexin neurons in mice preceding and during waking, as well as their fading firing during sleep, reveal a wakefulness promoting effect of orexin (Lee et al., 2005). Furthermore, it has been shown that c-Fos expression in orexin neurons of rats correlate positively with wakefulness and negatively with the amount of sleep (Estabrooke et al., 2001) and ICV injection of orexin A increases wakefulness and behaviours associated with arousal, such as elevated locomotor activity, grooming and food consumption, while it attenuates sleep (Sakurai et al., 1998; Hagan et al., 1999; Ida et al., 1999; Willie et al., 2001).

1.3.2 Orexin receptors

The respective receptors for orexins are the GPCRs orexin receptor type 1 (OX_1R) and type 2 (OX_2R), with its mRNA expression widely distributed in several regions of the brain

(Trivedi et al., 1998; Marcus et al., 2001). *OX_1R* and *OX_2R* mRNA expression has also been shown in peripheral tissues, although there is no evidence of circulating orexin in the body (Jöhren et al., 2001). GPCRs consist of 7 transmembrane domains, an extracellular, N-terminal loop and an intracellular C-terminus. Ligands bind to specific domains of the GPCR, leading to a change in its conformation and activating the associated G-protein. OX_1R and OX_2R have also been identified to couple with $G_{i/o}$ and G_s subtypes of G-proteins but are considered to be mostly coupled to the G_q-protein (Leonard, 2014). The G_q-Protein in turn is coupled to phospholipase C (PLC), which's activation leads to IP_3 (inositol trisphosphate) being cleaved from PIP_2 (phosphatidylinositol 4,5-bisphosphate) and opening calcium channels, leading to an influx of Ca^{2+} into the cytoplasm and depolarisation of the cell. The other product from PIP_2 hydrolysis, DAG (diglyceride) activates protein kinase C, that phosphorylates proteins, e. g. mitogen-activated protein kinase (MAPK), activating the respective signalling pathway (Lund et al., 2000; Ammoun et al., 2006b; Johansson et al., 2007; Tang et al., 2008; Leonard, 2014). It has also been shown that phospholipase D (PLD) was activated independently of PLC via the OX_1R (Jantti et al., 2012). Furthermore, orexin A and orexin B treatment activated mTORC1 (mechanistic Target of Rapamycin complex 1), an enzyme acting as nutrient and energy sensor and playing an important role in cell growth and proliferation, in OX_1R or OX_2R expressing immortalised embryonic hypothalamic cell lines (mHypoE-N41-OX_1R / mHypoE-N41-OX_2R) in an ERK-independent but extracellular Ca^{2+}-influx reliant pathway (Wang et al., 2014b). OX_1R exhibits a higher affinity for orexin A then orexin B, whereas OX_2R has a similar affinity for both peptides (Sakurai et al., 1998).

1.3.3 Orexins in regulating appetite and feeding behaviour

The lateral hypothalamus, where orexins are expressed was known as the 'feeding-centre' of the brain, after lesioning studies lead to a decrease in food intake (Anand and Brobeck, 1951). The first orexin effects discovered after identifying them were the increase in food intake after ICV injection of orexin A and orexin B as well as the enhanced *PPO* mRNA expression in the lateral hypothalamus upon fasting (Sakurai et al., 1998). Due to their orexigenic effects, the peptides were named after the Greek word for appetite, *orexis*. Their effects on feeding behaviour have been established by multiple studies supporting the initial findings, although few studies suggest OX_2R activity inhibits food intake in high-fat, albeit not low-fat diet fed mice (Funato et al., 2009). For example, injection of OX_1R antibodies or antagonists and the genetic ablation of orexin neurons leads to a decreased feeding

(Haynes et al., 2000; Yamada et al., 2000; Rodgers et al., 2001). The effect of fasting on orexin effects has been confirmed immunohistochemically by an increase of c-Fos activity in orexin neurons (Diano et al., 2003; Leinninger et al., 2011) and behaviourally by the increase of orexigenic effect in food deprived animals (Kotz et al., 2002). However, orexin induced feeding by ICV injection seems to be transient, since long-term application does not lead to change in 24-hour food intake or bodyweight, by increasing food intake during the day but decreasing it during the active night phase (Yamanaka et al., 1999; Szekely et al., 2002; Girault et al., 2012) and variable depending on the time and doses of application and diet composition (Tsuneki et al., 2010; Girault et al., 2012).

Although orexin increases food intake, disruption of the orexin system leads to overweight and obesity, because at the same time as elevating appetite and increasing food intake, orexins also increase energy expenditure independently of food restriction in mice (Lubkin and Stricker-Krongrad, 1998; Hara et al., 2001; Wang et al., 2001; Funato et al., 2009). Analog to these studies it has been shown that human patients with the sleeping disorder narcolepsy, where the disruption of the orexin system is a key factor, show a higher prevalence for obesity (Dahmen et al., 2001; Nishino et al., 2001).

Orexin expression and neuron activity are regulated by peripheral nutritional and hormonal signals like changes in blood glucose level and circulating leptin. Hypoglycaemia induced by insulin increased orexin neuron activity, demonstrated by c-Fos immunohistochemistry (Moriguchi et al., 1999; Cai et al., 2001) and elevation of *prepro-orexin* mRNA (Griffond et al., 1999). Up- and downregulation of the glucose level has been shown to inhibit or activate orexin neuron activity *in vitro* and ex vivo but independent of insulin (Muroya et al., 2001; Yamanaka et al., 2003b).The finding that glucose induced hyperpolarisation of orexin neurons is inhibited by the presence of intracellular energy sources like pyruvate, lactate or ATP, indicates that the sensitivity of orexin neurons to glucose depends on the availability of intracellular energy (Venner et al., 2011). The effect of orexin seems to shift in regard to energy balance (Kotz et al., 2002; Thorpe et al., 2003; Thorpe et al., 2005). Leptin also increases *orexin* mRNA expression and c-Fos activity in orexin neurons (Louis et al., 2010; Leinninger et al., 2011; Cui et al., 2012). Furthermore it has been published that the leptin receptor is expressed in the LH (Scott et al., 2009). A retrograde tracing system designed specifically for orexin neurons revealed that they get inputs from many brain regions, e.g. several nuclei of the hypothalamus, brains stem and the forebrain showing the complexity of the orexin system (Sakurai et al., 2005; Yoshida et al., 2006).

Orexin neurons, in turn, also project to numerous regions in the central (Figure 1.3.2) and the peripheral nervous system, the spinal cord and other organs involved in feeding and metabolism (Antunes et al., 2001; van den et al., 2003; Stanley et al., 2010; Perez et al., 2011; Tadataka Tsuji, 2011). Most of the orexinergic efferences in the CNS project to the nuclei of the hypothalamus. Regarding food intake and energy expenditure it has been shown that administration of orexin to the PVN (paraventricular nucleus), DMH (dorsomedial hypothalamus) and PFH (perifornical hypothalamus) increases food intake (Dube et al., 1999), to the VMH (ventromedial hypothalamus) elevates skeletal muscle glucose uptake via the sympathetic nervous system (Shiuchi et al., 2009) and to the arcuate nucleus augmented food intake and energy expenditure (Wang et al., 2003; Muroya et al., 2004b).

1.4 Leptin and leptin receptors

Leptin, named after the Greek word '*leptos*' (thin) is a 146 amino acid long protein released by adipocytes into the blood (Zhang et al., 1994).

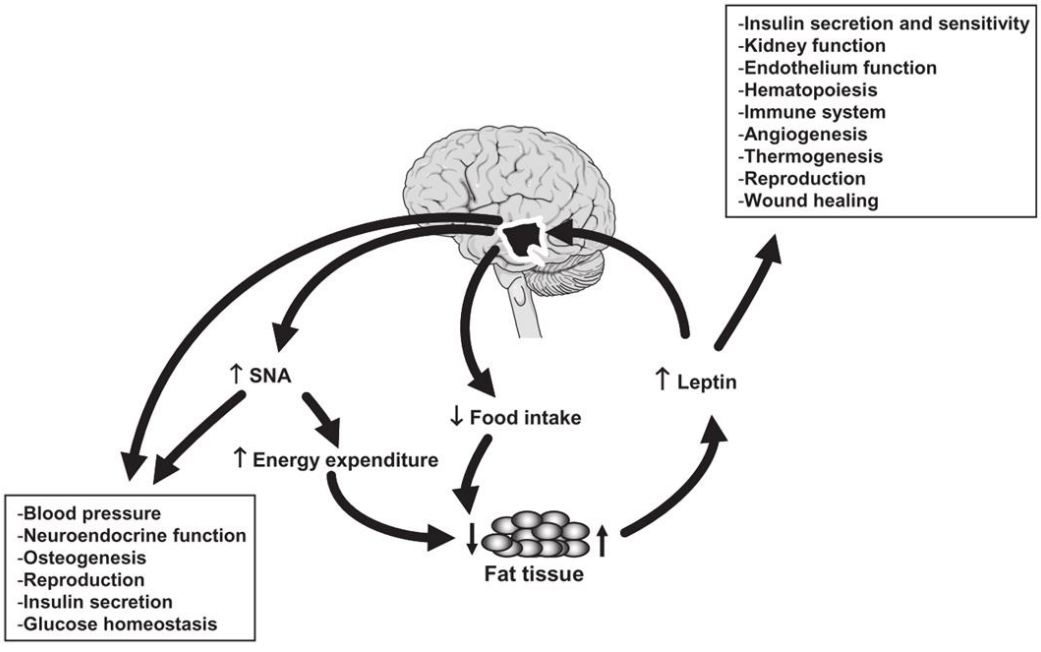

Figure 1.4.1.: Leptins negative feedback involved in bodyweight. Leptin is secreted from the fat tissue into the blood and circulates through the body, where it influences processes such as insulin secretion and sensitivity, kidney function and others (compare upper box) and transported to the brain, where it increases energy expenditure and the sympathetic nervous system activity (SNA) (compare lower box) and inhibits food intake (Rahmouni, 2012).

It was discovered after positional cloning of a gene discovered as mutation in a mouse strain with early onset obesity, called *obese* (*ob*) gene (Ingalls et al., 1950; Jeffrey M. Friedman, 1995). As an adipokine leptin reduces food intake and increases energy expenditure (Campfield et al., 1995; Seeley, 1996; Morton et al., 2006; Scott et al., 2009) in a negative feedback circuit (Figure 1.4.1) involving the hypothalamus (Kennedy, 1953). Leptin is secreted proportionally to the amount of adipose tissue, which results in very high levels of circulating leptin in the blood of obese individuals (Frederich et al., 1995; Hiroaki Masuzaki, 1995; Schwartz et al., 1996). If obesity is not a consequence of genetically caused leptin or leptin receptor deficiency it is usually accompanied by leptin resistance, causing the increase in leptin blood levels due to reduced central leptin effects or even diminishing leptin activity (Heymsfield et al., 1999; Morton et al., 2006).

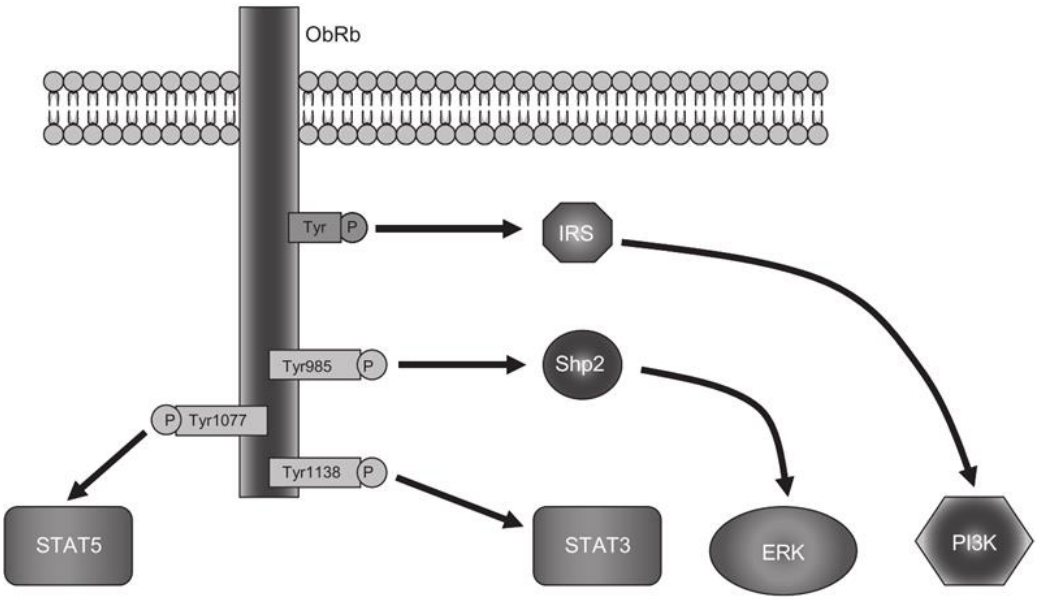

Figure 1.4.2.: Pathways activated by LepRb/ObRb activation. Upon activation of the ObRb different tyrosines (Tyr) can be phosphorylated and in turn activate phosphatidylinositol-3-kinases (PI3K) through insulin receptor substrate (IRS), extracellular signal-regulated kinases (ERK) through src homology region 2 domain-containing phosphatase-2 (Shp2), signal transducer and activator of transcription 5 (STAT5) or signal transducer and activator of transcription 3 (STAT3) (Rahmouni, 2012).

The leptin receptor was discovered in a similar way as leptin, in a mouse line with a diabetic phenotype resulting from a mutation in the *diabetes* (*db*) gene which was identified as leptin receptor (Coleman, 1978; Jeffrey M. Friedman, 1995). There are 6 isoforms of the leptin receptor due to alternative splicing, called LepR/ObR a to f, that differ in their intracellular

domain (Jeffrey M. Friedman, 1995; Louis A. Tartaglia, 1995; Streamson C. Chua, 1997). Only the LepRb/ObRb has been shown to be able to convert extracellular leptin signals to intracellular signals, e.g. the STAT3 or ERK pathway (Figure 1.4.2) (Jeffrey M. Friedman, 1995; Louis A. Tartaglia, 1995; Rahmouni, 2012). LepRb/ObRb are highly expressed within the hypothalamus, especially the arcuate nucleus (Scott et al., 2009) where leptin suppresses feeding/hunger by inhibiting orexigenic neuropeptide Y (NPY) expressing neurons or by activating anorexigenic proopiomelanocortin (POMC) expressing neurons (Balthasar et al., 2004; van de Wall et al., 2008; Rahmouni, 2012). Circulating leptin at normal levels and leptin receptor activity are crucial for maintaining a bodyweight within the range considered healthy (Coleman, 1978; Seeley, 1996; Balthasar et al., 2004; Rahmouni, 2012).

1.5 Orexin and leptin interaction

Orexin being known for its effect in food intake and energy homeostasis and leptin known as the satiety hormone would be logical opponents in the regulation of bodyweight. It has been shown that both orexin and leptin system impairment concludes in obesity (Campfield et al., 1995; Dahmen et al., 2001; Balthasar et al., 2004) and both peptides have effects on neurons in the hypothalamus, especially the arcuate nucleus (Horvath et al., 1999; Balthasar et al., 2004; Scott et al., 2009; Rahmouni, 2012). On a phenotypic and behavioural level it has also been shown that orexin when overexpressed in mice prevented diet induced obesity mediated by OX_2R and dependent on the presence of leptin (Funato et al., 2009).These results indicate an interaction between orexin and leptin not as opponents but rather as orexin enhancing leptin sensitivity (Funato et al., 2009). Another study found, that fasting induced *PPO* mRNA upregulation in WT mice depended on the co-application of leptin (Tritos et al., 2001) Already shortly after the discovery of orexins the interaction of orexin and leptin systems were addressed.

1.5.1 Regulation of orexin, PPO, and orexin receptors in genetically leptin deficient or resistant rodents

Rodents with spontaneous mutations in leptin or leptin receptor coding genes develop obesity and diabetes and serve as models for obesity studies. Most prominently are obese (*ob*/*ob*) mice, that are leptin deficient, diabetic (*db*/*db*) mice and Zucker fatty (*fa*/*fa*) rats, that are both leptin resistant as a result of mutated receptors (Wang et al., 2014a). *PPO*

expression has been shown to be significantly reduced in *ob*/*ob* and *db*/*db* mice, when fed ad libitum but is upregulated by food restriction in a leptin independent manner (Yamamoto et al., 1999; Yamamoto et al., 2000). Although more studies confirmed decreased *PPO* mRNA and orexin A levels in *ob*/*ob* mice (Stricker-Krongrad et al., 2002), others did not find a difference in *PPO* mRNA expression of *ob*/*ob* versus control mice and orexin A or *PPO* mRNA levels in obese versus lean Zucker rats (Taheri et al., 1999; Taheri et al., 2001; Tritos et al., 2001). Some even found increased orexin peptide levels in the LH of *ob*/*ob* but decreased levels in *db*/*db* mice (Mondal et al., 2002). Orexin A and orexin B levels were shown to not differ in the LH but other brain regions of Zucker rats, which indicates a reduced orexin neuron activity and orexin secretion (Mondal et al., 1999). Other studies claim a decrease of *PPO* but an increase of OX_1R and OX_2R mRNA in Zucker rats (Beck et al., 2001) or decrease in *PPO* and OX_2R mRNA levels (Yamamoto et al., 2002). Together these findings indicate that orexin levels and the expression of orexin receptors are at least partly dependent on or regulated by leptin.

1.5.2 Orexin effect on leptin target neurons

On a cellular and molecular level, the sites and pathways involved in this interaction have not been clearly identified yet. A possible interaction site for orexin and leptin could be a mutual target cell, expressing both LepR and orexin receptors. Leptin responsive cells in the arcuate nucleus were activated via orexin A application (Rauch et al., 2000), orexin neurons innervate NPY and POMC neurons containing the LepR (Horvath et al., 1999; Funahashi et al., 2000; Guan et al., 2001; Muroya et al., 2004b) and co-localisation studies found NPY and POMC neurons in the arcuate nucleus to be immuno-reactive for OX_1R (Funahashi et al., 2003). On top of expressing orexin receptors, NPY expressing neurons in the arcuate nucleus were also shown to be activated by orexin (van den et al., 2004). Findings on the effect of orexin on POMC neurons are controversial, since some groups found that they are electrically inhibited, while others saw excitation by orexin application in POMC neurons (Ma et al., 2007; Acuna-Goycolea and van den Pol, 2009). Furthermore, orexin neurons evoke Ca^{2+} influx in LepR positive NPY and POMC neurons (Muroya et al., 2004b). Either of these interaction pathways does not exclude the others and they could exist in parallel.

1.5.3 Leptin effect on orexin neurons

Controversial results show that on the one hand, leptin seems to impede the activity of orexin neurons as well as fasting induced upregulation of *PPO* RNA (Lopez et al., 2000; Yamanaka et al., 2003b), for example chronic treatment with leptin led to a reduction of *PPO* mRNA levels in mice (Yamanaka et al., 2003b), while on the other hand fasting induced increase of PPO mRNA levels seems to be dependent on co-treatment with leptin (Tritos et al., 2001). Some publications postulate LepR expression (Horvath et al., 1999; Iqbal et al., 2001) and STAT3 activation in lateral hypothalamic orexin neurons (Hakansson et al., 1999) indicating a direct regulation of orexin neurons by leptin, like the direct inhibition of isolated orexin neurons by leptin (Yamanaka et al., 2003b).

Contrariwise, other groups could not find LepR in orexin neurons but distinct cells in the lateral hypothalamus (Leinninger et al., 2009). These neurons in the lateral hypothalamus expressing the LepR appear to be neurotensin positive neurons that inhibit orexin neurons as a result of leptin stimulation (Louis et al., 2010; Leinninger et al., 2011; Goforth et al., 2014), demonstrating an indirect, inhibiting effect of leptin on orexin neurons.

1.6 Hypothesis and Aim

Numerous studies indicate an interaction of orexin and leptin, but little is known about the underlying molecular mechanisms. Whereas some data show an indirect effect of leptin on orexinergic neurons (Figure 1.6.1 possibility 2.), others claim that leptin receptors (LepRb) are expressed on the orexinergic neurons, leading to the conclusion that leptin may have also a direct effect on these neurons (Figure 1.6.1 possibility 1.). Other studies again show orexin receptor expression and orexin reactivity in leptin reactive NPY and/or POMC neurons in the arcuate nucleus, indicating that orexin and leptin both affect these neurons, where their interaction could merge on a molecular level, involving for example the MAPK/ERK pathway (Figure 1.6.1 possibility 3.).

Experiments in this work should investigate the following hypotheses:

- Leptin regulates orexin neurons directly requiring the expression of leptin receptors on orexin neurons, besides its indirect effect on orexin neurons.
- Leptin and orexin signalling converge at shared target neurons within the hypothalamus, for example NPY or POMC neurons in the arcuate nucleus.

The possible direct effect of leptin on orexin neurons was investigated by anatomical identification of the long version of the leptin receptor (LepRb) on orexin neurons in co-localisation studies using fluorescent *in-situ* hybridisation (FISH) against *prepro-orex*in (*PPO*) mRNA in a cre knock-in LepRb-ZsGreen mouse line.

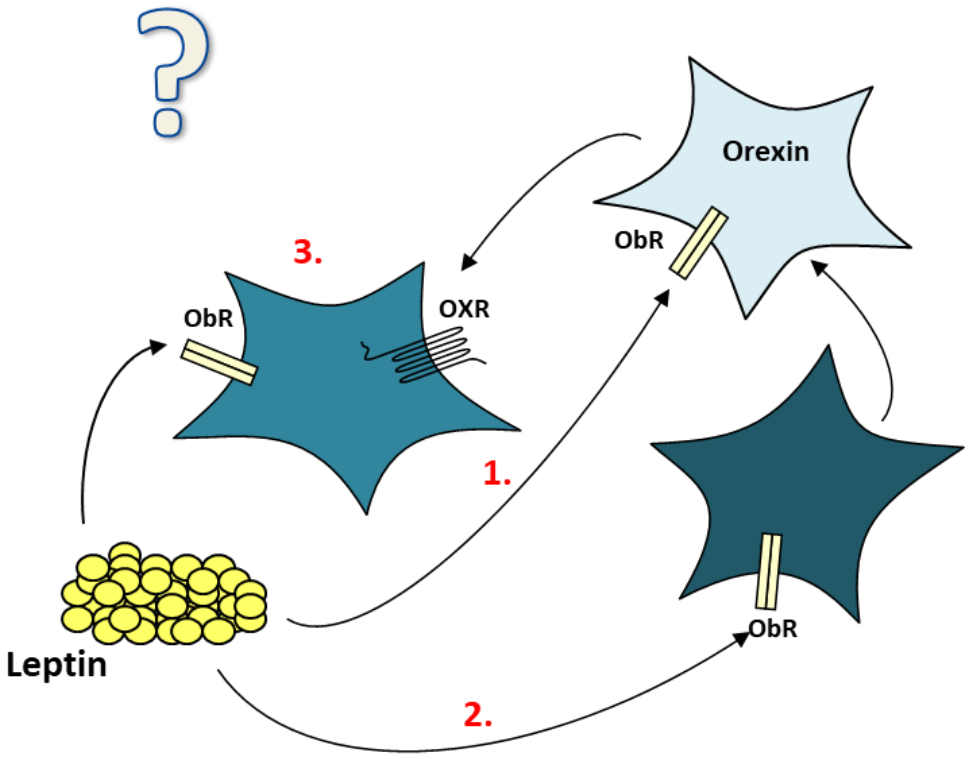

Figure 1.6.1.: Theoretically possible interaction sites for orexin and leptin. Leptin is secreted by the adipocytes and transported to the brain, where it could act on orexin neurons directly, if they express the leptin receptor (ObR) (**1.**), or indirectly via ObR expressing interneurons (**2.**), a third possibility of leptin-orexin interaction is a shared target neuron that expresses both ObR and orexin receptors (OXR) (**3.**).

Co-operative intracellular leptin-orexin signalling in shared target neurons was supposed to be anatomically and functionally identified and characterised using FISH against OX_1R and OX_2R mRNA and fluorescent activated cell sorting (FACS) in LepRb-ZsGreen mice, as well as phosphorylation and mRNA regulation studies, reporter gene assay and calcium measurements in murine immortalised, hypothalamic neurons, serving as *in vitro* models.

2 Methods

2.1 Cell culture

2.1.1 General cell culture

All methods were performed under sterile conditions in a Laminar-Flow-workbench. Cells grew in the appropriate flasks or dishes in incubators set to 5 % CO_2 and 37°C in water vapour saturation.

2.1.2 Cell lines immortalised, murine, embryonic/adult, hypothalamic (mHypoE/A) cell lines

Hypothalamic cells, previously isolated from embryonic or adult mice, were immortalized using SV40 virus. Infected cells were isolated and screened for neuron specific markers and other properties and distributed via CELLutions Biosystems (Ontario, Canada) (Belsham et al., 2004; CellutionsBiosystemsInc., 2009). Based on the advertised expression profile the cell lines mHypoE N41, mHypoE N25/2 and mHypoA 2/23 were purchased and used for studies on the orexin system.

Furthermore, the cell lines mHypoE-N41-OX_1R and mHypoE-N41-OX_2R were acquired. These cell lines are based on mHypoE N41 cells and stably transfected with the human OX_1R or OX_2R by infection with retroviruses (Wang et al., 2014b).

2.1.3 Starting a culture of mHypoE/A

Cells were cryoconservated in liquid nitrogen at a concentration of 1 to 5 x 10^6 cells/ml in freezing medium (40 % standard culture medium, 50 % FCS, 10 % DMSO sterile filtered). To revitalise the cell lines and start the cell culture a 1 ml aliquot of the cryovials were thawed in a water bath at 37°C. To wash out the freezing medium 10 ml cold culture medium (high glucose Dulbecco's modified Eagle's medium (DMEM; high glucose (25 mM), with L-glutamine (4 mM) with 10 % heat inactivated FCS and 100 µg/ml Penicillin/Streptomycin was added to the cell suspension and cells pelleted via centrifugation at 200 g for 5 min. The pellet was resuspended in 15 ml culture medium and transferred to a 75 cm^2 cell culture flask with filter vented caps (Greiner Bio-One International).

2.1.4 Sub cultivating mHypoE/A cell lines

Two times per week adherent, confluent cells grown in a 75 cm^2 cell culture flask with filter vented caps were washed with phosphate buffered saline (PBS; pH 7.4) to remove trypsin inactivating substances in the medium. Cells were detached from the culture flask with 3 ml of trypsin for a five-minute incubation. The detached cells were washed down and pelleted by 5 min centrifugation at 200 g. The pellet was re-suspended in 10 ml culture medium. One ml of the cell suspension was transferred to a new cell culture flask and filled up with 13 ml of fresh medium. For experiments cells were diluted and seeded in the needed concentration using a Fuchs-Rosenthal cell counting chamber to determine the cell amount in the cell suspension.

2.1.5 Seeding cells for protein or mRNA expression analysis experiments

For protein extraction 3 x 10^5 mHypoE/A cells were seeded in 2 ml high glucose Dulbecco's modified Eagle's medium (DMEM; high glucose (25 mM), with L-glutamine (4 mM)) with 10 % heat inactivated FCS and 100 µg/ml Penicillin/Streptomycin in a 6-well cell culture plate. For mRNA expression analysis 0.75 x 10^5 cells were seeded in 0.5 ml medium in a 24-well cell culture plate.

2.1.6 Treatment of cultured mHypoE/A cells for protein activation or mRNA expression analysis

24 h after seeding and 24 h prior treatment the cell culture medium with 10 % heat inactivated FCS and 100 µg/ml Penicillin/Streptomycin was changed to strep medium without serum or antibiotics. For mRNA expression analysis 4 wells of a 24-well cell culture plate per condition were treated with 1 µM orexin A (OA) with or without 0.1 µM leptin, 1 µM orexin B (OB) with or without 0.1 µM leptin, only leptin or PBS as control for 12, 6, 3, 1, 0.5 or 0.25 h. Following the treatment cells were washed with PBS and lysed with lysis buffer from NucleoSpin® RNA purification kit (Macherey-Nagel) for RNA extraction. For protein activation analysis cells were treated in a 6-well cell culture plate with 1 µM orexin A with or without 0.1 µM leptin for 5 or 30 min or PBS as control, washed with 1 x PBS and lysed with cell lysis buffer (CLB) with Phenylmethylsulfonylfluorid (PMSF) for protein extraction. In another experiment the cells were treated with medium without serum or antibiotics, that was primed for 48 h by adipocytes in culture for 5 or 30 min or medium without serum or antibiotics primed for 48 h by mHypoE/A cells as a control. Protein concentration was

determined after Lowry while RNA concentrations were measured via spectrophotometer (NanoDrop 2000, Thermo Scientific™) (Lowry et al., 1951).

2.1.7 Cultivation of immortalized cells from the epididymal white adipose tissue (WAT) of male C57BL/6 wild type mice and production of adipocyte primed medium

Epididymal adipocytes, that where immortalized and generated from male C57BL/6 wild type mice (Klein et al., 2000), where cultured from Lisa Cheradi in the research group Experimental and Clinical Endocrinology at the department of Internal Medicine I of the University of Lübeck.

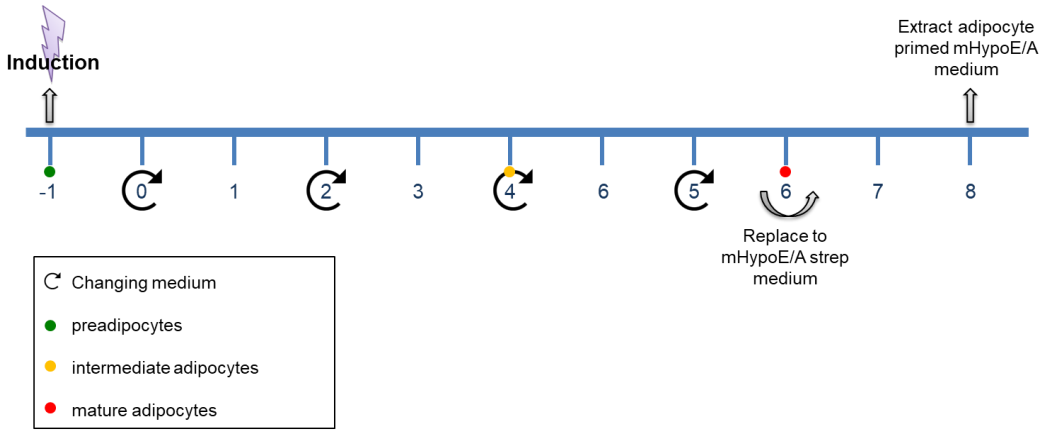

Figure 2.1.1.: Schematic overview of differentiation protocol for cultured epididymal adipocytes and the production of adipocyte primed medium. Preadipocytes grown to 100 % confluency where induced to differentiate for at day -1 for 24 h. During the next 6 to 7 days lipid droplet formation was controlled microscopically as a marker for differentiation status until the cells became mature adipocytes. The medium was changed to mHypoE/A medium without FCS or antibiotics for 48 h and then harvested from the cells for further experiments.

The immortalized preadipocytes were kept in culture in basic medium and to a maxiumum of 70 to 80 %. To differentiate the cells to mature adipocytes, the cells were grown to 100 % confluency in differentiation medium (mDM) and 100 mm petri dishes, before differentiation was induced by changing to mDM with dexamethasone, indomethacine und isobotylmethylxanthin (IBMX) at day -1, to change proliferation to differentiation signals, that induce the incorporation of lipids into lipid droplets.

After 24 h the medium was changed back to mDM and the cells monitored for their lipid droplet formation as an indicator for their differentiation status. The medium was changed every 1 to 2 days and the cells reached maturity at da 6 to 7. The medium of mature adipocytes was changed to mHypoE/A medium for 48 h and then harvested as adipocyte primed medium for further experiments.

2.2 RNA extraction protocols

2.2.1 RNA extraction from cultured cells or hypothalamic brain tissue

RNA extraction from cultured cell lines mHypoE N41, mHypoE N25/2, mHypoA, mHypoE-N41-OX_1R and mHypoE-N41-OX_2R and hypothalamic brain tissue followed the NucleoSpin® RNA protocol for RNA purification from cultured cells and tissue delivered within the kit from Macherey-Nagel.

2.2.2 RNA extraction after fluorescent activated cell sorting (FACS)

For further investigation of the RNA expression patterns of LepRb expressing ZsGreen cells compared to non-fluorescent cells, RNA was extracted from sorted samples. The ZsGreen positive samples had cell numbers ranging from 5 x 10^5 to 1.5 x 10^6 while non-fluorescent samples contained around 1 x 10^8 cells.

2.2.2.1 RNA extraction with NucleoSpin® RNA kit from samples with cell numbers < 5 x 10^6

If the cell number in FACSed samples was above 5 x 10^6 RNA extraction was performed with the NucleoSpin® RNA kit (Macherey-Nagel). Samples were centrifuges at 100 g for 10 min and cell pellets lysed in 250 µl of the Lysis Buffer from the kit. The extraction itself was performed following the protocol for RNA purification from cultured cells and tissue provided within the kit.

2.2.2.2 RNA extraction via Nanoprep for lower cell numbers

Due to low cell numbers in fluorescent samples the Nanoprep kit from Stratagene was used for RNA extraction. First samples were centrifuged at 100 g for 10 min, sorting buffer was

removed, and the cell pellet lysed in 100 µl of the provided Lysis buffer with 0.7 µl ß-ME. The lysate was mixed with 100 µl 70 % Ethanol by 5 s of vortexing. The sample was transferred to the RNA-binding nano-spin cup placed on a 2-ml cup and centrifuged for 60 s at 12 000 g. Once the RNA was bound in the nano-spin cup, the membrane was washed with 300 µl 1 x Low-Salt Buffer by centrifugation at 12 000 g for 60 s and dried by 2 min centrifugation at the same speed. DNase was eliminated from the sample by 15 min incubation at 37°C with a mixture of 2.5 µl reconstituted RNase-Free DNase I and 12.5 µl DNase digestion buffer directly pipetted onto the membrane. After DNA digestion, the membrane was washed once with 300 µl 1 x High-Salt Buffer and twice with 300 µl of 1 x Low-Salt Buffer, each time centrifuged for 60 s at 12 000 g. Before RNA elution the membrane was dried by 3 min centrifugation at 12 000 g and transferred to a fresh cup. RNA was eluted via 5-6 min incubation at RT with 11 µl Elution Buffer, that was previously heated to 60 °C. Following 5 min of centrifugation at 12 000 g, 2 µl of the elution were used to quantify RNA concentration via spectrophotometer (NanoDrop 2000, Thermo Scientific™) and the remaining 9 µl were reversely transcribed into cDNA for PCR analysis.

2.2.2.3 RNA extraction with Trizol® Reagent

To increase the amount of RNA yields and have an identical extraction method for all samples, the protocol was changed to Trizol® Reagent (ambion® life technologies™) as lysis buffer followed by ethanol precipitation. FACSed cells were pelleted at 100 g for 10 min, sorting buffer was removed, and cells lysed and homogenised with 350 µl Trizol® Reagent by pipetting. The sample was incubated at RT for 5 min and transferred to a 1.5 ml Eppendorf tube®. For phase separation 0.2 ml chloroform (CarlRoth®) per ml Trizol® Reagent was added to the lysate, mixed by shacking for 15 s and incubated at RT for 2-3 min. Subsequently the samples were centrifuged for 15 min and 12 000 g at 4°C. The upper, aqueous phase (now containing DNA and RNA) was transferred to a fresh tube,1/10 of the volume ammonium acetate (Sigma-Aldrich®) was added and the sample mixed by vortexing. RNA was precipitated from the sample by adding 3x the sample volume cold 100 % isopropanol, 1h incubation at -20°C followed by 20 min centrifugation at 13 200 rpm and 4°C. Supernatant was discarded and the RNA pellet washed with 0.5 ml cold 70 % ethanol (EtOH) for 15 min at 13 200 rpm and 4°C. The pellet was dried for 5 to 10 min prior to being resuspended in 20 µl RNAse free diethyl pyrocarbonate (DEPC) treated water. To purify the RNA yield samples were treated with 2.2 µl Turbo™ DNase (Invitrogen™) for 30 min at 37°C. DNase was washed out of the sample by phenol-chloroform-isoamyl precipitation by

adding 110 µl of phenol-chloroform-isoamyl (Sigma-Aldrich®) to the sample, vortexing, centrifugation at 14 000 g for 1 min and transferring the upper aqueous phase, now containing only RNA to a fresh tube. An equal amount chloroform (CarlRoth®) was added to the sample, mixed by vortexing and centrifuged at 14 000 g for 1 min to purify the sample from a possible phenol contamination that would influence further processing of the RNA by denaturing proteins as for example reverse transcriptase for cDNA synthesis. The upper aqueous phase was again transferred to a fresh tube, 1/10 ammonium acetate (Sigma-Aldrich®) added and RNA was precipitated, washed and finally resuspended in 15 µl RNase free DEPC treated water as described in this chapter. RNA concentration was determined via spectrophotometer (NanoDrop 2000, Thermo Scientific™).

2.3 Polymerase chain reaction (PCR)

2.3.1 Reverse transcriptase

RNA extracted from various samples was reversely transcribed into cDNA by First-Strand cDNA Synthesis Reaction using the Cloned AMV First-Strand cDNA Synthesis Kit (Invitrogen™) following the protocol for oligo(dt) provided within the kit in a T-Gradient Thermocycler (Biometra). Depending on the amount of extracted RNA samples were diluted 1:1 with DEPC treated water.

2.3.2 Quantitative real-time (q)PCR

For each PCR reaction 2 µl cDNA were used with the Platinum™ SYBR™ Green qPCR SuperMix-UDG w/ROX (Invitrogen™) kit following the protocol delivered within the kit. If RNA concentration was very low in samples the amount of cDNA could be increased up to 11 µl replacing the DEPC water in the PCR reaction mix (Table 2.3.1Table 2.3.1).

To quantify gene expression in the samples for every gene a standard was measured within each experiment. A housekeeping gene served as an internal control. qPCRs were performed in an ABI PRISM® 7000 Sequence Detection System (Applied Biosystems™).

Table 2.3.1.: Formula for one qPCR reaction

Component	µl
cDNA	2-11
qPCR SuperMix	12.5
Sense Primer (10 µmol/µl)	0.75
Antisense Primer (10 µmol/µl)	0.75
DEPC-H_20	0-9

The standard protocol for qPCR consisted of an initial cycle at 50 °C for 2 min, followed by one cycle of 95 °C for 2 min, continued for 40 cycles containing of 95 °C for 15 s to 60 °C for 1 min and finished with a final cycle of 95 ° C for 15 s to 60 °C for 20 s and 95 °C lasting 15 s.

2.3.3 PCR to investigate fluorescent activated cell sorting efficacy

To determine results of fluorescent activated cell sorting by checking for LepR positive vs. LepR negative samples *LepR* was multiplied by PCR with DyNAzyme II DNA Polymerase (Thermo Scientific™) using 2 µl of sample cDNA and the pipetting instructions delivered with the DNA polymerase. The PCR was performed by a T-Gradient Thermocycler (Biometra) following cycling instructions with 35 cycles. The PCR products were applied to a 1.5 % agarose (Table 2.3.2) gel to visualise PCR results.

Table 2.3.2.: 1.5 % Agarose gel

Substance	Amount
TRIS-Borsäure-EDTA- (TBE-) buffer	100 ml
Agarose	1.5 g
Ethidiumbromid (EtBr)	2 µl

2.4 Western Blot

2.4.1 Sample preparation

After protein quantification according to Lowry protein assay, 120 µl of each cell lysate were mixed with 40 µl 4x SDS-2-Mercaptoethanol and denaturised at 95°C for 10 min. All samples were diluted with 1x SDS (4x SDS diluted with 1x CLB) to the lowest protein concentration measured.

2.4.2 Sodium dodecyl sulphate polyacrylamide gel electrophoresis (SDS-PAGE)

Proteins were separated by size via self-made 10 % acrylamide gels in a vertical mini gel electrophoresis system (Mini-PROTEAN® Tetra Vertical Electrophoresis Cell; Bio-Rad) under 100 V for 2.05 h. The acrylamide gel containing the separating and stacking gels were prepared after and in the order shown in and Table 2.4.1. The chamber was filled with SDS electrophoresis buffer (3.03 g Tris Base, 14.4 g Glycine and 1 g SDS/51 per litre H_2O). The first pocket of the stacking gel (

Table 2.4.2) was loaded with Presision Plus Protein™ Standards (Bio-Rad) while the other pockets were loaded with 50 to 100 µg of protein.

Table 2.4.1.: Separating acrylamid gel (10 %)

Component	Amount
H_2O	4.05 ml
Tris-HCL pH 8.8 (1.5 M)	2.5 ml
SDS (10 %)	100 µl
Acrylamid (30 %)	3.3 ml
Ammonium Persulphate (APS)	50 µl
Temed	10 µl

Table 2.4.2.: Stacking acrylamid gel

Component	Amount
H_2O	3.05 ml
Tris-HCL pH 6.5 (0.5 M)	1.25 ml
SDS (10 %)	50 µl
Acrylamid (30 %)	0.67 ml
APS	25 µl
Temed	5 µl

2.4.3 Semi dry protein transfer

After SDS-PAGE the separated proteins were transferred from the separating gel to a Immobilon-P membrane (Millipore) by semi dry protein transfer. Membrane and filters were soaked in Towbin blotting buffer (3.03 g Tris Base, 14.41 g glycine and 1 g SDS in 800 ml and 200 ml Methanol (MeOH), pH 8.2 - 8.4) and stacked in a Hoefer® SemiPhor™ Electophoresis Blotter TE-70 (Amersham Pharmacia Biotech). The transfer ran for 1.5 h at 100 V.

2.4.4 Immuno-Staining

The proteins, now transferred to the membrane, where blocked with 5 % Bovine Serum Albumin (BSA, Sigma-Aldrich®) and immune-stained first with antibodies against phosphorylated ERK1/2 (rabbit anti-Phospho-p44/42 MAPK (Thr202/Tyr204) from Cell Signaling Technology®) in a 1:1000 dilution in 5 % BSA in Tris-buffered saline (TBS) at 4°C, over night. The following day membranes were washed with 1 x PBS and incubated in a horseradish peroxidase (HRP) secondary antibody (Goat anti-Rabbit IgG Secondary Antibody, HRP from Invitrogen™), 1:5000 in 5 % BSA in TBS for 1h at room temperature (RT). The secondary antibody bound to the respective protein was made visible by a 1:4 dilution of the HRP enhanced-chemiluminescent-substrate SuperSignal® West Femto-Substrate (Thermo Scientific™) in H_2O using a FUSION SOLO S (Vilber). Subsequently the antibodies were stripped off the membrane by 15 min incubation with 1x Re-Blot Mild Solution (10x (Millipore) diluted in ddH_2O) and washing with TBS-T washing buffer. The staining protocol was then rerun using antibodies against whole ERK1/2 (rabbit anti-p44/42 MAPK (Thr202/Tyr204) from Cell Signalling Technology®).

2.4.5 Analysis

The pictures taken in the Fusion SOLO S (Vilber) where analysed by quantification with the help of the EvolutionCapt software delivered with the system. For each sample the quantity of phosphorylated ERK1/2 relative to the amount of whole ERK1/2 was calculated and normalised to the control sample.

2.5 Brain tissue preparation

2.5.1 Mouseline

To visualise cells that express/expressed LepRb the knock-in mouse line $LepRb^{IRES\text{-}Cre}$ was crossed with the $ROSA26^{LoxP\text{-}STOP\text{-}LoxP\text{-}ZsGreen1}$ mouse line. $LepRb^{IRES\text{-}Cre}$ mice express Cre from an IRES element inserted downstream of the obr (LepR) gene directly after the stop codon in the last exon of ObRb (Jeff DeFalco, 2001). In ZsGreen mice, a loxP-flanked ('floxed') stop cassette followed by a sequence coding for the fluorescent protein ZsGreen is inserted into the Rosa26 locus after the CAG promoter (Madisen et al., 2010). LepRb-ZsGreen mice express ZsGreen in all cells expressing LepR at present or at any time point during the life of the cells.

2.5.2 Brain tissue preparation for cryostat sections

Mice were euthanised by intraperitoneal (IP) injection of a letal dose of a 2.5 % avertin solution in 0.9 % NaCl. By severing the diaphragm, the heart was exposed, whereupon a cannula was inserted into the left ventricle while the right atrium was opened by a small incision. The blood was washed out of the circuit by a pre-perfusion with 1x PBS before fixating the whole body-tissue by perfusing with 4 % paraformaldehyde (PFA). Following fixation, the brain was dissected from the cranium, post fixed in 4 % PFA for 2 h and dehydrated in 30 % sucrose solution at 4°C. Dehydrated brains were frozen and cut into 20 µm thick sections using a cryostat CM3050 (Leica Biosystems).

2.5.3 Brain tissue preparation for vibratome sections

LepRb-ZsGreen mice were anaesthetised with isoflurane and decapitated. The brains dissected from the skull were fixed in 4 % Paraformaldehyde (PFA) in 1x PBS at 4°C, over night before sectioning in 50 µm slices at a vibrating blade microtome (VT1200 S, Leica Biosystems). Brain sections were kept at 4°C in PBS with 0.02 % sodium azide until further use but a maximum of 4 weeks.

2.5.4 Cell dissociation for fluorescent activated cell sorting (FACS)

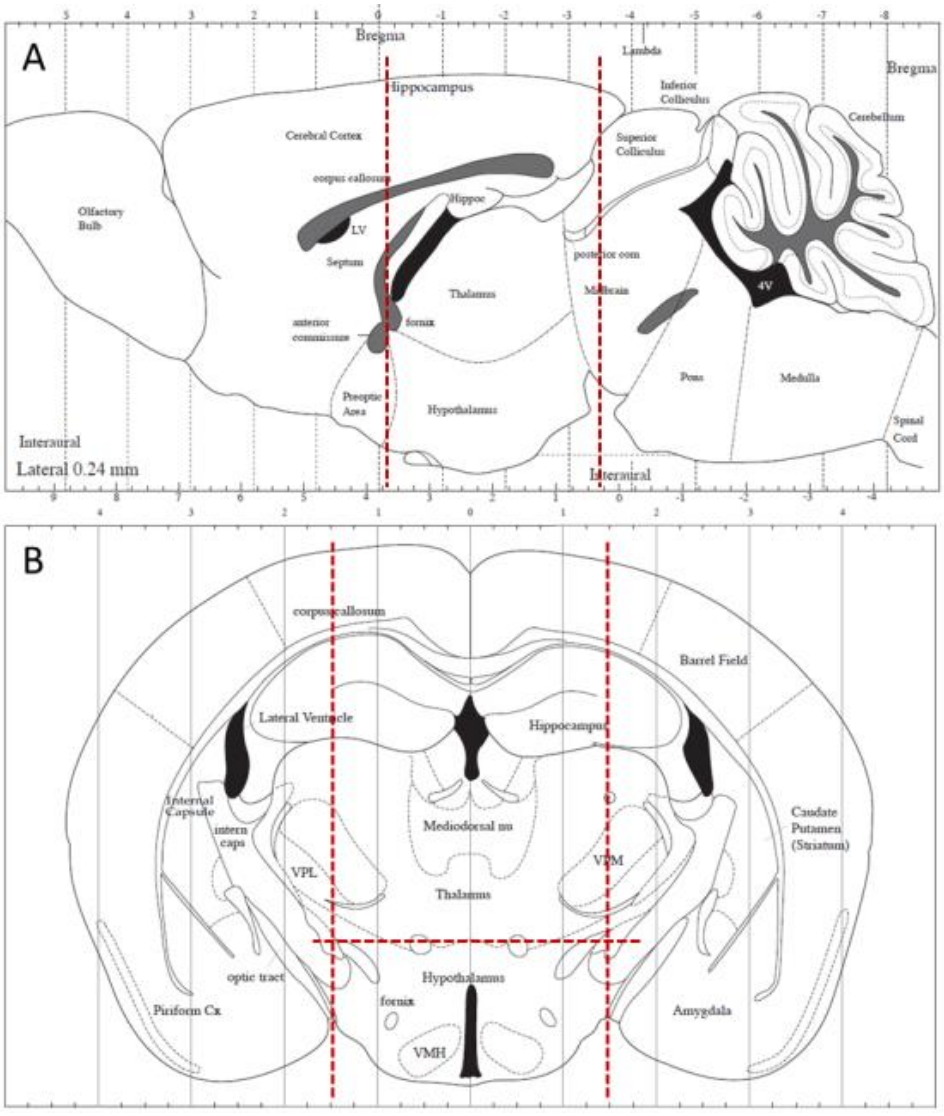

Figure 2.5.1.: Schematic overview of the preparation of LepRb-ZsGreenmice hypothalami. Two frontal cuts at Bregma level 0 and 3.5 mm were performed to dissect the area containing the hypothalamus (**A**), followed by two sagittal cuts and a final transversal cut at approximately 1.5 mm laterally and ventrally (**B**).

The hypothalamus of LepRb-ZsGreen mice was harvested after decapitation by frontal cuts in the tissue at Bregma level 0 and 3.5 mm followed by two sagittal cuts at 1.5 mm laterally and a final transversal cut 1.5 mm ventrally (Figure 2.5.1). Hypothalamic cells were dissociated using the Worthington papain dissociation kit following the protocol for RNA extraction from sorted neuronal subtypes "Trehalose-enhanced isolation of neuronal subtypes from adult mouse brain" (Saxena et al., 2012). To get rid of any cell clumps the samples were additionally filtered through a sterile nylon-mesh filter with a 70 µm pore size (Falcon™ Cell Strainers, fisher scientific or CellTrics®, Sysmex).

2.6 Fluorescent *in situ* hybridisation (FISH)

2.6.1 Subcloning of *mouse prepro-orexin* (*mPPO*), *orexin 1 receptor* (*mOX$_1$R*) and *orexin 2 receptor* (*mOX$_2$R*) for RNA probe production

To produce RNA probes in anti-sense to *mPPO*-, *mOX$_1$R- and mOX$_2$R*-RNA the distinctive sequences had to be cloned into the pCR®4-TOPO®-vector (TOPO® TA Cloning® Kit for Sequencing, Invitrogen™) containing the required T7 and T3 promoter for the employed *in vitro* transcription kit (MAXIscript®T7/T3, Ambion). First the gene of interest (GOI) was multiplied by PCR (Platinum® *Taq* DNA Polymerase High Fidelity, Invitrogen™) using 50 ng of existing vectors that hold the specific DNA sequence as a template in a T-Gradient Thermocycler (Biometra). The PCR products were applied to a 1.5 % agarose (CarlRoth®) gel (Table 2.3.2) to confirm the right DNA-fragment size by gel electrophoresis (SubCell® GT Bio-Rad). The gels were transferred to a gel documentation chamber with UV table (Phase) where they were processed for gel purification and documented.

The proper band was then cleaved from the gel and purified (NucleoSpin® Gel and PCR clean up, Macherey-Nagel). As the resulting DNA-fragment has a sticky 3`-End though blunt ends are needed for pCR®4-TOPO®-vector ligation, the end was filled by adding 2 µl of a polymerase solution (5 µl 10x Buffer, 2.5 µl dNTP Mix, 2 µl $MgSo_4$, from the Cloned AMV First-Strand cDNA Synthesis Kit, Invitrogen™ and 1 µl DyNAzyme II DNA-Polymerase, Thermo Scientific™) to the gel purification product and incubated for 30 min at 72°C. Subsequently the respective DNA-fragment was ligated to the pCR®4-TOPO®-vector (TOPO® TA Cloning® Kit for Sequencing, Invitrogen™).

2.6.2 Transformation

To amplify the cloned plasmid, 1 µl of the TOPO® Cloning reaction was added to a vial of One Shot® Top10 Electrocomp™ *E. coli* cells (Invitrogen™) and transferred to a chilled electroporation cuvette on ice. The cell-plasmid suspension was electroporated at 1800 V in the Eppendorf® Electroporator 2510. Afterwards 250 µl of room temperature S.O.C. medium (Invitrogen™) were immediately added and the whole solution brought to a 1.5 ml Eppendorf Tube®, that was then incubated in a heating block shaking at 200 rpm at 37°C for 1 h. After 1 h the antibiotic resistance gene, incorporated in the distinctive DNA – fragments, was expressed and 20 µl or 50 µl of the transformation were spread on a prewarmed LB agarose plate containing the relevant antibiotic. The plates were incubated at 37°C, overnight. Only colonies from cells containing the plasmid with the antibiotic resistance gene could grow on the plates and selected to grow further in LB medium (Invitrogen™) with ampicillin shaking at 37°C, overnight.

2.6.3 Plasmid DNA purification

Cultivated cells were harvested in autoclaved 2 ml Eppendorf Tubes® at 11 000 g for 30 s and plasmids purified from the pellet using the NucleoSpin® kit Plasmid QuickPure kit (Macherey-Nagel™) according to the protocol provided within the kit. DNA concentration determination of the product was performed via spectrophotometer (NanoDrop 2000, Thermo Scientific™). The purified plasmids were tested for the GOI by restriction digest benefiting from gene and vector specific restriction sides. Choosing one restriction side on the vector sequence and one laterally on the GOI sequence provides not only the possibility to determine if the gene was properly ligated to the vector, but also the configuration of the gene sequence within the vector. After digestion, the fragments of the sample were separated by size via 1.5 % agarose gel (Table 2.3.2) electrophoresis. When the sample showed fragments of the proper size the corresponding *E. coli* colony was further cultivated for Plasmid DNA purification (NucleoBond® Xtra Midi/Maxi kit, Macherey-Nagel™) following the Midi Plus protocol provided within the kit. Final concentrations were again determined via spectrophotometer (NanoDrop 2000, Thermo Scientific™).

2.6.4 Linearisation

The plasmids were digested with the restriction enzymes *SpeI* or *NotI* (New England BioLabs® *Inc*.) and incubated at 37°C for 2 h (Figure 2.6.1 A). After the incubation the restriction was confirmed via gel electrophoresis. A phenol-chloroform precipitation was performed to separate the DNA from proteins such as the restriction enzymes. Therefore, the samples were mixed with an equal amount of phenol-chloroform and centrifuged for one minute at 14 000 rpm the lower organic phase containing the proteins was discarded, while the upper aqueous phase containing the DNA was further processed. Because phenol denatures proteins and might influence further experiments employing the DNA samples, possible phenol contamination was removed by chloroform precipitation. This time an equal amount of chloroform (CarlRoth®) was added to the samples and again centrifuged for 1 min at 14 000 rpm. The DNA was precipitated from the upper aqueous phase by adding sodium acetate (1/10 of the sample volume) and 100 % ethanol (2.5 times the sample volume), incubation at -20°C for 1 h followed by 15 min centrifugation at 4°C and 14 000 rpm. The pellet was washed with 70 % ethanol, then resuspended in DEPC water and stored at -20°C until further use.

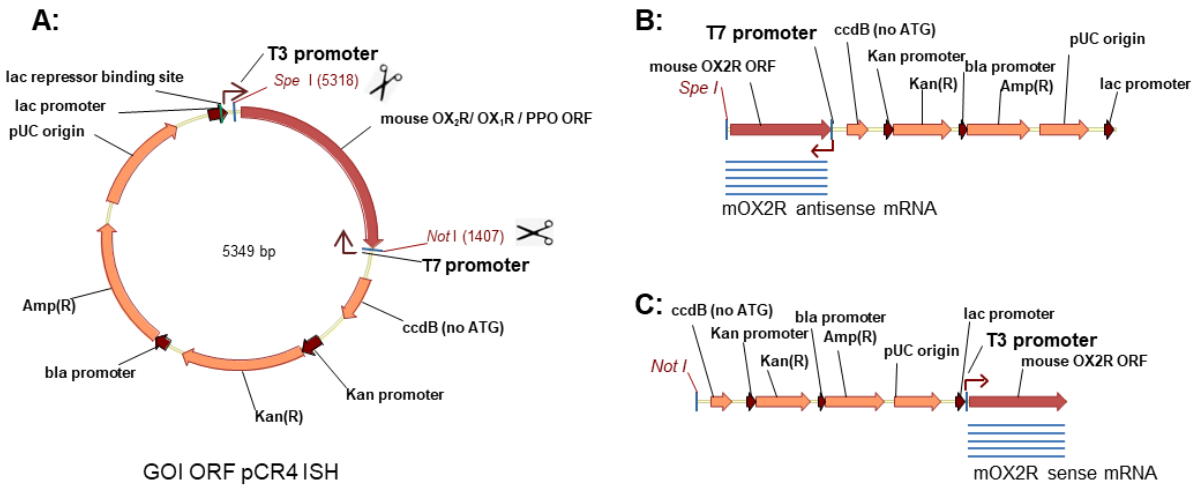

Figure 2.6.1.: Overview of FISH probe production. First the pCR4 vector containing the GOI (mPPO, mOX_1R or mOX_2R) was linearised by digestion with either *SpeI* or *NotI* restriction enzyme (**A**). The linearised plasmid served as template to transcribe the plasmid DNA into RNA probes in antisense configuration to the GOI after digestion with *SpeI* using the T7 promoter (**B**) or in sense configuration to the GOI after *NotI* digestion using the T3 promoter (**C**).

2.6.5 *In vitro* transcription

The previously linearised plasmid DNA was used as a template to synthesise RNA probes complementary to the GOI via *in vitro* transcription following the protocol provided with the MAXIscript®T7/T3 Transcription Kit (Ambion). When the GOI sequence had the sense configuration in the plasmid, T3 promoter was applied to produce sense RNA probes for negative control (Figure 2.6.1 C) and T7 promoter to produce antisense RNA probes to detect mRNA in brain sections via *in situ* hybridisation (Figure 2.6.1 B) and vice versa if the plasmid contained the GOI in antisense configuration. After *in vitro* transcription the RNA was extracted by ethanol precipitation adding 1/6 of the sample volume ammonium acetate (Sigma-Aldrich®) and 3 times the sample volume 100 % ethanol and incubation for 1 h at -20°C followed by 20 min of centrifugation at 13 200 rpm and 4°C. The ammonium acetate increases the efficiency of the extraction by lowering the pH to a slightly acidic value and, in contrast to for example sodium acetate, prevents precipitation of oligonucleotides and free dNTPs. The RNA pellet was washed with 70 % ethanol and resuspended in DEPC water. The precipitation was performed twice to assure the purity of the RNA probes. RNA probes were stored at -80°C for a maximum of one year.

2.6.6 Orexin receptor probe hydrolysis

To shorten the orexin receptor RNA-probes for better access and binding to the membrane bound receptors, they were hydrolyzed. To calculate the time of hydrolysis (t), difference between the initial length of the probe in kb (L_0) and the final length in kb (L_f) was divided by the product of the cuts per kb per minute, the L_0 and the L_f, following the formula: $t = (L_0 - L_f)/(k\ L_0\ L_f)$. The probe was mixed with five times the volume of carbonate buffer (Table 2.6.1) and incubated at 60°C for the calculated time.

Table 2.6.1.: Carbonate buffer

Substance	Volume in µl
Na_2CO_3 (1 M)	60
DTT (0.5 M)	10
Dep-DI	430

The reaction was neutralised by adding 1/10 volume of acetic acid and precipitated over night at -70°C after adding 1/10 volume 3 M Sodium acetate and 2.5 volumes of cold 100 % EtOH. The following day the pellet was washed with 70 % EtOH and centrifugation at 14 000 rpm for 20 min at 4°C. The supernatant was removed and after drying the pellet resuspended in 50 µl Dep-DI and 0.5 µl Superase Rnase inhibitor. The RNA concentration was determined via spectrophotometer (NanoDrop 2000, Thermo Scientific™).

2.6.7 Free floating fluorescent *in situ* hybridisation with RNA probes (FISH)

Brain sections, previously prepared as described in 2.5.3*,* were post fixed in 4 % PFA in PBS for 10 min and washed with PBS followed by 30 min of incubation in PBS with 0.1 % active DEPC. DEPC inactivates ribonucleases to prevent degeneration of RNA probes used for *in situ* hybridisation (ISH). Subsequently endogenous peroxidases of brain sections were quenched via incubation in 5 % H_2O_2 in PBS for 30 min. The hybridisation was performed in hybridisation mix, containing 0.8 % ribomix (yeast tRNA (Invitrogen™) and single stranded salmon testes DNA (Sigma-Aldrich®), 1:1 for 10 min at 70°C and then on ice), 500 ng / ml RNA probe, 0.6 % DEPC water, 0.2 % 10 % SDS (Sigma-Aldrich®) and 90 % hybridisation buffer, prepared as shown in Table 2.6.2, at 54°C overnight.

Table 2.6.2.: Hybridisation buffer

Substance	Volume in µl
Formamid	2500
Dextransulfat (50 %)	1000
DEPC-H_2O	490
NaCl (5 M)	300
50x Denhardt's	100
Tris (1 M, pH 7.5)	100
EDTA (0.5 M)	10

The next day brain section were washed with 4x saline-sodium citrate (SSC) buffer (Invitrogen™) and incubated for 30 min in RNase A in NTE-Buffer followed by other washing steps with 1x SSC and 0.1x SSC for 5 min each. Subsequently brain sections were

incubated for 30 min in 0.1x SSC at 54°C and washed again with 0.1x SSC at RT. Blocking was performed with TNB buffer for 30 min at RT. DIG-labelled hybridised RNA probes were stained with 1:50 Anti-Digoxigenin-POD Fab-fragment from sheep (Roche Life Science™) in TNB buffer by incubating the slices for 2 h at RT. Afterwards brain slices were washed three times 5 min in TNT buffer. The hybridisation signal was amplified via the tyrosine signal amplification (TSA™ Plus Cyanine 5 System, PerkinElmer™) by incubating the brain slices in a 1:100 dilution of Cy5 in amplification diluent for 10 min at RT. In the following step 4',6-diamidino-2-phenylindole (DAPI) staining was performed for 15 min in a 1:1000 dilution in TNT buffer, which was succeeded by two final washing steps for 5 min each in TNT buffer. The ready stained brain slices were mounted on object slides with Dako Fluorescent Mounting Medium (DakoNorthAmerica, *Inc*.).

2.6.8 Free floating fluorescence *In situ* hybridisation with oligonucleotide probes (FISH)

For ISH with oligonucleotide probes, 100 pmol oligonucleotides (Gibco) were diluted to 10 µl with DEPC water and DIG labelled (DIG Oligonucleotide Tailing Kit, Roche Life Science™) following the provided protocol. Brain sections were post fixed for 10 min in 4 % PFA in 1x PBS, washed two times in 1x PBS for 1 min each and incubated at 42°C, overnight in hybridisation mix, containing 10 µl oligonucleotide probe in 60 µl ribomix (Table 2.6.3) per ml hybridisation buffer (Table 2.6.2).

Table 2.6.3.: Ribomix

Substance	Volume in µl
Yeast tRNA	40
Salmon testes DNA	36.4

The following day stringent washing steps were performed on the brain sections starting with 1 min in 1x SSC at RT, followed by 30 min 1x SSC at 55°C, 1 min 1x SSC at RT and 1 min 0.5x SSC at RT. DIG-labelled hybridised oligo probes were stained with anti-DIG POD fragment and TSA-Amplification as described in “2.6.7.: Free float fluorescent In situ hybridisation with RNA probes (FISH)”.

2.6.9 Detection of hybridisation and analysis of possible co-localisation of LepR and GOI

As soon as the mounting medium was dried brain sections were analysed via fluorescent and confocal microscopy (Leica TCS SP5, Leica Microsystems™). The green fluorescent protein ZsGreen was excited at 488 nm with the Argon laser set to 40 %, the Cy5 labelled probes were excited at 633 nm (Figure 2.6.2) with the HeNe633 laser set to 45 % and DAPI, which ranges in the UV spectrum was excited with the 405 Diode laser set to 6 %.

Pictures were taken at 200 Hz, the resolution of 1024 x 1024 pixels, a line average of 2 and a frame average of 4 scans. Smart gain settings were set according to. Overviews of whole sections were stitched from single pictures taken at a fluorescent microscope (DMI 6000B, Leica Microsystems™) using the software Leica Application Suite Advanced Fluorescence (Version 2.5.0.6735).

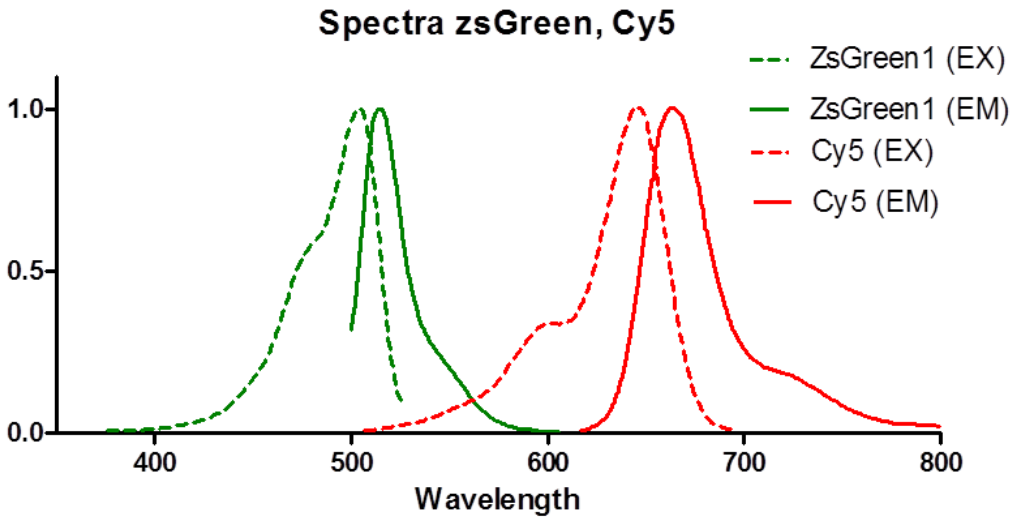

Figure 2.6.2.: Excitation and emission spectra of the fluorescent proteins ZsGreen and Cy5. Excitation spectra are shown in dashed lines and emission spectra in continuous lines in the colour of the respective fluorescence of the Protein (ZsGreen = green lines and Cy5 = red lines) in nm of the wavelength.

The single pictures, taken in a 10-fold magnification, were merged from three channels with the filter cubes A4 for UV, L5 for ZsGreen or Y5 for Cy5 (all Leica Microsystems™).

Table 2.6.4.: *Settings of gain used in different magnifications at the confocal microscope to analyse FISH*

Magnification	Dapi	ZsGreen	Cy5
2.5 x	1050	1050	800
10 x	830	870	490
20 x	710	770	460
63 x	820	690	600

2.6.10 Co-localisation analysis

After hybridisation, the brain sections were analysed using the JACoP (**J**ust **A**nother **Co**-localisation **P**lugin) plugin for ImageJ software. The images of 20-fold magnification were split back into their separate colour channels (red, green, blue) and the software analysed pixels in each channel of the images for their fluorescent intensity to calculate the correlation in form of the Pearson's Coefficient (Manders et al., 1992) and the Manders split coefficient, allocating the amount of co-localizing pixel fluorescence intensity in one channel when expressing fluorescence above threshold in the other colour channels (Manders et al., 1993). Whenever pixel based analysis came out positive, the sections were re-analysed on an object based method using JACoP. The number of labelled objects (=cells) were counted and objects labelled positive for co-localisation visually monitored.

2.7 Fura-2-Acetoxymethyl ester (Fura-2AM) Calcium Measurements

To investigate calcium influx caused by orexin A or orexin B treatment in mHypoE N41, mHypoE N41 OX_1R and mHypoE N41 OX_2R, the cells were seeded in a l-ornithin coated 96 Well Cell Culture Microplate, µClear® (Greiner Bio.One International). Cell culture medium was discarded and each well was incubated in 100 µl of a 2 µM Fura-2AM-solution (Table 2.7.1), containing the cell permeant Fura-2AM (Molecular Probes™), sterile filtered physiological buffer (Table 2.7.2) with a pH of 7.4, probenecid (life technologies™) and pluronic F127 (life technologies™) for 30 min at 37°C.

Table 2.7.1.: Fura-2AM-Solution

Substance	Volume in µl
Fura-2AM	2
Physiological Buffer	998
Probenecid	10
Pluronic F127 (20%)	1

Acetoxymethyl (AM) ester transports the Fura-2AM complexes through the cell membrane into the cell body, where it is digested by esterase, which leads to the release of Fura-2 into the cytoplasm. Fura-2 is a fluorochrome that builds a chelate complex with free Ca^{2+} ions. With increased calcium concentration in the cells more chelate complexes are build and the wavelength of the Fura-2 excitation maximum shifts from 340 to 380 nm, while the emission maximum stays at 510 nm. After incubation, the cells were washed twice with 50 µl/well assay buffer (probenecid 1:100 in physiological buffer) and again incubated for 30 min at 37°C, this time in assay buffer.

Table 2.7.2.: Physiological buffer in a total volume of 50 ml sterile H_2O, pH 7.4

Substance	Amount
NaCl	410 mg
KCl	18.64 mg
$CaCl_2$ (50nM)	500 µl
Glucose	99.08 mg
HEPES	275 µl

Finally, the cells were treated with 0.1 or 1.0 µM of orexin A or orexin B or 1x PBS as control and the fluorescence intensity of the samples measured over 15 s before and 60 s after treatment, in a CLARIOstar® High Performance Microplate Reader (BMG Labtech). Samples were excited at 340 nm and 380 nm and emission measured at 510 nm. The

amount of intracellular calcium is determined by the ratio of the emissions of the two excitation wavelengths.

2.8 Dual-Luciferase® Reporter Assay

2.8.1 Transfection

Dual-Luciferase® Reporter Assay experiments were performed in the Department of Veterinary Biosciences, Veterinary Biochemistry and Cell Biology at the Faculty of Veterinary Medicine of the University of Helsinki under the supervision of Jyrki Kukkonen. The cell lines mHypoE N41 OX_1R and mHypoE N41 OX_2R were seeded in a 96 well plate and at 80 % confluency co-transfected with pSG-Gal4-Elk-1 containing the transcription factor *elk-1* as reporter gene and Gal4 DNA-binding side, pGL3G5E4Δ38 containing the Gal4 binding site and therefore controlling the expression of firefly luciferase, pRL-TK (Promega) constitutively expressing renilla luciferase under the control of herpes simplex virus-thymidine kinas promoter (TK) and the empty vector pUC18 to keep an equal amount of DNA in all transfections (Jantti et al., 2013). A total amount of 0.1 µg plasmid DNA in 5 µl Optimem medium and 0.3 µl of the transfection reagent Lipofectamine® 2000 (Invitrogen™) in 5 µl Optimem medium in a volume of 100 µl culture medium per well was divided into 75 % pGL3 G5 E4Δ38 + 2 % pRL-TK + 23 % pUC18 (bright yellow in Table 2.8.1) for the control conditions or 0.9 % pSG-GalElk-1 + 75 % pGL3 G5 E4Δ38 + 2 % pRL-TK + 22.1 % pUC18 (dark yellow in Table 2.8.1) to test Elk-1 regulation as a result of treatment. 4 h after transfection the medium was changed to full culture medium with FCS and pen/strep for 60 min and then again to strep medium to starve the cells 12 h prior treatment.

2.8.2 Treatment

If treatment included the dual orexin receptor antagonist TCS 1102 (Tocris Bioscience) or the MAP kinase kinase, MEK-1 and MEK-2 inhibitor UO126 (Tocris Bioscience) or PD98059 (Tocris Bioscience), the cells were pre-treated 30 min with 10 µM of these substances before adding 1 µM orexin A/B or 100 % adipocyte primed medium.

Table 2.8.1.: Example treatment plan for Elk-1 Dual-Luciferase® Reporter Assay

	1	2	3	4	5	6	7	8	9	10	11	12
A	ctrl	ctrl	ctrl									
B	ctrl	OA 1 nM	OA 10 nM	OA 100 nM	OA 1 µM	OB 1 nM	OB 10 nM	OB 100 nM	OB 1 µM	Nag26 20µM	Nag26 50µM	Adip. Med
C	ctrl	OA 1 nM	OA 10 nM	OA 100 nM	OA 1 µM	OB 1 nM	OB 10 nM	OB 100 nM	OB 1 µM	Nag26 20µM	Nag26 50µM	Adip. Med
D	ctrl	OA 1 nM	OA 10 nM	OA 100 nM	OA 1 µM	OB 1 nM	OB 10 nM	OB 100 nM	OB 1 µM	Nag26 20µM	Nag26 50µM	Adip. Med
E												
F	U0126 10 µM	U0126 10 µM OA 1 µM	U0126 10 µM OB 1 µM	U0126 10 µM Adip. Med,					TCS 10 µM	TCS 10 µM OA 1 µM	TCS 10 µM OB 1 µM	TCS 10 µM Adip. Med.
G	U0126 10 µM	U0126 10 µM OA 1 µM	U0126 10 µM OB 1 µM	U0126 10 µM Adip. Med.					TCS 10 µM	TCS 10 µM OA 1 µM	TCS 10 µM OB 1 µM	TCS 10 µM Adip. Med.
H	U0126 10 µM	U0126 10 µM OA 1 µM	U0126 10 µM OB 1 µM	U0126 10 µM Adip. Med.					TCS 10 µM	TCS 10 µM OA 1 µM	TCS 10 µM OB 1 µM	TCS 10 µM Adip. Med.

shows an overview of all substances and concentrations tested. The cells were treated in triplicates and for 5 h to ensure the expression of firefly luciferase resulting from Elk-1 activation.

2.8.3 Dual-Luciferase® Reporter Assay

The Dual-Luciferase® Reporter Assay System (Promega) detecting firefly (*Photinus pyralis*) luciferase activity from the reporter gene and Renilla (*Renilla reniformis*) luciferase activity as an internal control sequentially within the same sample. Measurements were performed as described in Jantti et al., 2013.

2.9 Fluorescent activated cell sorting (FACS)

2.9.1 Cell sorting

The dissociated cells (described in 2.5.4) were sorted at the Cell Analysis Core (CAnaCore) facility in the Institut für Systemische Entzündungsforschung (ISEF) of the University Lübeck, using a MoFlo Legacy Cell Sorter (BeckmanCoulter). For detection of the green fluorescent protein ZsGreen, which is expressed in all cells containing the LepR, the Lyt 200 S Solid State Laser System was applied exciting the protein at its optimal excitation wavelength at 488 nm (Figure 2.9.1 C).

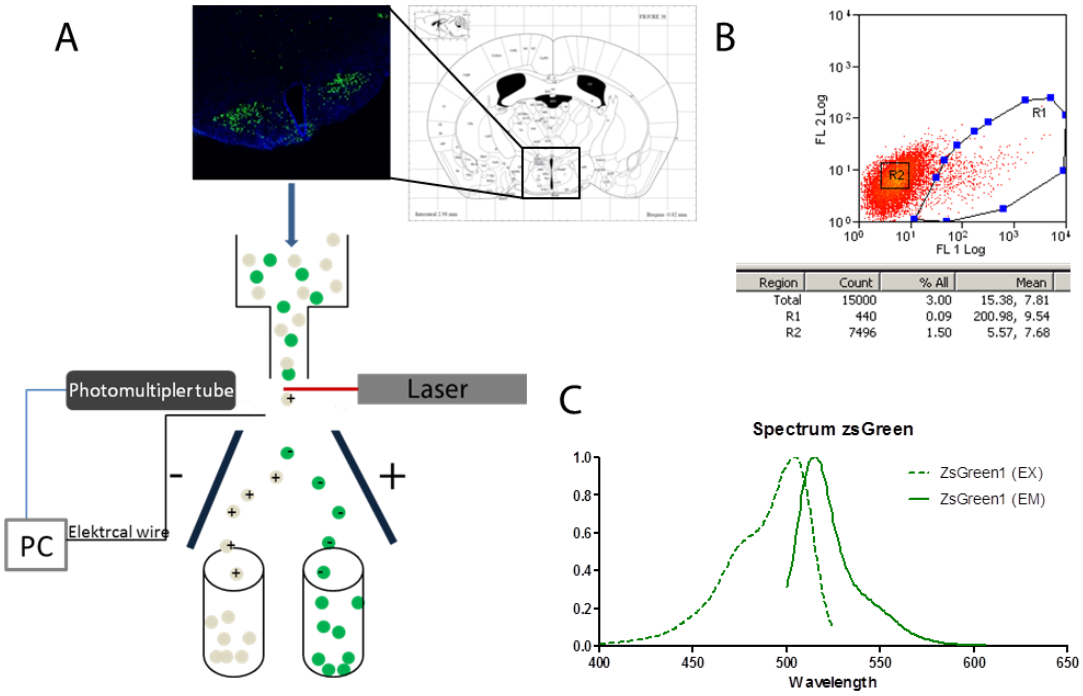

Figure 2.9.1.: Simplified overview of fluorescent activated cell sorting. Cells are detected by their fluorescent and contrariously polarised. An electrical field produced by two electromagnets sorts the now differently charged cells into another vial than the rest and non-fluorescent cells (**A**). A forward scatter side scatter scattergram helps to determine healthy fluorescent (R1) and non-fluorescent (R2) cells. Therefore, the forward scatter (cell size) is plotted against the side scatter (fluorescence) (**B**). The spectrum of ZsGreen shows the fluorescent protein is best excited at a wavelength of 488 nm (**C**).

A scattergram plotting the forward scatter, that detects the size of healthy/dead cells against the side scatter, which detects fluorescents helps to choose the thresholds to recognise healthy green fluorescent (R1) or non-fluorescent (R2) cells (Figure 2.9.1 B).

The cell suspension must pass through a nozzle with the diameter of 100 µm so that every single cell is detected by the laser. If the photomultiplier gives the signal for fluorescence to a PC, this cell is contrariously polarised. When the cells pass through an electrical field, which is created by two electromagnets, they are sorted according to their polarisation and thereby sorted into fluorescent and non-fluorescent samples (Figure 2.9.1 A).

2.9.2 Microscopic verification of sorting outcome

The sorting outcome was determined by fluorescent microscopy. The sorted samples were centrifuged at 100 g for 10 min and the pellet was resuspended in 20 µl of medium. Two µl of the cell suspension were stained with DAPI (1:2000) and mounted on a slide. The cover glass was distanced from the slide by lying on another cover glass on each side. This way the cells were protected from being crushed. Pictures were taken at the fluorescent microscope (DMI 6000B, Leica Microsystems^{TM}) with three channels using the A4 filter cube in the UV range for detection of DAPI, the Y5 filter cube to detect ZsGreen fluorescence and using the bright field to show the morphology of the cells.

2.10 Statistics

Statistical analyses were performed with the GraphPad Software version 5 or 7. When cells were treated with 2 factors, the 2-way-ANOVA determined, if either factor had significant effects and if this effect was isolated from or influenced by the other factor. Significant effects with a p value under 0.05 ($p<0.05$) or even 0.001 ($p<0.001$) were marked with * or *** respectively in the corresponding figures. Experiments that were not independently repeated at least three times were not statistically investigated. Possible outliers were identified with the help of the Grubb`s test at the GraphPad Software-website (https://graphpad.com/quickcalcs/Grubbs1.cfm) and excluded from the analysis.

3 Results

3.1 Mapping of ZsGreen expression in LepRb-ZsGreen *mice*

Cryotome sections from LepRb-ZsGreen mice were analysed by fluorescent microscopy at 20-fold magnification and pictures were stitched to an overview of whole coronal slices. The fluorescent protein ZsGreen is very strong and the emission is detectable already at very low excitation power levels. To analyse the specificity of ZsGreen expression cells, that are or have been LepRb positive, ZsGreen expression pattern (Figure 3.1.1) was mapped for comparison to previously described areas and densities of rat *LepRb* mRNA and mouse LepRb-GFP distribution and prevalence of leptin-sensitive neurons in the adult and postnatal mouse brain (Juel K. Elmquist, 1998; Scott et al., 2009; Caron et al., 2010). Highest expression of ZsGreen was found in neurons of the granular layer of the dentate gyrus, the CA3 field of the Ammon's horn, the retrosplenial granular cortex and cells of the choroid plexus (Figure 3.1.1 A.-D.). Within the hypothalamus, the arcuate nucleus and the dorsomedial hypothalamic nucleus showed a similarly high ZsGreen expression (Figure 3.1.1 D.). The density of ZsGreen expressing cells in the external capsule (Figure 3.1.1 A.-D.), the posterior hypothalamic nucleus, the lateral hypothalamic area and the ventromedial hypothalamus (Figure 3.1.1 C.) as well as the medial amygdaloid nucleus (Figure 3.1.1 D.) was slightly lower than in the highest expressing areas but still explicit. A moderate amount of ZsGreen expression was found in the nucleus of reuniens, the suprachiasmatic nucleus (Figure 3.1.1 B.), the mediodorsal thalamic nucleus (Figure 3.1.1 C.) and the median eminence (Figure 3.1.1 D.), whereas the density of ZsGreen expression in the paraventricular nucleus was rather low.

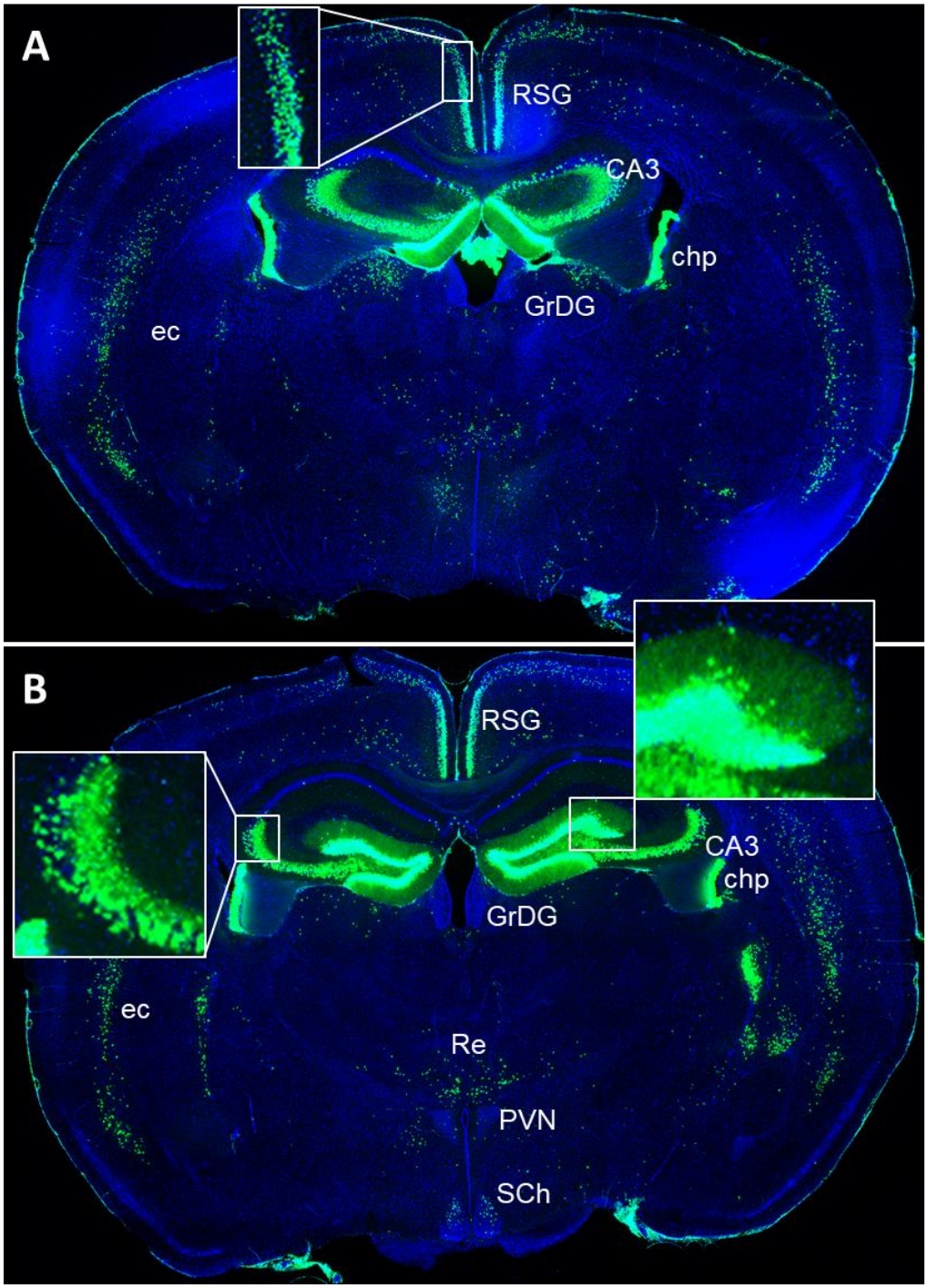

Figure 3.1.1.: Overview of LepRb-ZsGreen *mice* brain sections showing ZsGreen expression cells. RSG (retrosplenial granular cortex), CA3 (CA3 field of the Ammon's horn), chp (choroid plexus), GrDG (granular layer of the dentate gyrus), ec (external capsule), Re (nucleus of reuniens), PVN (paraventricular nucleus), SCh (suprachiasmatic nucleus), MD (mediodorsal thalamic nucleus), PH (posterior hypothalamic nucleus), DM (dorsomedial hypothalamic nucleus), LH (lateral hypothalamic area), VMH (ventromedial hypothalamic area), Arc (arcuate hypothalamic nucleus), MePV (medial amygdaloid nucleus, posteroventral part), ME (median eminence)

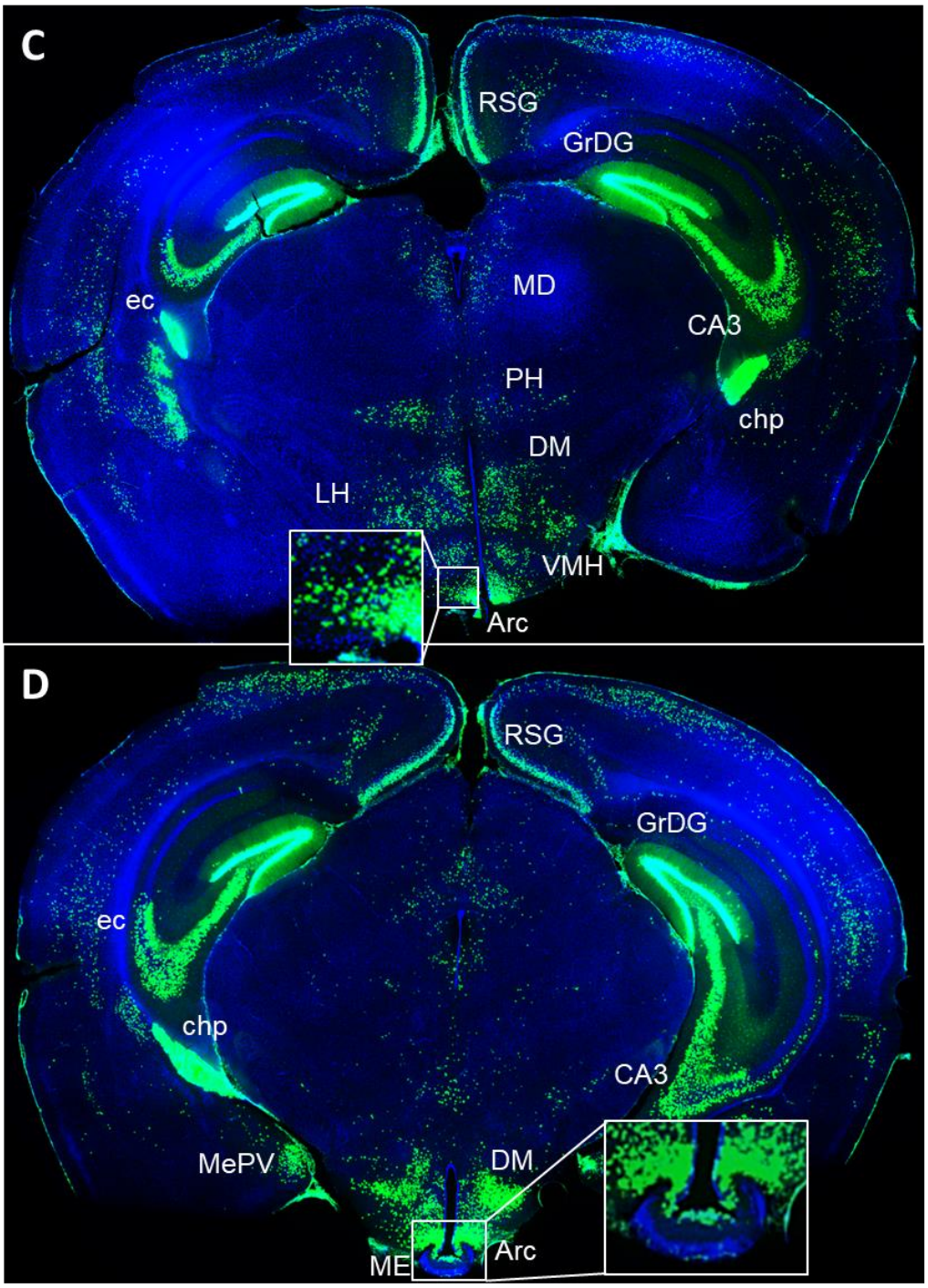

Figure 3.1.1 (continued from previous page)

Occasionally, some LepRb-ZsGreen mice showed ectopic expression of ZsGreen throughout the whole brain and body. These mice could be distinguished by their yellow ears, tale and paws and cloudy eyes. Mice showing this phenotype were eliminated from the colony and not used for further experiments or breeding.

3.2 Mapping of *prepro-orexin* mRNA expression in LepRb-ZsGreen *mice*

To investigate the presence of LepRb in orexin neurons a co-localisation study of ZsGreen and *prepro-orexin* mRNA was performed in brain sections of LepRb-ZsGreen mice. LepRb positive cells are labelled by expressing ZsGreen, orexin neurons were labelled via fluorescent *in situ* hybridisation (FISH) with RNA probes in antisense orientation of mouse *prepro-orexin* (*PPO*) RNA.

For *in vitro* transcription of sense and anti-sense RNA probes, a mouse *PPO* cDNA was cloned into the pCR4 vector (Figure 3.2.1) After PCR amplification of mouse *PPO*, gel electrophoresis of samples with 50°C and 55°C showed a product of the expected size of 406 bp (Figure 3.2.1 A.). This product was purified and cloned into the pCR4 vector (Figure 3.2.1 B.).

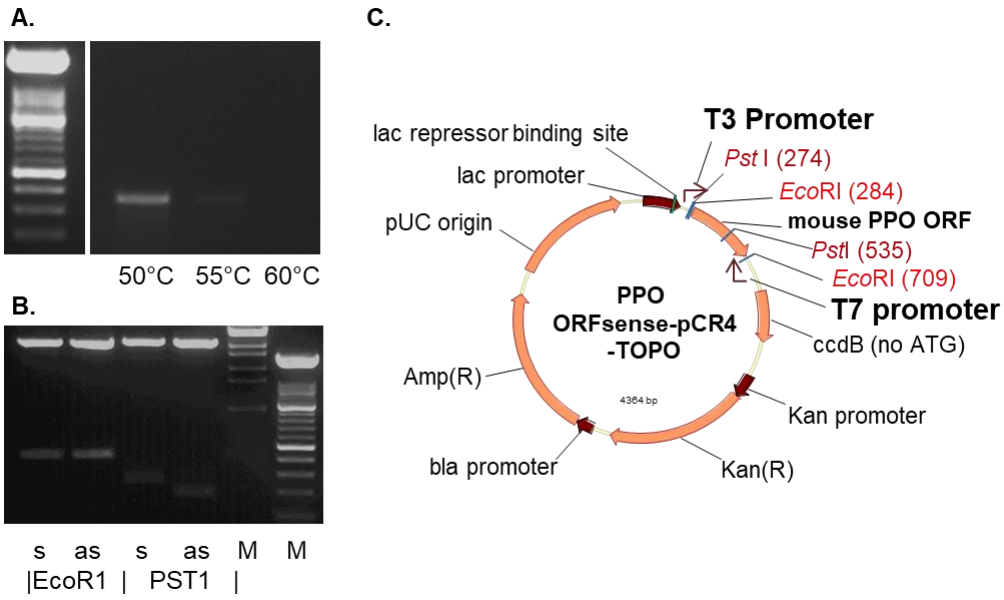

Figure 3.2.1.: Cloning of mouse *PPO* for *in vitro* transcription of FISH RNA probes. Mouse *PPO* sequence was amplified by PCR using different annealing temperatures (**A**) and the product was cloned into the pCR4-TOPO vector (**B**). A test restriction with *EcoR*I gave information about the cloning success and with *Pst*I about gene orientation within the plasmid (**C**).

The resulting plasmid was digested with the restriction enzymes *EcoR*I and *Pst*I, which have their restriction sides at bp position 284 and 709 (*EcoR*I), that are flanking the *PPO* sequence and 274 and 535 (*Pst*I), upstream of the *PPO* sequence and on the sequence, itself. Only a plasmid containing the *PPO* sequence shows two bands after *EcoR*I digestion,

which cleaves the plasmid into 3939 bp and 425 bp fragments. Digestion with *Pst*I cuts unsymmetrically within the inserted *PPO* DNA leading to fragment sizes of either 4103 and 261 bp if the gene was inserted into the vector in sense orientation or 4172 and 192 bp if it was inserted in anti-sense orientation when transcribed from the promoter specific for the bacteriophage T3 RNA polymerases (Figure 3.2.1 C.). The plasmid containing the *PPO* sequence in sense orientation from T3 was used for probe production by *in vitro* transcription.

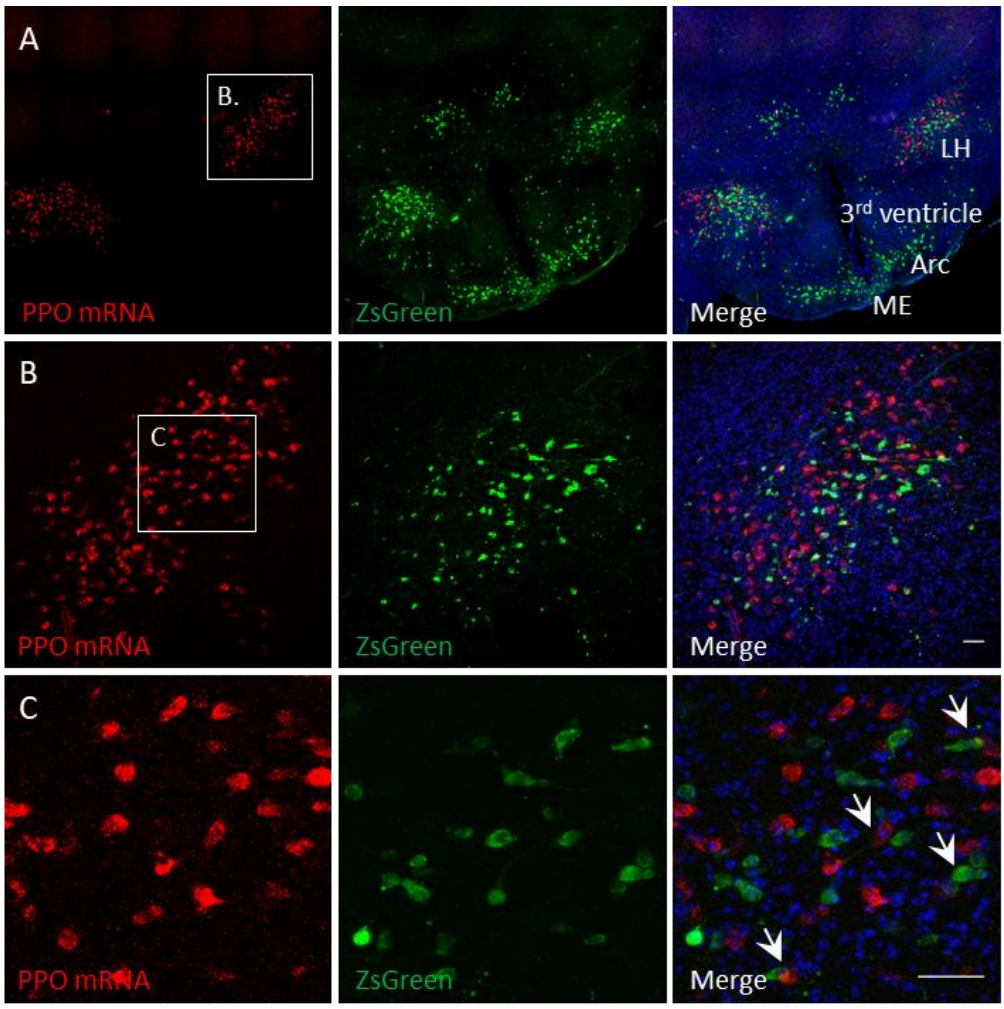

Figure 3.2.2.: *PPO* FISH in LepRb-ZsGreen mice brain sections. Hybridised RNA-probes in *PPO* antisense orientation are labelled with Cy5 (Red) and LepRb expressing cells with ZsGreen (green). Both Channels were merged to each other and DAPI (blue) to investigate possible co-localisations in (**A.**) a stitched overview of the hypothalamic area, with the lateral hypothalamus (LH), 3rd ventricle, arcuate nucleus (Arc) and median eminence (ME) labelled (**B.**) a 20-fold and (**C.**) 63-fold magnification. Arrows pointing at PPO labelled cells proximate to ZsGreen and bars indicate 50 µm.

The overview of the hypothalamic area after FISH with Cy5 (red) labelled hybridised *PPO* anti-sense RNA probes showed a distinct population of neurons in the LH with red fluorescence besides cells expressing ZsGreen (green) (Figure 3.2.2. A.). At higher magnification Cy5 fluorescence was clearly limited to the cytoplasm surrounding the cellular nucleus (Figure 3.2.2 C.). ZsGreen positive cells were also found in other areas like the arcuate nucleus.

At 20-fold magnification no cells were found showing co-localisation of Cy5 and ZsGreen expression, but *PPO* mRNA and ZsGreen were found in cells with very close proximity to each other (Figure 3.2.2 B.). These results were confirmed in a closer analysis at 63-fold magnification (Figure 3.2.2 C.) showing no co-localisation of ZsGreen and Cy5 but expression of the two in proximate cells (arrow).

The same procedure was performed using probes in sense orientation to *PPO* RNA as negative control for *PPO* FISH and conformation for hybridisation specificity. When the probe had *PPO* sense orientation no distinct Cy5 labelled cells were detected via fluorescent microscopy, but the brain sections exhibited relatively high background, as shown in the slice overview (Figure 3.2.3).

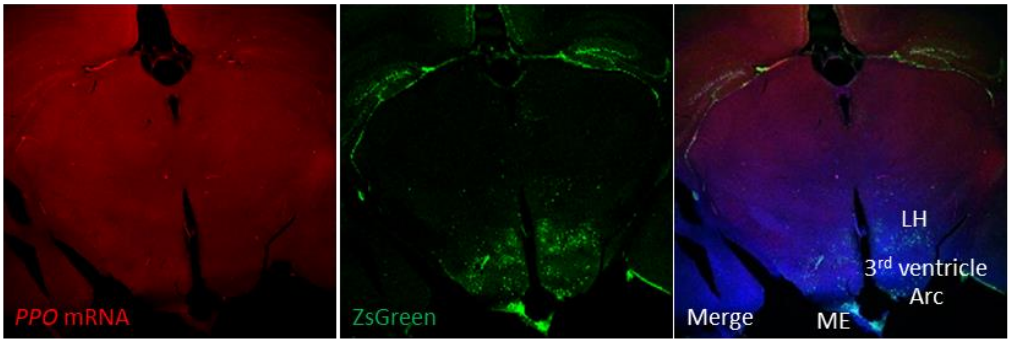

Figure 3.2.3.: Negative control for *PPO* FISH. FISH procedure in LepRb-ZsGreen mice brain section using labelled *PPO* RNA-probes in sense orientation served as negative control for the specificity of *PPO* FISH.

The visual analysis of Cy5 and ZsGreen co-localisation was completed by image analysis using the software ImageJ with the plugin JACoP (Just Another Co-Localisation Plugin). The different channels of confocal microscopy images in 20-fold magnification were analysed after setting a threshold for background subtraction. The program analysed red (A) and green (B) pixiels, and calculated the Pearson's correlation coefficient (Figure 3.2.4 B.), which indicates the intensity and direction of linear correlation between the red and

green fluorescence (Manders et al., 1992) as well as Manders split coefficients M1 and M2, values indicating the amount of co-localizing pixel fluorescence in both colour channels (Manders et al., 1993) (Figure 3.2.4. A.).

A.

Pixel based

Pearson's Coefficient	0.16 ± 0.00
M1 (A overlapping B)	0.04 ± 0.00
M2 (B overlapping A)	0.05 ± 0.01

Object based

Cy5 cells colocalizing with zsGreen	4% ± 0.3%
ZsGreen cells colocalizing with Cy5	2% ± 0.4%
Cy5 cells/hypothalamus	1318 ± 249
ZsGreen cells/hypothalamus	2467 ± 406

B.

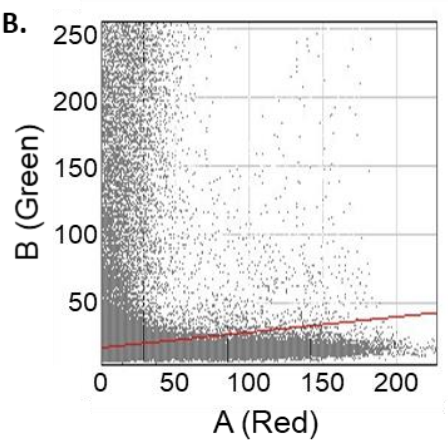

Figure 3.2.4: Pixel based co-localisation analysis of *PPO* and ZsGreen. (**A.**) Tabular results showing mean values obtained from serial sections of three whole hypothalami (mean ± SEM). Pearson's coefficient is a value for linear correlation of Cy5 and ZsGreen, M1 and M2 are Manders split coefficients, a measurement for the intensity of fluorescence in pixels in one colour channel that show fluorescence above threshold in the other colour channel, the percentage of Cy5 and ZsGreen cells found positive for co-localisation based on overlapping pixels and mean amount of Cy5 and ZsGreen labelled cells per hypothalamus. (**B.**) Exemplary cytofluorogram, blotting fluorescence of each pixel within a confocal image of one brain section, with ZsGreen on the y-axis against Cy5 on the x-axis. The red line indicates the linear correlation between Cy5 and ZsGreen with a Pearson's Coefficient close to 0, the value for no linear correlation.

The mean value of Pearson's Coefficient from three hypothalami of 0.16 ± 0.00 (mean ± SEM) as obtained by pixel-based cytofluorogram is close to 0, indicating a very low linear correlation between Cy5 and ZsGreen labelling (Figure 3.2.4 B.). The Pearson's Coefficient is also indicated by the red line in the cytofluorogram blotting fluorescent colour and its intensity for each pixel, with Cy5 on the x-, against ZsGreen on the y-axis (Figure 3.2.4 B.). Manders split coefficients (M1: Cy5 overlapping ZsGreen and M2: ZsGreen overlapping Cy5) "expressing the fraction of intensity in a channel that is located in pixels where there is above zero (or threshold) intensity in the other colour channel" (https://imagej.net/Colocalization_Analysis) using a value between 0 and 1, were with 0.04 ± 0.00 for M1 and 0.05 ± 0.01 for M2 also close to 0 (Manders et al., 1993).

Because pixel based JACoP analysis indicated a very low correlation of *PPO* mRNA and ZsGreen, the program was also used for object based analysis, that counts and identifies Cy5 and ZsGreen cells co-localising ZsGreen and Cy5 respectively, based on the distance between their geometrical centres.

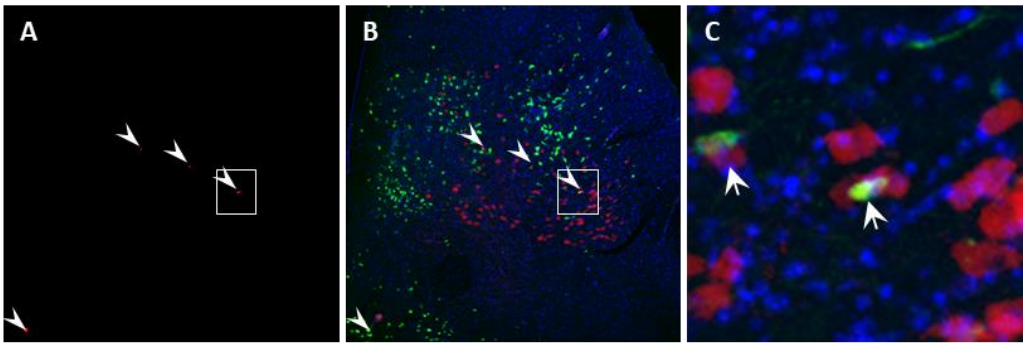

Figure 3.2.5.: Object based co-localisation analysis of *PPO* and ZsGreen. (**A**) The image of cells JACoP found positive for co-localisation of ZsGreen and Cy5 (arrowheads) was compared to (**B**) the original confocal image of *PPO* FISH and results visually re-investigated in (**C**) a higher magnification.

Objects-based analysis of Cy5 and ZsGreen co-localisation marked only few cells in a mask (arrowheads in Figure 3.2.5 A). Overall an average of 4 ± 0.3 % of 1318 ± 249 Cy5 labelled cells per brain section were also positive for ZsGreen and 2 ± 0.4 % of 2467 ± 406 ZsGreen labelled cells per brain section also show Cy5 fluorescence (Figure 3.2.4 A.). These cells were identified in the original confocal image (arrowheads in Figure 3.2.5 B) and re-inspected visually in a higher magnification (Figure 3.2.5 C). In all these cases the objects found positive for co-localisation by JACoP were two cells, each labelled by one of the fluorescent proteins, in very close proximity to each other (arrow in Figure 3.2.5 C) and therefore false positive results.

Proopiomelanocortin (POMC) neurons are known to express LepRb and therefore served as positive control for co-localisation of Cy5 and ZsGreen, to prove that both fluorescent proteins can co-localise and both signals can be detected by microscopy. FISH was conducted using *proopiomelanocortin* (*POMC)* anti-sense oligonucleotide probes labelled by tailing with DIG-UTP. Most Cy5 positive cells were found in the arcuate nucleus, a region for highest expression of LepRb and therefore ZsGreen in LepRb-ZsGreen mice (Figure 3.2.6 A). Confocal images at 63-fold magnification were visually evaluated for co-localisation of Cy5 and ZsGreen. Many Cy5 labelled cells were also positive for ZsGreen and a fraction of ZsGreen labelled cells also showed Cy5 fluorescence (Figure 3.2.6 B).

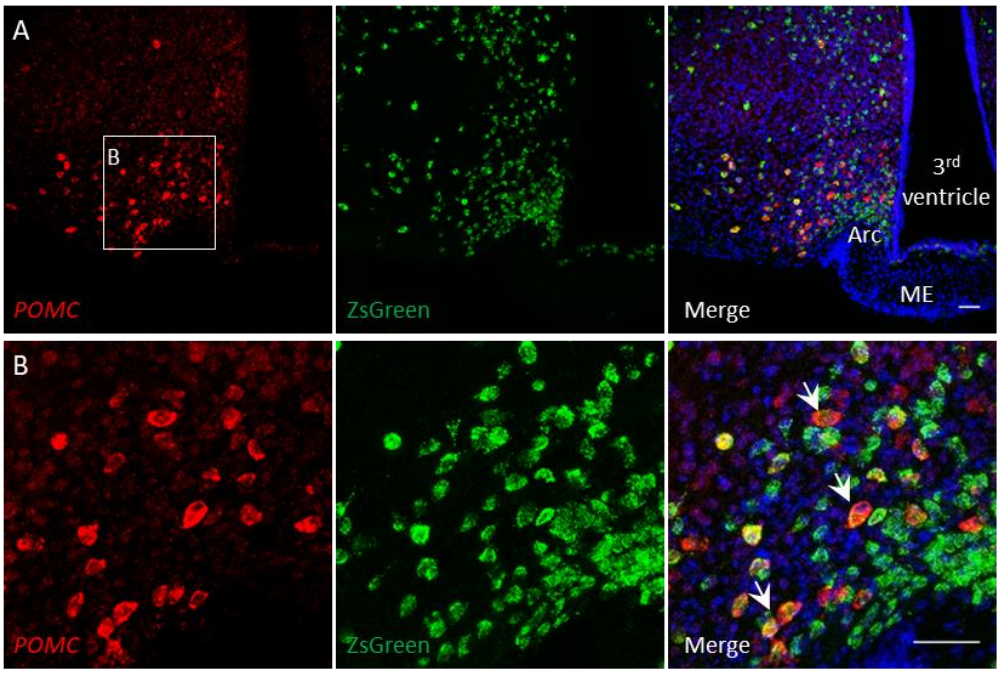

Figure 3.2.6.: Positive control for Cy5 and ZsGreen co-expression. FISH with labelled oligo anti-sense probes against *POMC* was employed as positive control for ZsGreen and Cy5 co-localisation. (**A**) In the 20-fold magnification Cy5 (red) labelled cells were mainly found in the arcuate nucleus (Arc), an area with highest density of ZsGreen expressing cells. (**B**) A closer look at 63-fold magnification reveals a part of the Cy5 labelled cells are also expressing ZsGreen and the other way around, some of them are indicated by arrows. Bars indicate 50 µm.

JaCop analysis of *POMC* FISH was performed for the arcuate nucleus of one animal to review if visually obtained results for co-localisation are reflected in data obtained by computational analysis. Pearson's Coefficient showed a mean value of 0.34 per analysed brain section, that is indicated as a red line in the cytofluorogram blotting ZsGreen fluorescence and its intensity on the y-axis against Cy5 fluorescence and its intensity on the x-axis, for each pixel (Figure 3.2.7 A. and B.). Mean Manders split coefficient per brain section was 0.27 for Cy5 overlapping ZsGreen and 0.18 for ZsGreen overlapping Cy5 pixels (Figure 3.2.7 A.).

A.

Pixel based

Pearson's Coefficient	0.34
M1 (A overlapping B)	0.27
M2 (B overlapping A)	0.18

Object based

Cy5 cells colocalizing with zsGreen	17 %
ZsGreen cells colocalizing with Cy5	10 %
Cy5 cells/hypothalamus	367
ZsGreen cells/hypothalamus	364

B.

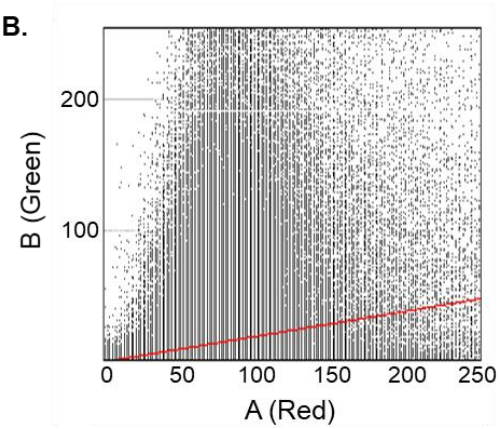

Figure 3.2.7.: JaCop Analysis of *POMC* control for *PPO* FISH. (**A.**) Tabular results show values from brain sections through the arcuate nucleus of one LepRb-ZsGreen mouse. Mean value per section for Pearson's coefficient showing linear correlation of Cy5 and ZsGreen, mean Manders split coefficients M1 and M2 per brain section are measuring the intensity of fluorescence in pixels in one colour channel that show fluorescence above threshold in the other colour channel, overall percentage of Cy5 and ZsGreen pixel found positive for co-localisation and total amount of Cy5 and ZsGreen labelled cells. (**B**.) The cytofluorogram blotting fluorescence of each pixel in the confocal image of one brain section, with ZsGreen on the y-axis against Cy5 on the x-axis. The red line indicates the linear correlation between Cy5 and ZsGreen.

Object based JaCop analysis, based on the distance between geometrical centres, revealed a similar amount of co-localising cells. Overall 17 % of the 367 Cy5 and 10 % of the 364 ZsGreen labelled cells were found to co-localise both fluorescent signals (Figure 3.2.7 A.). A small fraction of these cells was found to be false positive in visual screening of the results, but most cells were Cy5 labelled and expressed ZsGreen.

3.3 Orexin and leptin interaction at the same target cells

3.3.1 Immortalised embryonic hypothalamic cell lines mHypoE N41 and mHypoE N25/2 as *in vitro* model neurons

To serve as a model for interaction of leptin and orexin at the same target neuron, cells must express the $OX_{1/2}R$ and LepRb. The cell lines mHypoE N41 and mHypoE N25/2 were purchased from CELLutions Biosystems (Ontario, Canada), based on their description to express all three receptors, POMC and neuropeptide Y (NPY) (CellutionsBiosystemsInc., 2009). Before conducting further experiments with these cell lines, the expression of OX_1R, OX_2R and *LepRb* mRNA was confirmed via qPCR.

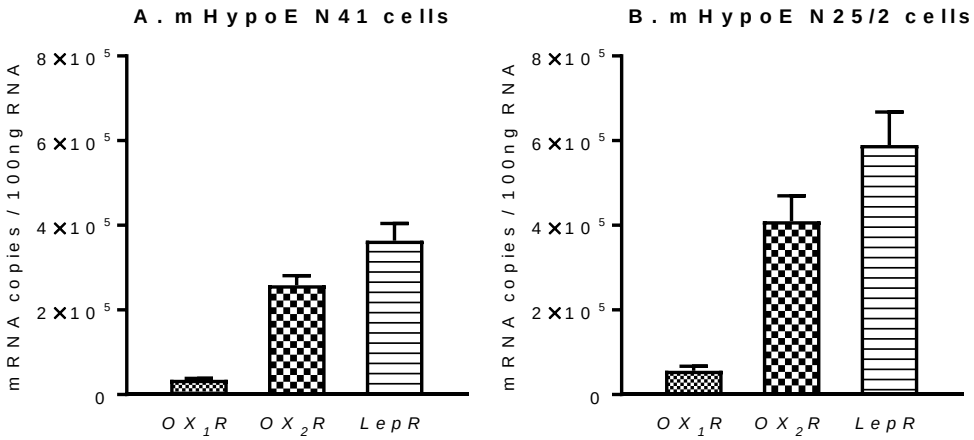

Figure 3.3.1.: mRNA expression of *OX$_1$R*, *OX$_2$R* and *LepRb* in mHypoE N41 and mHypoE N25/2 cell line. Number of mRNA copies were determined per 100 ng total RNA, from an n of 12 wells per receptor gained from 3 independent experiments.

The amount of mRNA copies was determined via standards and controlled by housekeeping gene *ß-actin* mRNA expression. All three receptors are expressed in both cell lines. Overall expression was higher in mHypoE N25/2 cells with an average of 5.66 x 10^4 ± 3.01 x 10^3 (mean ± SEM) copies/100 ng RNA of *OX$_1$R* mRNA, 4.1 x 10^5 ± 1.74 x 10^4 of *OX$_2$R* and 5.9 x 10^5 ± 2.24 x 10^4 of *LepR* mRNA copies/100ng RNA (Figure 3.3.1 B.). In mHypoE N41 cells mRNA copies/100ng RNA of *OX$_1$R* were an average of 3.47 x 10^4 ± 9.7 x 10^2, OX$_2$R 2.58 x 10^5 ± 6.49 x 10^3 and *LepR* 3.64 x 10^5 ± 1.17 x 10^4 (Figure 3.3.1 A.).

3.3.1.1 Regulation of *NPY* mRNA in mHypoE N41 cells after orexin A, orexin B and/or leptin treatment

NPY mRNA expression was investigated via qPCR after different durations of treatment with orexin A, B and/or leptin. The amount of mRNA copies was determined using dilution series of standards and the housekeeping gene *ß-actin* served as internal control. The graph shows the fold change of *NPY* mRNA expression relative to untreated control cells in 4 wells per condition in one initial experiment. In mHypoE N41 cells, *NPY* mRNA appeared to be 1.48 ± 0.46 (mean ± SEM) fold increased after treatment with orexin A for 15 min, while 15 min treatment with orexin B seemed to increase *NPY* mRNA. Leptin treatment appeared to decrease *NPY* mRNA expression in cells not treated with orexin, in orexin A treated and in orexin B treated cells (Figure 3.3.2 A.).

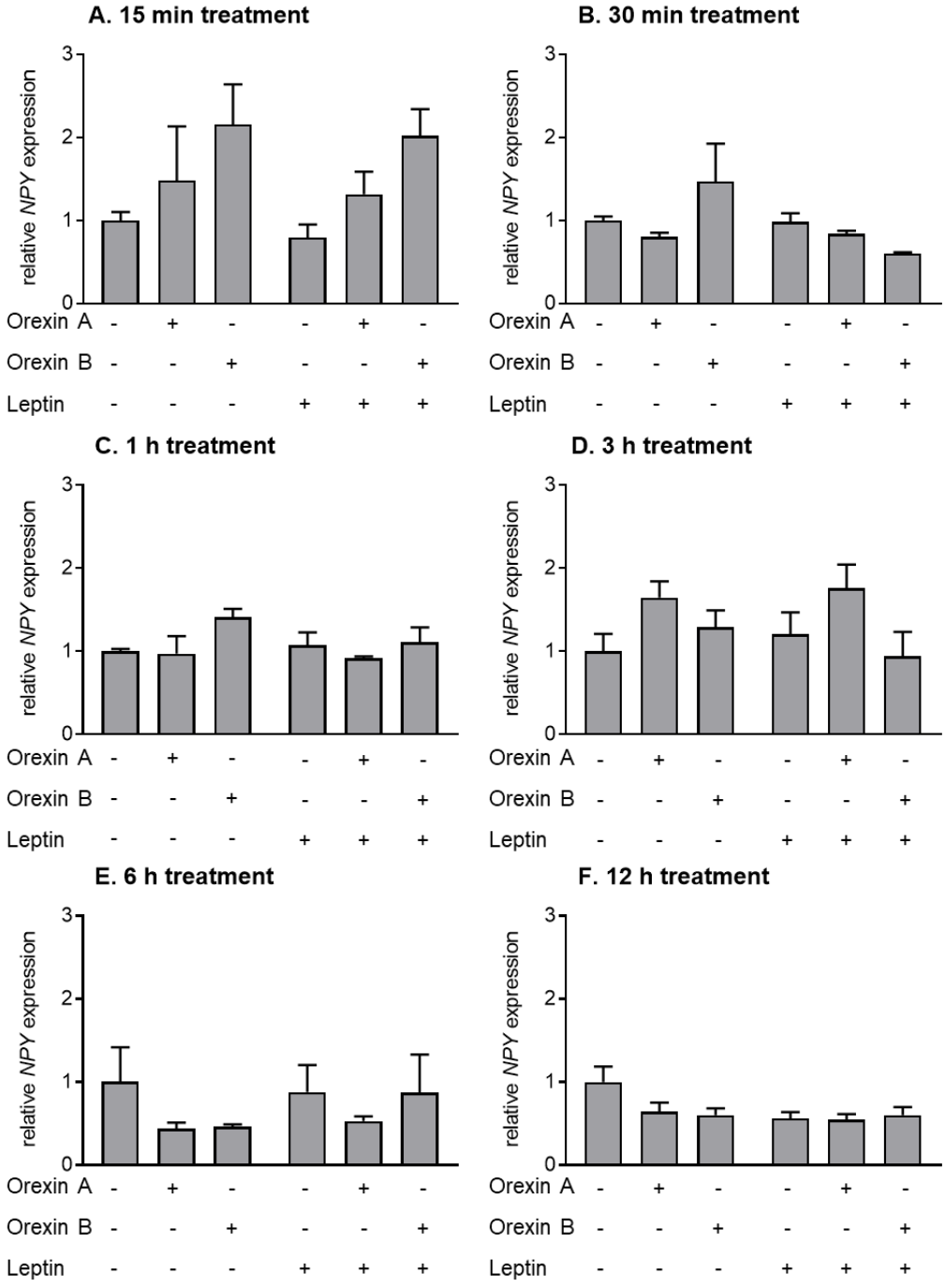

Figure 3.3.2.: *NPY* mRNA regulation in mHypoE N41 cells after orexin A/B and/or leptin treatment. Cells were treated for (**A**.) 15 min, (**B**.) 30 min, (**C**.) 1 h, (**D**.) 3 h, (**E**.) 6 h or (**F**.) 12 h, n = 4 wells per condition within one initial experiment.

30 min of orexin A treatment seemed to lead to a decrease in *NPY* mRNA expression, like orexin A and leptin co-treatment. Orexin B treatment on the other hand seemed to increase

NPY mRNA expression, which appeared to be decreased when co-treated with leptin (Figure 3.3.2 B.). Apparently, orexin A treatment did not change *NPY* mRNA expression after 1 h but orexin B treatment seemed to increase *NPY* mRNA. These seemingly increases appeared to be decreased by leptin co-treatment to (Figure 3.3.2 C.). Samples treated with orexin A or B for 3 h both seemed to show an increase in *NPY* mRNA expression. At this time-period *NPY* mRNA expression appeared to be further increased in samples treated without orexin and with leptin and orexin A and leptin, whereas co-treatment of leptin and orexin B seemed to decrease *NPY* mRNA expression (Figure 3.3.2 D.). After 6 h orexin A or B treatment *NPY* mRNA expression looked bisected in orexin A and in orexin B treated samples. Leptin co-treatment seemingly decreased *NPY* mRNA expression in cells without orexin and appeared to reduce this decrease in orexin A treated and in orexin B treated cells (Figure 3.3.2 E.). 12 h after treatment *NPY* mRNA seemed downregulated in all conditions (Figure 3.3.2 F.).

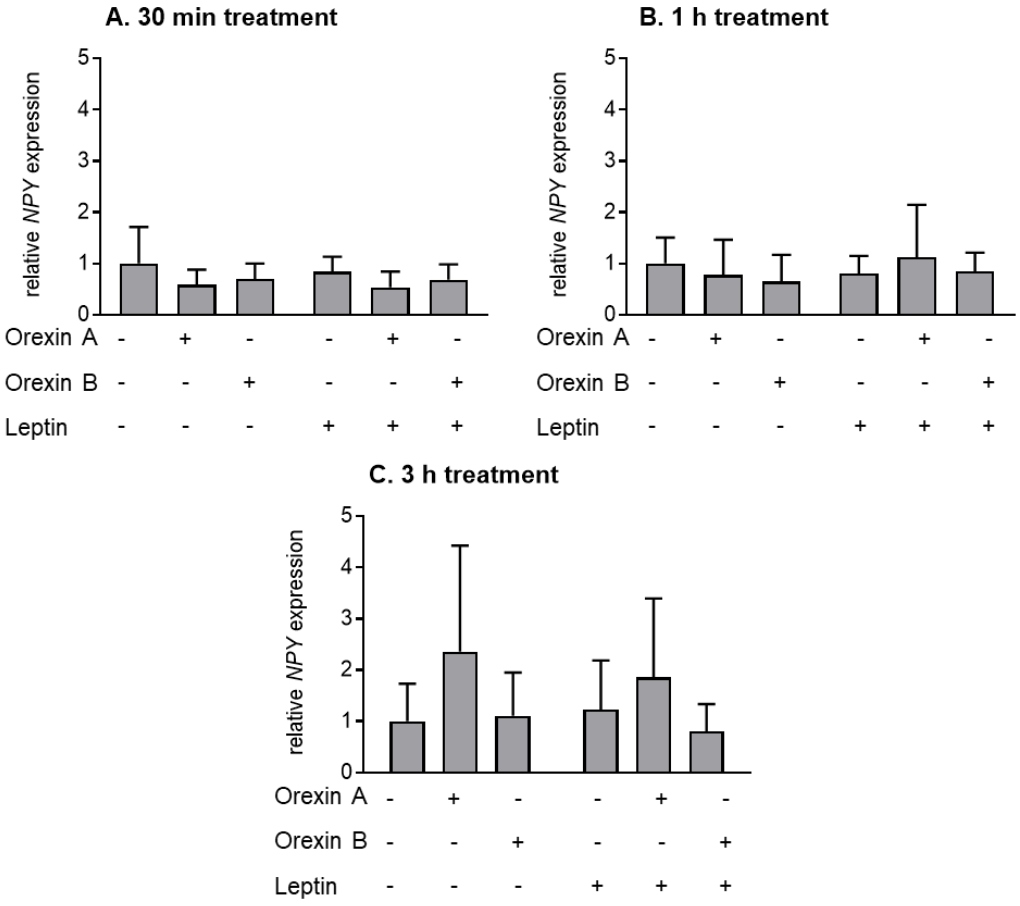

Figure 3.3.3.: *NPY* mRNA regulation in mHypoE N41 cells after orexin A/B and/or leptin treatment. Cells were treated for (**A**.) 30 min, (**B**.) 1 h or (**C**.) 3 h. Data are shown as fold change relative to untreated control cells. The means ± SEM of three independent experiments are shown.

To verify and statistically validate these results, the treatments were repeated for the 30 min-, 1 h- and 3 h time-period in 3 individual experiments, each having four samples per condition. In Figure 3.3.3 the averages of mean values of mRNA expression fold change relative to untreated control cells for each experiment are shown.

When cells were treated for 30 min with orexin A or B, *NPY* mRNA was seemingly 0.59 ± 0.17 (mean ± SEM) or 0.70 ± 0.17-fold, respectively, compared to controls like their corresponding leptin co-treated samples (orexin A + leptin: 0.54 ± 0.18-fold; orexin B + leptin: 0.68 ± 0.18-fold) (Figure 3.3.3 A.). Cells treated with leptin alone exhibited a 0.84 ± 0.17-fold change for this duration of treatment.

In samples collected after 1 h-treatment *NPY* mRNA expression appeared decreased after orexin A and B treatment and leptin treatment without orexin A or B. Co-treatment of leptin seemed to diminish the *NPY* mRNA decrease in orexin treated samples, increasing it in orexin A samples and in orexin B treated cells (Figure 3.3.3 B.). After treatment with orexin A, *NPY* mRNA expression seemed increased, after orexin B treatment and after leptin without orexin A or B increased in samples collected from the 3 h experiment (Figure 3.3.3 C.). Orexin A and leptin co-treatment and orexin B and leptin seemed to lead to a decrease in *NPY* mRNA expression.

In general, the experimental repetitions gave no uniform results and none of the results were statistically significant with high overall SEMs that were ranging from 0.17 up to 2.07 per sample.

3.3.1.2 Regulation of *NPY* mRNA in mHypoE N25/2 cells after orexin A, orexin B and/or leptin treatment

The same initial experiment for *NPY* mRNA regulation in 4 wells per condition for 6 time-periods was conducted in mHypoE N25/2 cells (Figure 3.3.4).

Samples treated with orexin A were seemingly increased in *NPY* mRNA expression after 3 h, 6 h and 12 h, that appeared diminished in samples co-treated with leptin after 3 h, 6 h and after 12 h treatment (Figure 3.3.4 D. – F.). After 3 h and 6 h, as well as 15 min, also orexin B treated samples showed higher *NPY* mRNA expression then their controls (Figure 3.3.4 A., D, and E) minimised by co-treatment with leptin. *NPY* mRNA expression seemed to be lowered in orexin A treated samples after 30 min and 1 h (Figure 3.3.4 B. and C.) and in orexin B treated samples after 30 min, 1 h and 12 h (Figure 3.3.4 B., C., F.). Only after

30 min the *NPY* mRNA expression appeared to be further decreased by leptin co-treatment with orexin A (Figure 3.3.4 B.).

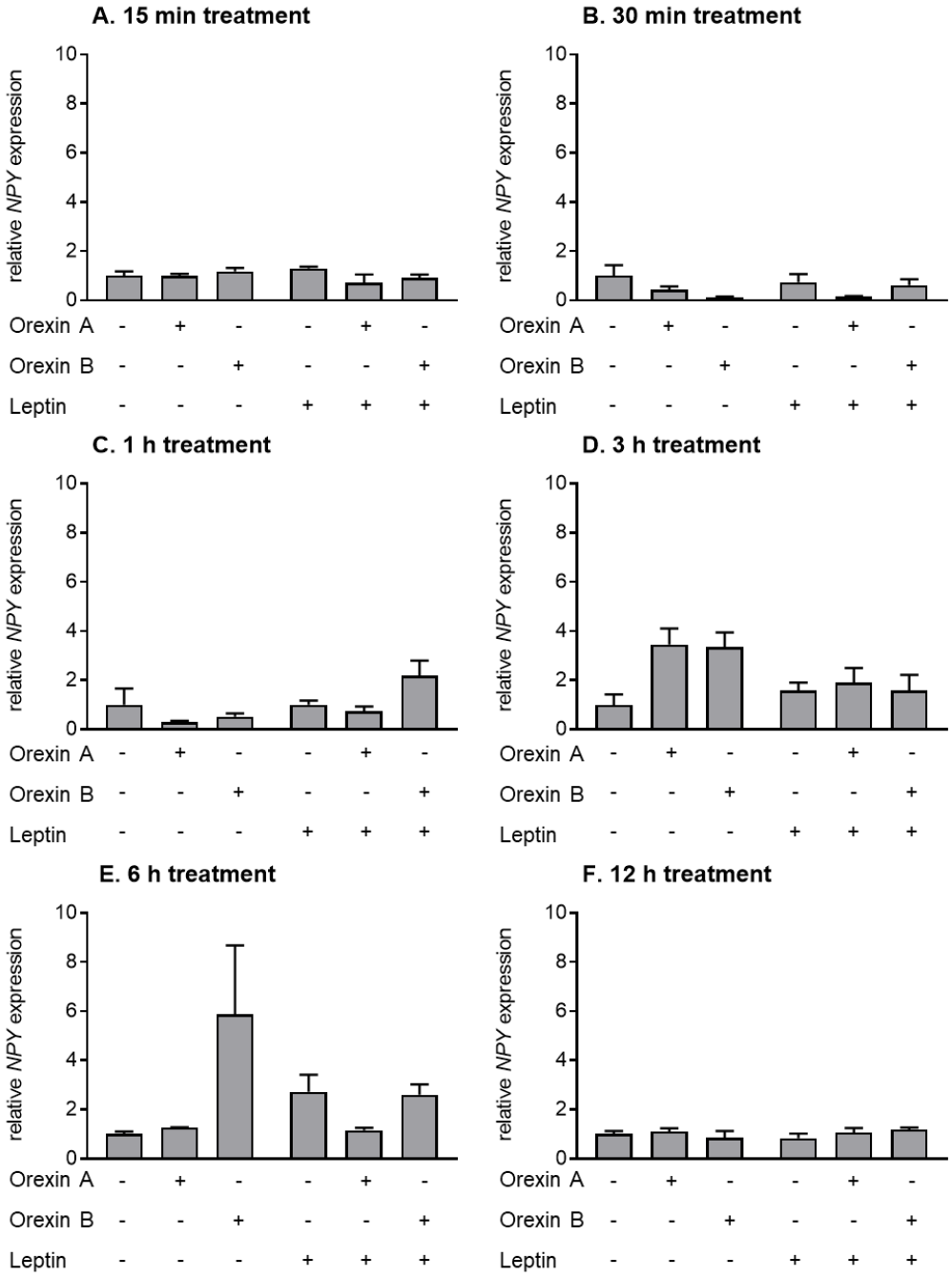

Figure 3.3.4.: *NPY* regulation in mHypoE N25/2 cells after orexin A/B and/or leptin treatment. Cells were treated for (**A**.) 15 min, (**B**.) 30 min, (**C**.) 1 h, (**D**.) 3 h, (**E**.) 6 h or (**F**.) 12 h, n = 4 wells per condition within one initial experiment.

All other time-periods, where orexin A or B treated cells showed lowered *NPY* mRNA expression, the leptin co-treated samples seemingly showed smaller decrease, like orexin A + leptin at 1 h and orexin B + leptin at 30 min (Figure 3.3.4 C. and B.), or even increase in the amount of *NPY* mRNA expressed, as orexin B + leptin after 1 h and 12 h (Figure 3.3.4 C. and F.). Samples did not show a change in *NPY* mRNA expression after 15 min treatment with orexin A and 1 h leptin treatment (Figure 3.3.4 A. and C.). After leptin treatment alone *NPY* mRNA appeared decreased after 30 min (Figure 3.3.4 B.) and after 12 h (Figure 3.3.4 F.). Otherwise *NPY* mRNA expression seemed increased after 15 min (Figure 3.3.4 A.), after 3 h (Figure 3.3.4 D.) and after 6 h (Figure 3.3.4 E.).

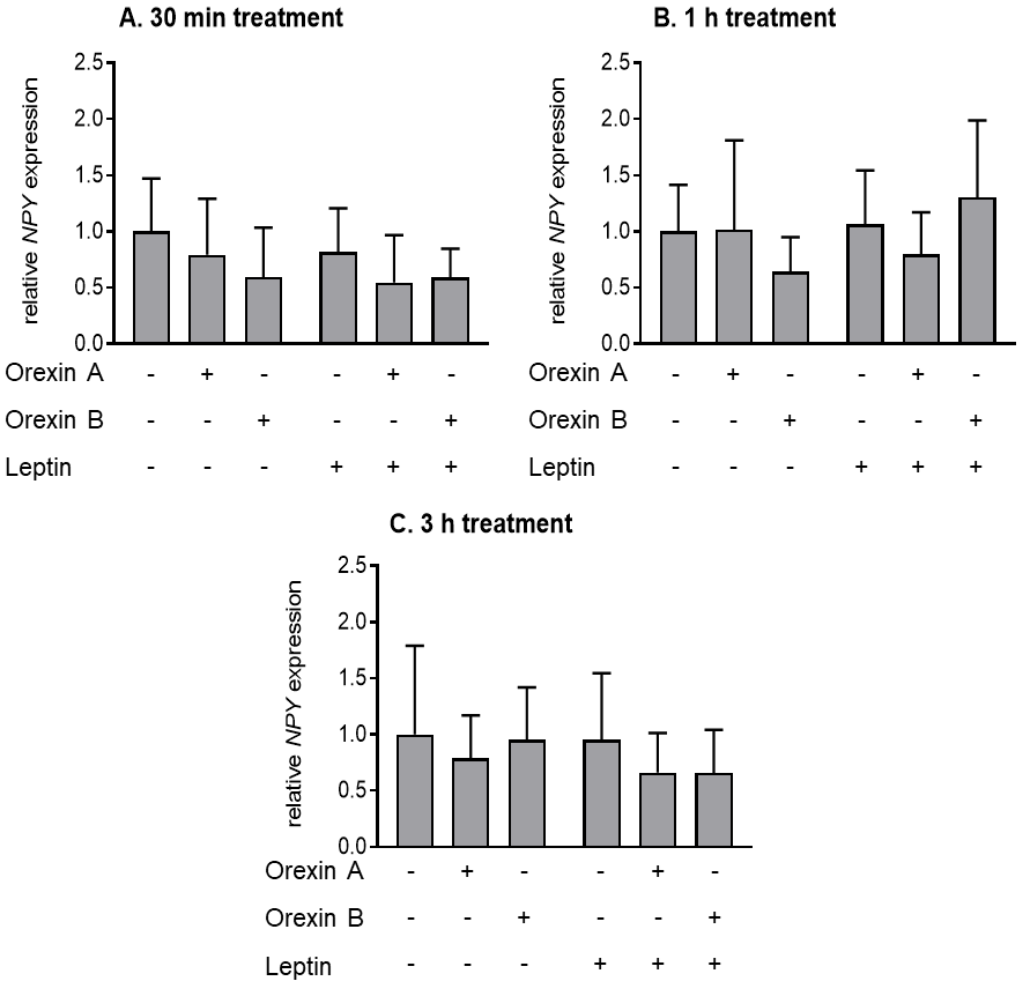

Figure 3.3.5*.: NPY* mRNA regulation in mHypoE N25/2 cells after orexin A/B and/or leptin treatment. Cells were treated for (**A**.) 30 min, (**B**.) 1 h or (**C**.) 3 h. Results are relative to untreated control cells and the mean of 4 wells per conditions for three independent experiments plotted.

The treatments were, like in mHypoE N41 cells, repeated in three independent experiments for the time-periods of 30 min, 1 h and 3 h treatment and the mean values of 4 wells per condition blotted (Figure 3.3.5). After 30 min orexin A, orexin B or leptin treated cells showed lower *NPY* mRNA expression then untreated control cells, seemingly further decreased by co-treating leptin with orexin A and with orexin B (Figure 3.3.5 A.). Leptin or orexin A treatment alone did not appear to change *NPY* mRNA expression after 1 h, whereas orexin B treated samples seemed to be decreased. Orexin A and leptin co-treated samples showed decreased *NPY* mRNA expression, orexin B and leptin co-treated samples on the other hand, showed increase, seemingly abolishing orexin B decrease (Figure 3.3.5 B.). Samples treated with orexin A appeared to show lower *NPY* mRNA expression then control cells, while there seemed to be no change in leptin or orexin B treated cells and their *NPY* mRNA expression levels. Orexin and leptin co-treated samples showed lowered *NPY* mRNA expression in orexin A + leptin and in orexin B + leptin samples (Figure 3.3.5 C.).

The changes in *NPY* mRNA expression were statistically not significant with SEMs ranging between 0.18 and 0.8.

3.3.1.3 Regulation of *POMC* mRNA in mHypoE N41 cells after orexin A, orexin B and/or leptin treatment

Proopiomelanocortin (*POMC*) mRNA expression was also investigated after treatment with orexin A, orexin B or leptin, as well as co-treatment of orexin A or orexin B and leptin for 30 min, 1 h and 3 h in mHypoE N41 cells. In Figure 3.3.6 the mean values of 4 wells per condition of three independent experiments are shown.

POMC mRNA levels seemed decreased after orexin A treatment for 30 min, (Figure 3.3.6 A.), after orexin A and after orexin B treatment for 1 h (Figure 3.3.6 B.). When samples were only treated with leptin for 30 min or 1 h, *POMC* mRNA levels did apparently not change (Figure 3.3.6 A. and B.). A 30-min treatment with orexin B (Figure 3.3.6 A.) and 1 h co-treatment of orexin B and leptin also does not indicate *POMC* mRNA regulation (Figure 3.3.6 B.). Co-treatment of orexin A or B with leptin seemed to lead to a decrease in *POMC* mRNA expression after 30 min (Figure 3.3.6 A.), whereas samples that were treated with orexin A and leptin for 1 h seemingly had a slight increase in *POMC* mRNA expression (Figure 3.3.6 B.).

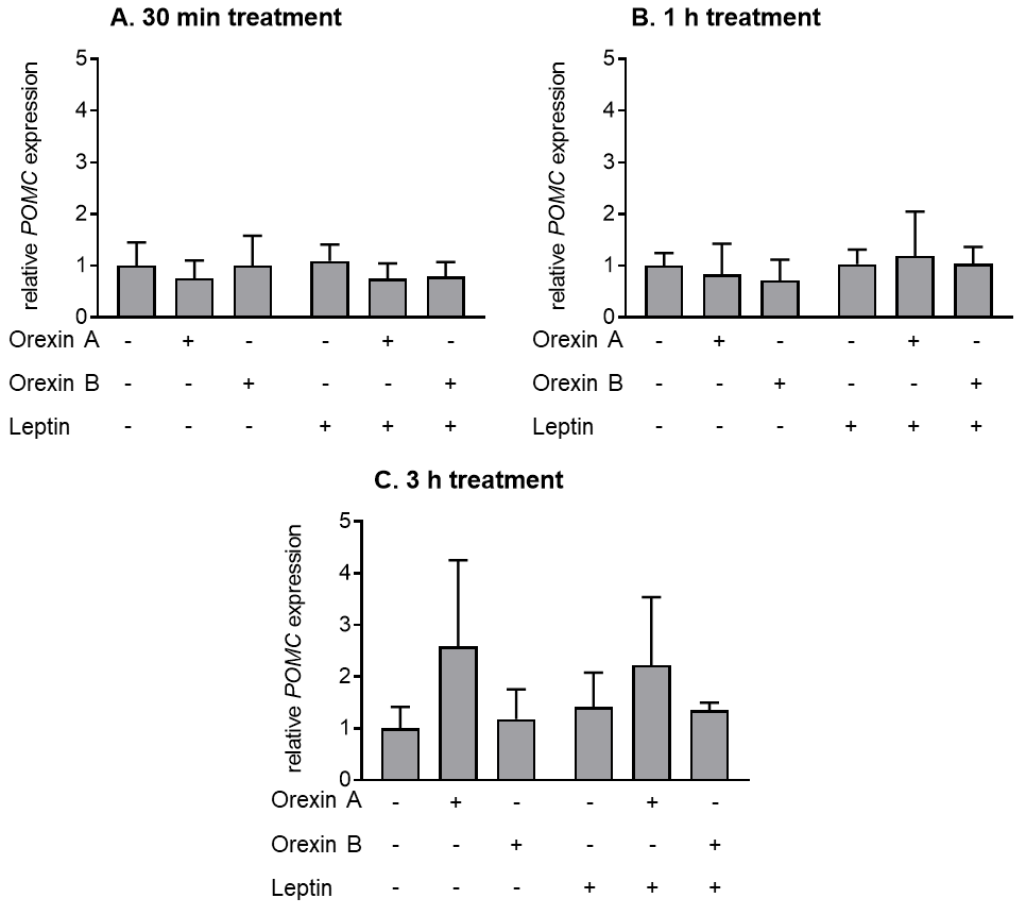

Figure 3.3.6.: *POMC* mRNA regulation in mHypoE N41 cells after orexin A/B and/or leptin treatment. Cells were treated for (**A**.) 30 min, (**B**.) 1 h or (**C**.) 3 h. Results are relative to untreated control cells and the mean of 4 wells per conditions for three independent experiments blotted.

The changes in *POMC* mRNA expression were statistically not significant with high variations, expressing SEMs as high as 1.66.

3.3.1.4 Regulation of *POMC* mRNA in mHypoE N25/2 cells after orexin A, orexin B and/or leptin treatment

The regulation of *POMC* mRNA in mHypoE N25/2 cells was investigated in the same conditions as in mHypoE N41 cells.

After 30 min of treatment all samples seemed to show a decrease in *POMC* mRNA levels, highest in orexin B treated and orexin A co-treated with leptin samples, followed by orexin

A treated and orexin B co-treated with leptin cells and lowest in merely leptin treated samples (Figure 3.3.7 A.).

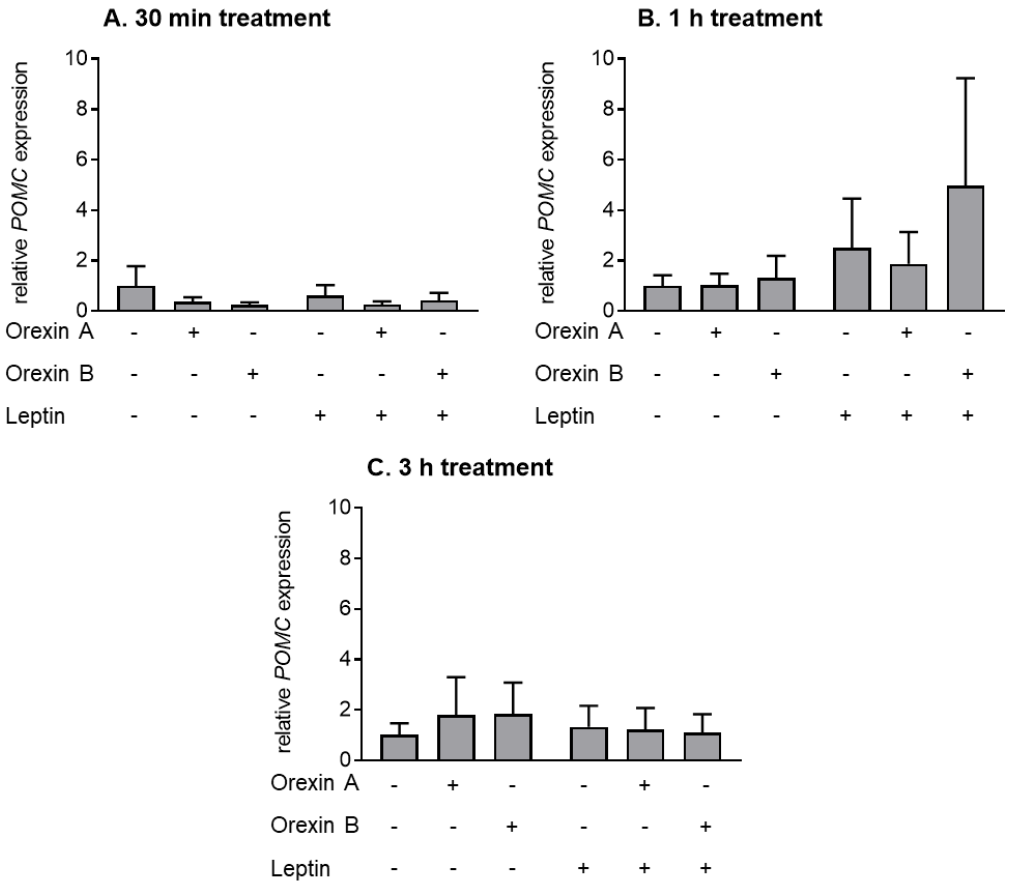

Figure 3.3.7.: *POMC* mRNA regulation in mHypoE N25/2 cells after orexin A/B and/or leptin treatment. Cells were treated for (A.) 30 min, (B.) 1 h or (C.) 3 h. Results are relative to untreated control cells and the mean of 4 wells per conditions for three independent experiments blotted.

Almost all samples treated with one of the conditions for 1 h showed elevated *POMC* mRNA levels, except for orexin A treatment that control *POMC* mRNA levels (Figure 3.3.7 B.). Orexin A and leptin co-treated samples seemed to almost have twice the control *POMC* mRNA expression level, samples only treated with leptin seemed even further elevated in their *POMC* expression, while orexin B alone and co-treated with leptin seemed to have highest increase in *POMC* mRNA levels (Figure 3.3.7 B.). After 3 h orexin A treated samples showed increase in *POMC* mRNA expression that seemed reduced in samples co-treated with leptin to, orexin B treated samples appeared to have increased *POMC* mRNA levels,

seemingly alleviated by co-treatment with leptin and in solely leptin treated samples *POMC* expression seemed increased (Figure 3.3.7 C.).

Statistically there were no *POMC* mRNA regulations that were significant, with SEMs going up to 4.26.

3.3.1.5 Activation of mitogen-activated protein kinase (MAPK) pathway by orexin A and/or leptin treatment in mHypoE N41, mHypoE N25/2 and mHypoA 2/23 cells

To address a possible common intracellular signalling pathway of orexins and leptin signalling the activation of the MAPK pathway was investigated via Western blot staining for whole and phosphorylated extracellular signal–regulated kinase (ERK1/2). Both, orexins and leptin have been shown to activate MAP kinases (Tang et al., 2008; Ramanjaneya et al., 2009; Rahmouni, 2012; Leonard, 2014). Quantification was performed with EvolutionCapt software and the difference between pERK1/2 and ERK1/2 for each sample relative to basic ERK1/2 phosphorylation in untreated control cells analysed (Figure 3.3.8).

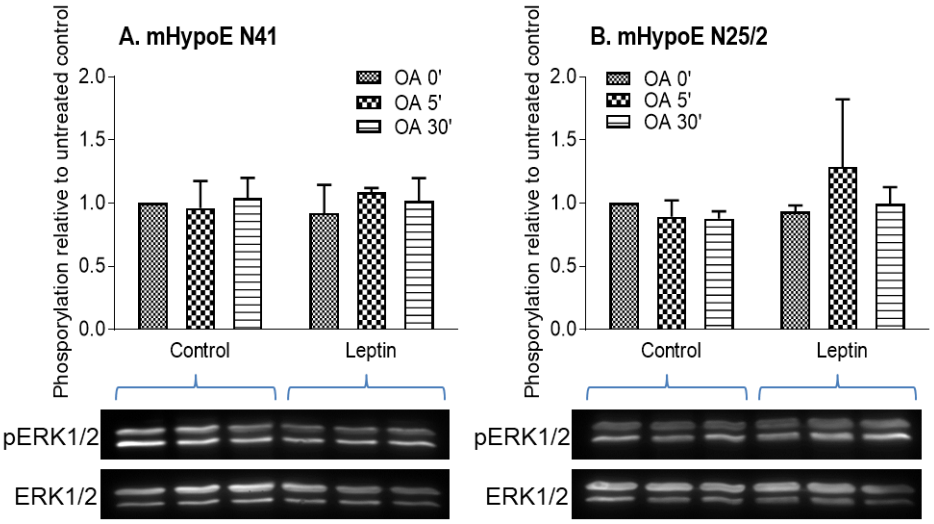

Figure 3.3.8.: ERK1/2 phosphorylation after orexin A and/or leptin treatment in (**A**.) mHypoE N41 and (**B**.) mHypoE N25/2 cells after OA for 30 min and 5 min with or without pre-treatment with leptin. Gel pictures are representative, one out of three independent experiments, while graphs show phosphorylation relative to untreated control of three independent experiments.

Phosphorylation of ERK1/2 was neither in- nor decreased by orexin A and/or leptin treatment in mHypoE N41 cells after 5 min or 30 or in merely leptin pre-treated samples (Figure 3.3.8 A.). ERK1/2 phosphorylation seemed slightly increased by 1.29 ± 0.31-fold (mean ± SEM) in samples treated with orexin A for 5 min after pre-treatment with leptin in mHypoE N25/2 cells while the other conditions did not change ERK1/2 phosphorylation (Figure 3.3.8 B.).

Since in mHypoE N41 and mHypoE N25/2 cells orexin A treatment did not lead to statistically significant ERK1/2 phosphorylation independent of the duration of the treatment or co-treatment with leptin, the range of cell lines used was extended by mHypoA 2/23 cells which were derived from adult hypothalamic neurons (https://www.cedarlanelabs.com /Products/Listing/Adult_Mouse_Hypothalamic).

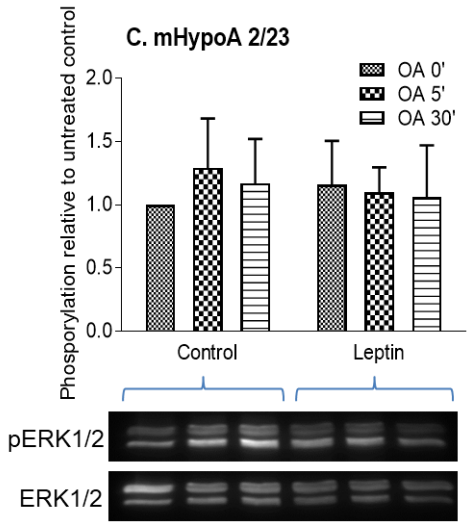

Figure 3.3.9.: ERK1/2 phosphorylation after orexin A and/or leptin treatment in mHypoA 2/23 cells after OA for 30 min and 5 min with or without pre-treatment with leptin. Gel pictures are representative, one out of three independent experiments, while graphs show phosphorylation relative to untreated control of three independent experiments.

In mHypoA 2/23 cells all conditions led to a slight increase in ERK1/2 phosphorylation with 1.29 ± 0.23 -fold increase after 5 min orexin A, 1.17 ± 0.20-fold after 30 min, 1.10 ± 0.11 -fold after 5 min orexin A with leptin and 1.16 ± 0.20-fold change after only leptin treatment (Figure 3.3.8 C.). SEMs of these values were usually higher then the measured increase and the results statistically not significant.

3.3.1.6 Activation of mitogen-activated protein kinase (MAPK) pathway by treatment with medium primed by cultured adipocytes in mHypoE N41, N25/2 and mHypoA 2/23 cells

To analyse a possible effect of adipokines or other signalling molecules derived from adipocytes the cell lines mHypoE N41, mHypoE N25/2 and mHypoA 2/23 were treated for 5 or 30 min with medium, that was primed by cultured epididymal adipocytes for 48 h, and MAPK pathway activation investigated as before after orexin A treatment.

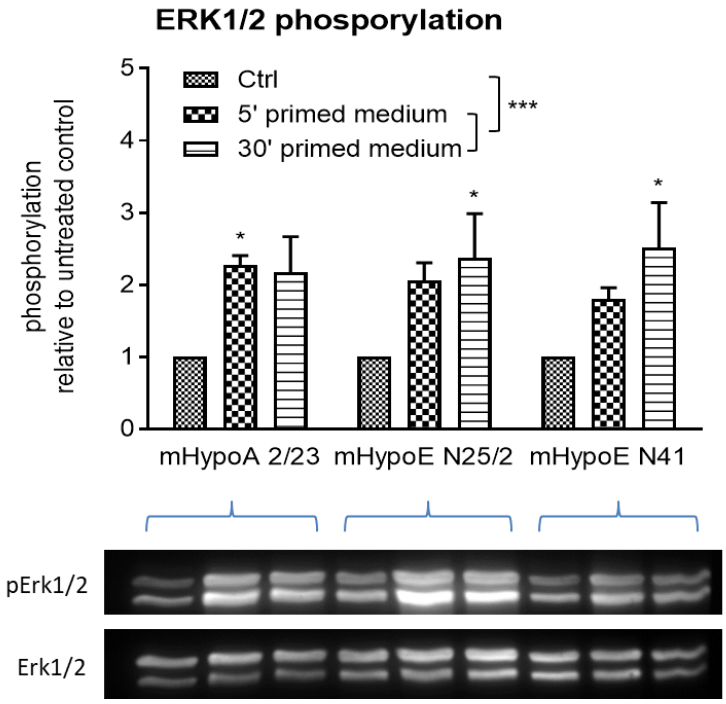

Figure 3.3.10.: ERK1/2 phosphorylation in mHypoA 2/23, mHypoE N41 and mHypoE N25/2 after treatment with adipocyte-primed medium for 5 and 30 min relative to basal phosphorylation in control cells, that were treated with mHypoE primed medium; n=3 independent experiments. * = $p \leq 0.05$ compared to controls (Ctrl); *** = $p \leq 0.001$.

In all three cell lines the treatment with adipocyte-primed medium led to increased ERK1/2 phosphorylation after 5 and 30 min of treatment (Figure 3.3.10). ERK1/2 phosphorylation was 2.27 ± 0.07-fold (mean ± SEM) over the basal ERK1/2 phosphorylation after 5 min and 2.18 ± 0.28-fold after 30 min with adipocyte-primed medium in mHypoA 2/23 cells. In mHypoE N25/2 cells the treatment with adipocyte-primed medium increased ERK1/2 phosphorylation 2.05 ± 0.14-fold after 5 min and 2.37 ± 0.35-fold after 30 min treatment.

1.80 ± 0.09-fold elevation of ERK1/2 phosphorylation was found in mHypoE N41 cells after 5 min treatment further increased after 30 min by 2.51 ± 0.36-fold.

The heightened phosphorylation of ERK1/2 was found to be statistically significant after 5 min treatment in mHypoA 2/23 ($p = 0.05$) and after 30 min treatment in mHypoE N25/2 ($p = 0.02$) and mHypoE N41 cells ($p = 0.01$) (Figure 3.3.10).

3.3.2 mHypoE N41 cells stably transfected with OX_1R and N41 OX_2R as *in vitro* model neurons

In mHypoE N25/2 and mHypoE N41 cells orexin receptor expression was at very low levels and the, for orexins well described, ERK1/2 phosphorylation was not detected. Therefore, mHypoE N41 cells, that were stably transfected with either human OX_1R or OX_2R were obtained (Wang et al., 2014b). These cell lines served as neuronal cell model for further experiments to test a possible interaction of orexin and adipokine signalling.

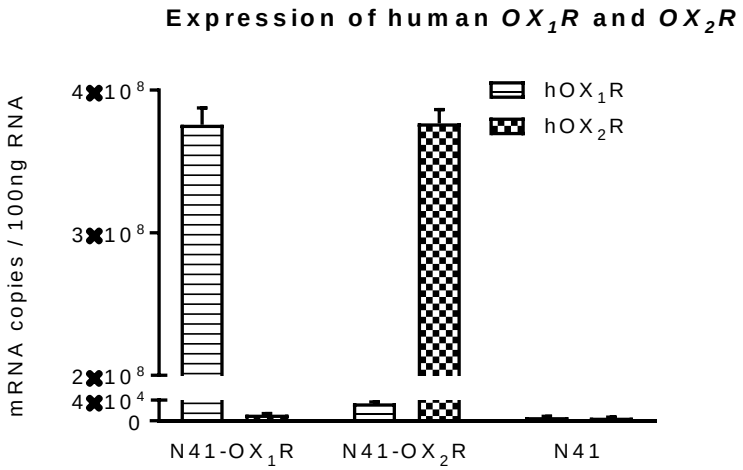

Figure 3.3.11.: Expression of *human OX_1R* and *OX_2R* in mHypoE-N41-OX_1R, mHypoE-N41-OX_2R and mHypoE N41 cells. Every column represents the mean value of mRNA copies / 100 ng RNA from 4 samples per cell line with the respective SEM.

First, the expression of OX_1R or OX_2R was confirmed in the cell lines by qPCR. From 4 samples per cell line RNA was extracted to serve as a template for qPCR for human orexin receptor expression, with non-transfected mHypoE N41 cells serving as a negative control

(Figure 3.3.11). The quantity of mRNA expression was determined via standards and calculated for 100 ng whole RNA extract used in one PCR reaction.

mHypoE-N41-OX_1R cells expressed 3.76 x 10^8 ± 5.85 x 10^6 (mean ± SEM) mRNA copies of the human OX_1R per 100 ng RNA and only low mRNA levels of the human *OX_2R* per 100 ng RNA. In mHypoE-N41-OX_2R cells, only low levels of human *OX_1R*, but 3.77 x 10^8 ± 4.78 x 10^6 copies of the human *OX_2R* were detected per 100 ng RNA. Non-transfected mHypoE N41 control cells showed only very low levels of human *OX_1R* or *OX_2R* copies in 100 ng RNA. Thus, a substantial expression of both orexin receptor subtypes was detected as expected.

3.3.2.1 Calcium responds to orexin A and orexin B in mHypoE-N41-OX_1R and mHypoE-N41-OX_2R cell lines

Activation of orexin receptor subtypes leads to a rapid increase in intracellular Ca^{2+} (Leonard, 2014). To test their responsiveness, mHypoE-N41, mHypoE-N-41-OX_1R and mHypoE-N41-OX_2R cells, that were loaded with the radiometric fluorescent Ca^{2+} indicator Fura-2 were treated with either 0.1 µM or 1.0 µM concentration of orexin A or orexin B.

The ratio of the emissions at 510 nm after excitation with 340 nm or 380 nm wavelengths is a direct indicator of Ca^{2+} concentration in the cells, as the excitation of Fura-2 shifts from 340 nm to 380 nm after building a chelate complex with Ca^{2+} ions (Kong, 1995). The samples were measured 15 s before and 60 s after orexin A or orexin B treatment that is displayed by the dotted line in the blots (Figure 3.3.12).

In mHypoE N41 control cells that do not express hOX_1R and hOX_2R the ratio of emissions did not change after adding 0.1 or 1.0 µM orexin A or orexin B to (Figure 3.3.12 A.). In mHypoE-N41-OX_1R cells (Figure 3.3.12 B.) the ratio increased from the basal ratio of 0.3 to 0.8 when 0.1 µM orexin A was added to the samples and was only slightly elevated to 0.9 at an orexin A concentration of 1.0 µM. Orexin B led to a shift in emission ratio to 0.5 at 0.1 µM and to 0.85 at 1.0 µM concentration. In mHypoE-N41-OX_2R cells orexin A and B both induced a similar shift in emissions ratio to 0.7 following treatment with a 0.1 µM and a 1.0 µM concentration (Figure 3.3.12 C.).

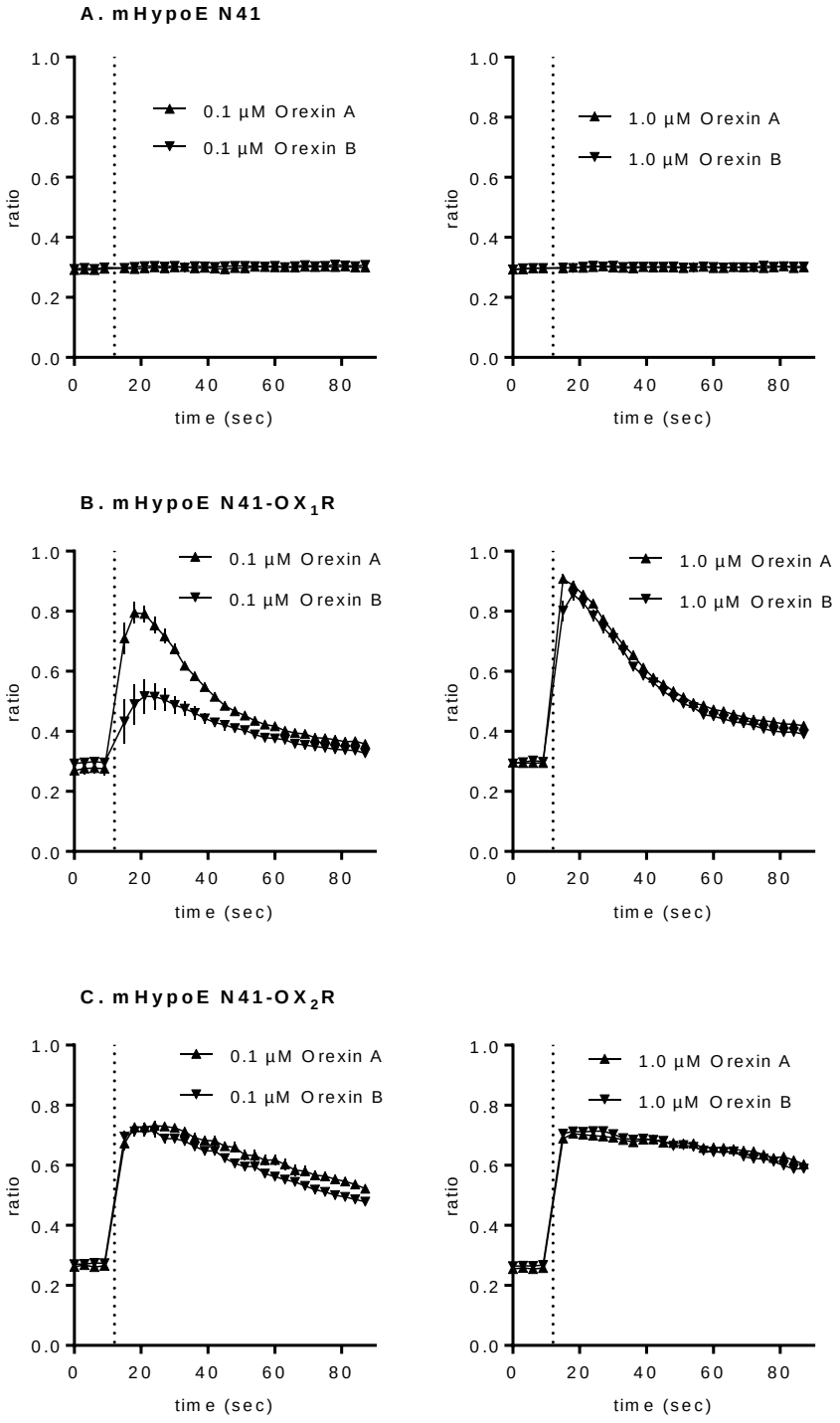

Figure 3.3.12.: Calcium measurements after orexin A or orexin B treatment. Fura-2 loaded (**A**.) mHypoE N41, (**B**.) mHypoE-N41-OX_1R and (**C**.) mHypoE-N41-OX_2R were treated with either orexin A or orexin B at 0.1 µM or 1.0 µM concentration. The vertical dotted line indicates the time point of orexin injection and ratio of emissions at 510 nm after excitation at 340 nm and 380 nm wavelength is plotted against time; n= 4 wells per condition in one experiment.

3.3.2.2 Activation of MAPK pathway by orexin A and/or adipocyte- primed medium treatment in mHypoE-N41-OX_1R and mHypoE-N41-OX_2R cells

In a further set of experiments, the effects of orexins and adipocyte-primed medium were tested. Therefore, the cell lines mHypoE-N41-OX_1R and mHypoE-N41-OX_2R were treated with either orexin A, adipocyte-primed medium or both and the activation of the MAPK pathway was investigated via Western blot with antibodies against phosphorylated (p)ERK1/2 and whole ERK1/2. The ratio of pERK1/2 to ERK1/2 was determined relative to untreated control cells in three individual experiments.

After treatment of mHypoE-N41-OX_1R cells with orexin A alone for 5 min pERK1/2 was increased 1.53 ± 0.26-fold (mean ± SEM) relative to untreated control samples, after 10 min 1.25 ± 0.12-fold. Single treatment with adipocyte-primed medium led to a 1.21 ± 0.18-fold elevation of pERK1/2, that was further increased to 1.44 ± 0.14-fold by co-treatment with orexin A for 5 min and 1.76 ± 0.35-fold for 10 min (Figure 3.3.13 A.).

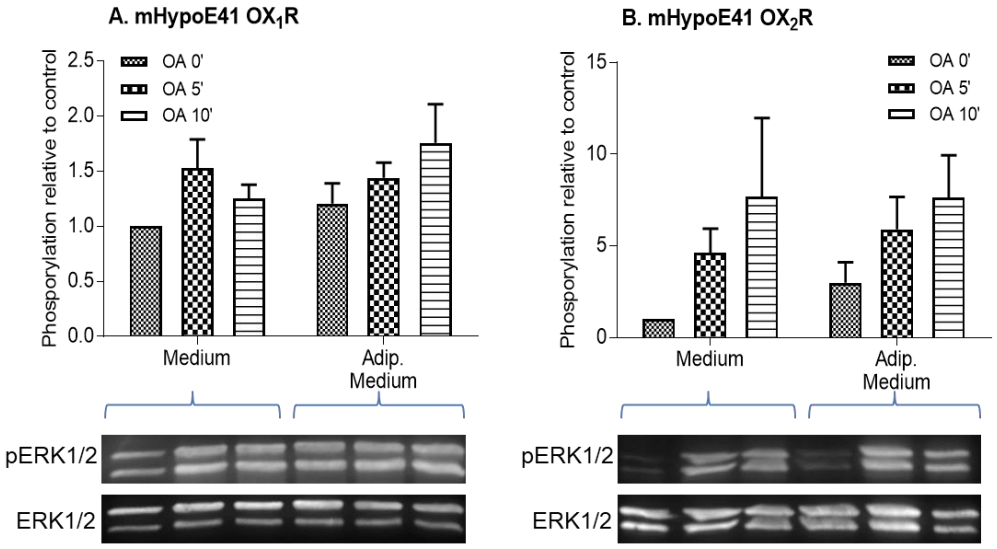

Figure 3.3.13.: ERK1/2 phosphorylation after orexin A and/or adipocyte-primed medium treatment in (**A**.) mHypoE-N41-OX_1R and (**B**.) mHypoE-N41-OX_2R cell lines after orexin A for 5 min or 10 min with or without co-treatment with adipocyte-primed medium. Gel pictures are representative, one out of three independent experiments, while graphs show the mean ratio ± SEM of phosphorylated (p)ERK1/2 to whole ERK1/2 relative to untreated control; n = 3 independent experiments.

In mHypoE-N41-OX_2R cells, pERK1/2 was increased 4.62 ± 1.32-fold in samples treated with orexin A for 5 min and 7.69 ± 4.3-fold with orexin A for 10 min A 2.99 ± 1.13-fold

increase was determined when samples were only treated with adipocyte-primed medium. Samples that were co-treatment of adipocyte-primed medium an orexin A had a 5.91 ± 1.78-fold pERK1/2 enhancement after 5 and 7.65 ± 2.29-fold after 10 min (Figure 3.3.13 B.).

3.3.2.3 Dual-Luciferase® Reporter gene Assay in mHypoE-N41-OX_1R and mHypoE-N41-OX_2R cells

Western blot analysis indicated a regulation of pERK1/2 phosphorylation by orexins and/or adipocyte-primed medium in mHypoE-N41-OX1R and mHypoE-N41-OX2R cells (3.3.2.2). However, Western blot analyses allow the measurement of only few samples per blot. To achieve a higher throughput of samples in the analysis of MAPK signalling pathways, a luciferase reporter gene assay was used that measures the activation of the transcription factor Elk-1 (Jantti et al., 2013). Phosphorylation by ERK1/2 activates Elk-1, which in turn induces the transcription of immediate-early genes, such as *c-Fos* (Janknecht R, 1992; Kortenjann M, 1994).

Before the Dual-Luciferase® Reporter gene assay could be performed with the different treatments, a transfection rate had to be determined to get feasible ratios of firefly luciferase (fLuc) / renilla luciferase (rLuc) values. The test revealed if transfections were successful and the Elk-1 system is functional. Different proportions of the plasmid that constantly expresses rLuc (pRL-TK) were transfected together with either pSG-GalElk-1 or pGal4 VP16 plasmids. pSG-GalElk-1 expresses the Gal part of a fusion construct that needs co-expression with a second plasmid coding for the second part of that system. When Elk-1 is activated in the transfected cells Gal is expressed, binds to the fusion construct and fLuc is expressed. The pGal4 VP16 contains the template for both fusion construct parts, that are constantly expressed and therefore also fLuc.

Transfections with 3, 6 and 12 % of plasmid DNA consisting of pRL-TK were tested and 3 as well as 6 % pRL-TK were found to deliver higher fLuc to rLuc ratios in pGal4 VP16 co-transfected cells then 12 %. To economise with plasmid DNA, 3 % pRL-TK were used for further reporter gene assays.

The functionality of the pSG-GalElk-1 system was tested by orexin A treatment in mHypoE-N41-OX_1R and mHypoE-N41-OX_2R cells with mHypoE N41 cells serving as control.

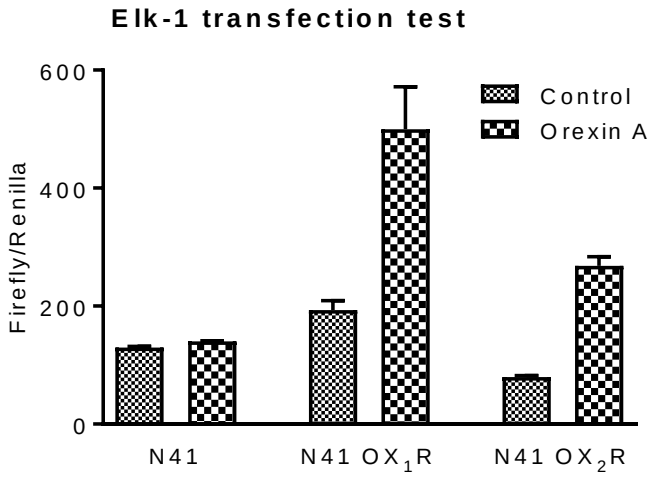

Figure 3.3.14.: Test for *Elk-1* reporter Gene Assay in mHypoE-N41-OX_1R and mHypoE-N41-OX_2R cells. Cells were transfected with 3 % pRL-TK plasmid and the pSG-GalElk-1 system, leading to firefly luciferase (fLuc) expression when *Elk-1* is activated. To determine if transfections were successful and if the system is functional samples were treated for with 1000 nM orexin A for 4 h. mHypoE N41 cells served as negative control; n =4 wells from one transfection experiment.

Orexin A treatment clearly increased fLuc and therefore Elk-1 activation in both, mHypoE-N41-OX_1R and mHypoE-N41-OX_2R cells, whereas mHypoE N41 cells exhibited no change due to orexin A treatment (Figure 3.3.14).

In an initial experiment mHypoE-N41-OX_1R and mHypoE-N41-OX_2R cells were treated with increasing concentrations (1, 10, 100 and 1000 nM) of orexin A or B to investigate if the response of Elk-1 to orexin A was doses dependent and applied for orexin B treatment as well (Figure 3.3.15).

Orexin A as well as orexin B treatment increased Elk-1 activation in mHypoE-N41-OX_1R and mHypoE-N41-OX_2R cells. This increase seemed to correlate with the applied concentration of orexin and was saturable. The half maximal effective concentration (EC_{50}) indicates the concentration of orexin, that induces 50 % of its effect and is 14 nM for orexin A and 174 nM for orexin B in mHypoE-N41-OX_1R (Figure 3.3.15 A.) and 25 nM for orexin A and 28 nM for orexin B in mHypoE-N41-OX_2R cells (Figure 3.3.15 B.). In mHypoE N41 cells, neither orexin A nor orexin B activated Elk-1 (Figure 3.3.15 C.).

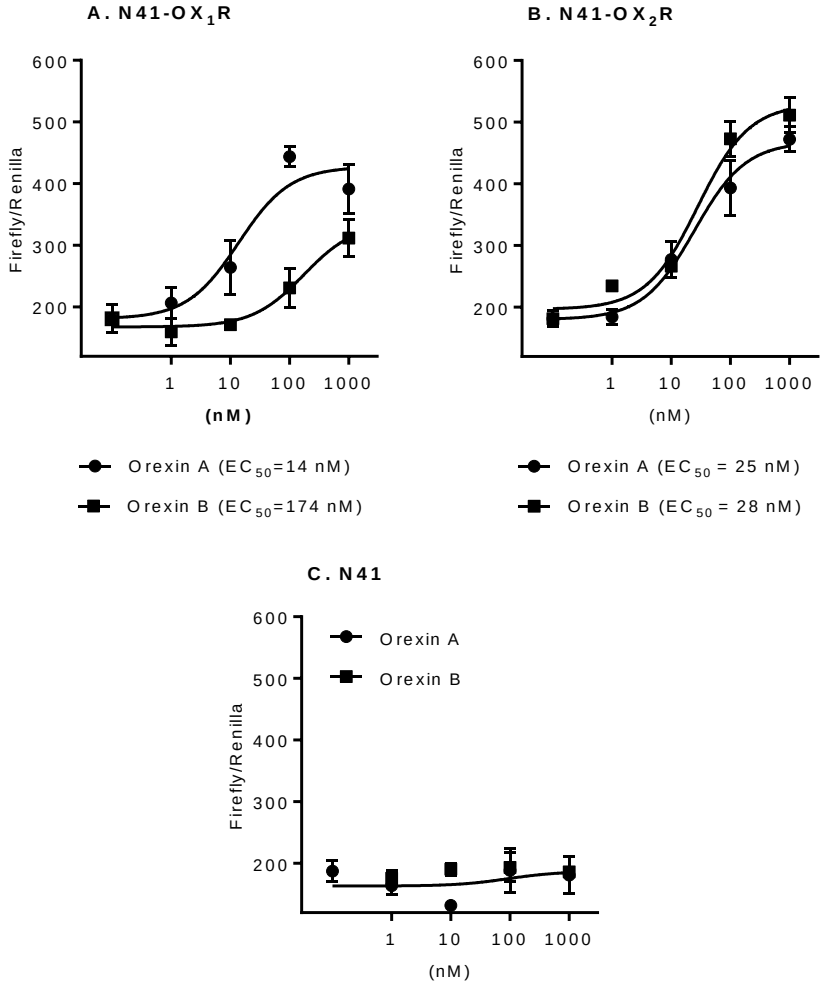

Figure 3.3.15.: Orexin A and orexin B doses dependent Elk-1 activation in mHypoE-N41-OX$_1$R and mHypoE-N41-OX$_2$R cells. *Elk-1* reporter gene assay was performed using different concentrations of orexin A and B in (**A**.) mHypoE-N41-OX$_1$R, (**B**.) mHypoE-N41-OX$_2$R cells and (**C**.) mHypoE N41 cells as negative control; n = 4 wells from one transfection experiment.

The effect of the more potent orexin A was also tested in adipocyte primed medium compared to normal medium to investigate a possible interaction between compounds secreted by adipocytes and orexin (Figure 3.3.16).

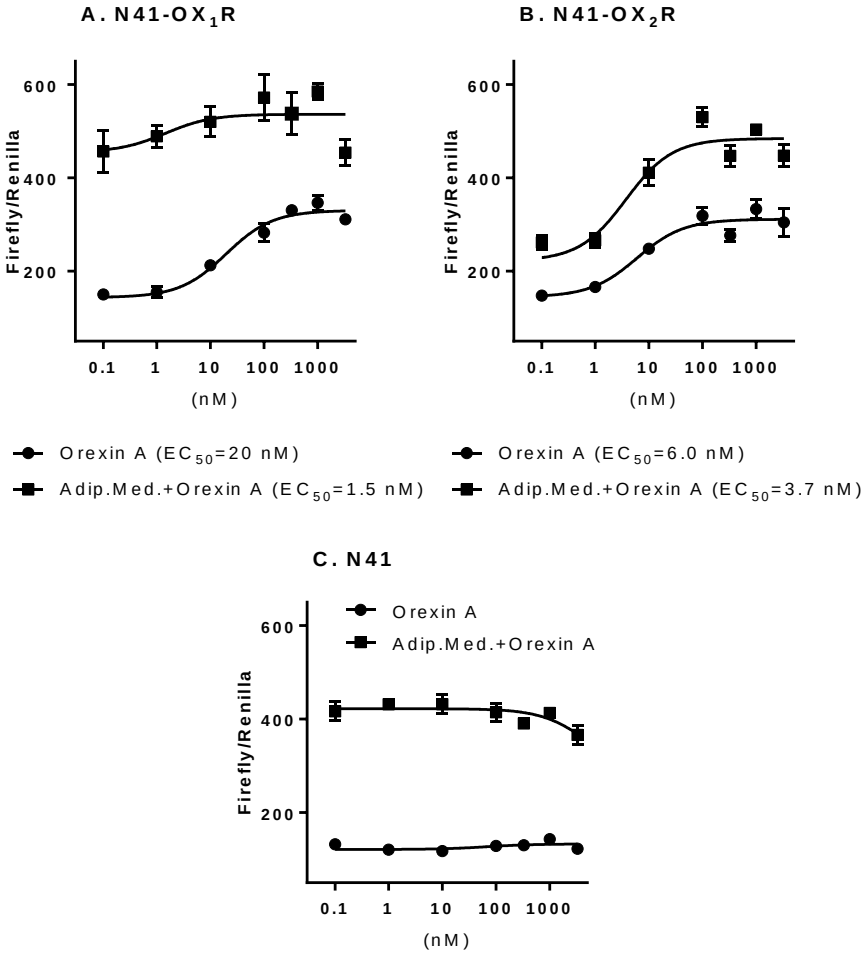

Figure 3.3.16.: Orexin A and orexin A plus adipocyte primed medium doses dependent Elk-1 activation in mHypoE-N41-OX_1R and mHypoE-N41-OX_2R cells. *Elk-1* reporter gene assay was performed using different concentrations of orexin A in control or adipocyte primed medium in (**A**.) mHypoE-N41-OX_1R, (**B**.) mHypoE-N41-OX_2R cells and (**C**.) mHypoE N41 cells as negative control; n = 4 wells of one transfection experiment.

In all three cell lines, Elk-1 activity was higher in cells incubated with adipocyte primed medium compared to control medium. Elk-1 activity in mHypoE-N41-OX_1R cells seems to be already above orexin saturation in adipocyte primed medium without orexin A and slightly increased with raising orexin A concentrations. The curve does not clearly indicate saturation of the orexin A effect in adipocyte primed medium but the EC_{50} shifted from 20 nM in control medium to 1.5 nM in the presence of adipocyte primed medium (Figure 3.3.16 A.). In mHypoE-N41-OX_2R cells the orexin A effect is elevated in adipocyte primed medium, but still shows a distinct doses response and saturation, with EC_{50} values of 6.0 nM in control medium and 3.7 nM in the presence of adipocyte primed medium (Figure 3.3.16 B.).

In mHypoE N41 control cells the adipocyte medium leads to a high increase in Elk-1 activity that appears to be slightly inhibited with higher concentrations of orexin A, whereas orexin A did not change Elk-1 activity in control medium (Figure 3.3.16 C.)

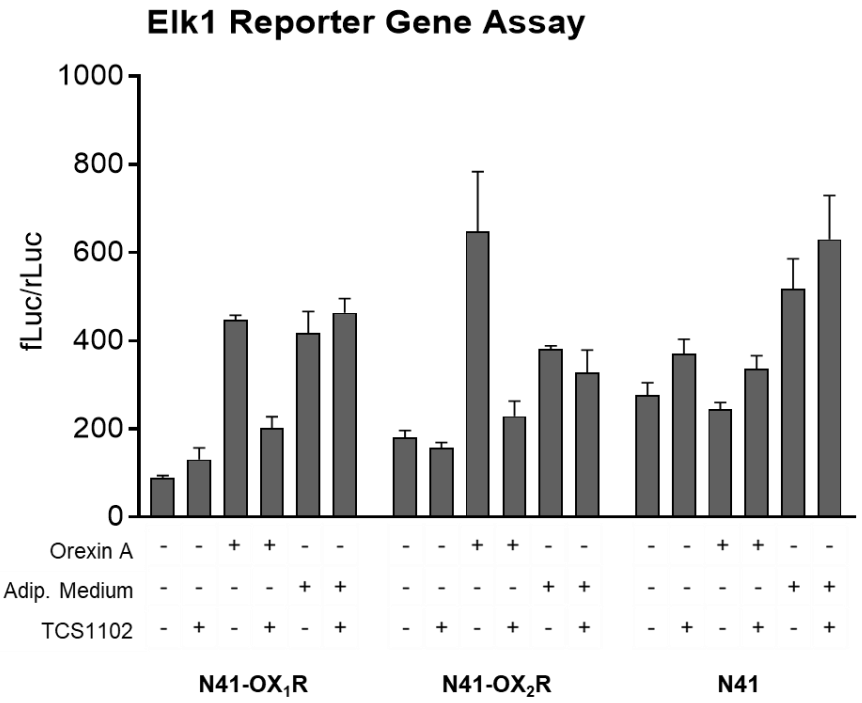

Figure 3.3.17.: Elk-1 reporter gene assay in mHypoE-N41-OX_1R and mHypoE-N41-OX_2R cells. Fold change of fLuc/rLuc after 5 h treatment with 1000 nM orexin A or adipocyte-primed medium alone or after pre-incubation with 10 µM dual orexin receptor antagonist TCS 1102, mHypoE-N41 cells served as control; n = 3 samples from one transfection experiment.

In a follow-up experiment mHypoE-N41-OX_1R, mHypoE-N41-OX_2R and mHypoE N41 control cells were treated with 1000 nM orexin A or with adipocyte-primed medium without pre-treatment or pre-treated with the dual orexin receptor antagonist TCS 1102 (Figure 3.3.17). Inhibition with the orexin receptors inhibitor TCS 1102 tests the involvement of orexin receptors in Elk-1 activation after the different treatments.

All samples showed an increase after orexin A or apipocyte-primed medium treatment in fLuc/rLuc ratio relative to control samples without treatment. This increase was reduced in orexin A but not in adipocyte-primed medium treated cells when cells were pre-incubated with 10 µM TCS 1102. TCS1102 pre-incubation alone did not result in an increase in Elk-1 activity. In mHypoE N41 control cells, only the adipocyte-primed medium influenced Elk-1

activity, which was also not clearly inhibited or reduced when cells were pre-incubated with TCS1102.

The effect of TCS1102 pre-incubation on Elk-1 activation was further investigated by testing different concentrations of TCS1102 in control medium, with 1000 nM orexin A or adipocyte-primed medium treatment in mHypoE-N41-OX_1R, mHypoE-N41-OX_2R and, as control, mHypoE N41 cells (Figure 3.3.18).

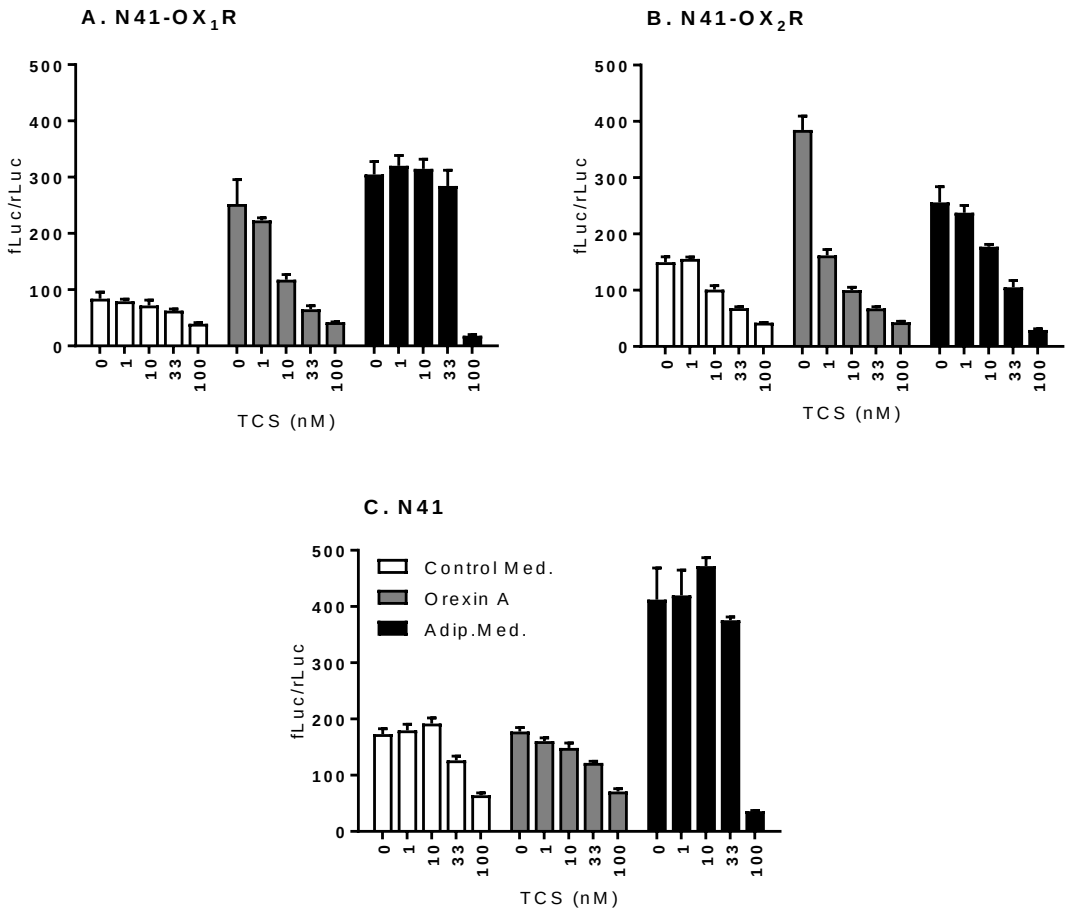

Figure 3.3.18.: Effect of TCS1102 concentration on *Elk-1* reporter gene assay in mHypoE-N41-OX_1R and mHypoE-N41-OX_2R cells. Fold change of fLuc/rLuc after pre-incubation with different concentrations of the dual orexin receptor antagonist TCS1102 and 5 h treatment with either 1000 nM orexin A or adipocyte-primed medium in (**A.**) mHypoE-N41-OX_1R, (**B.**) mHypoE-N41-OX_2R and (**C.**) mHypoE N41 cells as control; n = 4 wells of one transfection experiment.

TCS1102 inhibited orexin A-induced Elk-1 activation in both, mHypoE-N41-OX_1R and mHypoE-N41-OX_2R cells in lower starting at concentrations of 10 nM in mHypoe-N41-OX_1R cells (Figure 3.3.18 A.) and of 1 nM in mHypoE-N41-OX_2R cells (Figure 3.3.18 B.). This inhibition was even more effective with increasing TCS1102 concentrations. A pre-incubation with 100 nM even inhibits adipocyte-primed medium- incuced Elk-1 activation in all three cell lines.

In addition to orexin receptor antagonism, MAPK/ERK and SHP1/2 pathway inhibition were tested regarding their effect on Elk-1 activation induced by treatment with either orexin A or adipocyte-primed medium in mHypoE-N41-OX_1R, mHypoE-N41-OX_2R and as control mHypoE N41 cells (Figure 3.3.19).

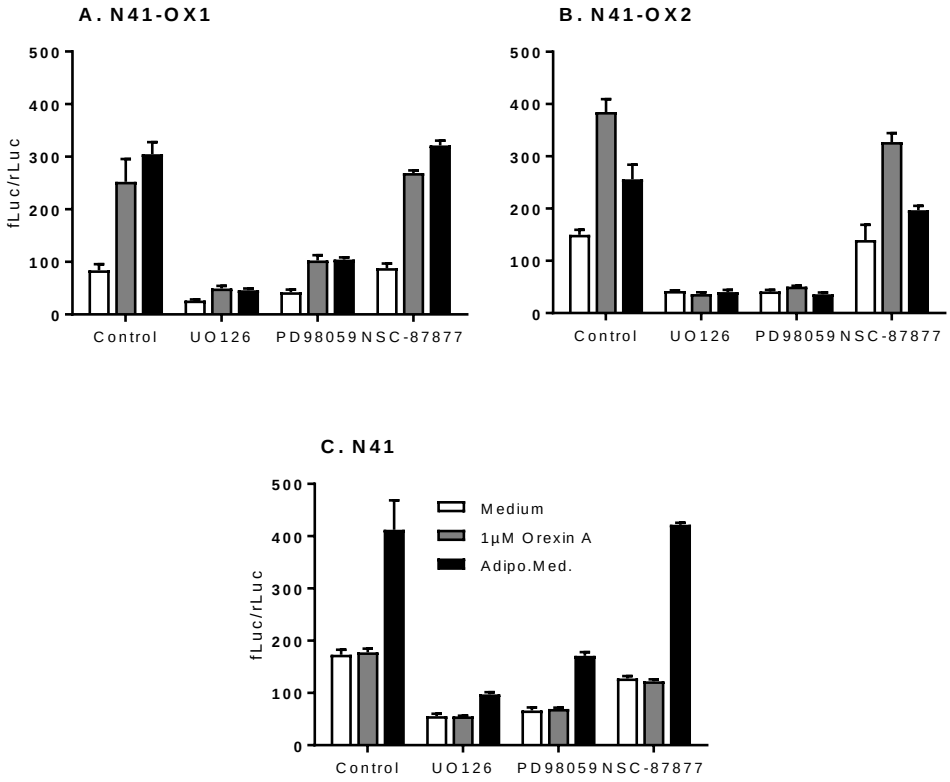

Figure 3.3.19.: Effect of different antagonists on *Elk-1* reporter gene assay in mHypoE-N41-OX_1R and mHypoE-N41-OX_2R cells. Fold change of fLuc/rLuc after pre-incubation with 10 µM MAPK/ERK inhibitor UO126 and PD98059 or the inhibitor of SHP-1 and SHP-2 protein tyrosine phosphatases (NSC-87877) and 5 h treatment with either 1000 nM orexin A or adipocyte-primed medium in (**A.**) mHypoE-N41-OX_1R, (**B.**) mHypoE-N41-OX_2R and (**C.**) mHypoE N41 cells as control; n = 4 wells of one transfection experiment.

Both MAPK/ERK pathway inhibitors, UO126 and PD98059 clearly inhibited Elk-1 activation induced by orexin A or adipocyte-primed medium in mHypoE-N41-OX_1R and mHypoE-N41-OX_2R (Figure 3.3.19 B.) cells, although Elk-1 activation was not completely reduced in mHypoE-N41-OX_1R cells (Figure 3.3.19 A.). When SHP-1 and SHP-2 protein tyrosine phosphatases were inhibited by pre-incubation with NSC-87877, the orexin A and the adipocyte-primed medium stimulated Elk-1 activity was not affected.

3.3.3 LepRb-ZsGreen *mice as model*

3.3.3.1 Co-localisation study of LepR and orexin receptors via FISH

For FISH experiments, that were designed to determine possible shared target neurons for orexins and leptin via co-localisation of OX_1R or OX_2R and LepR in LepRb-ZsGreen mice, RNA probes in antisense orientation to OX_1R and OX_2R were prepared.

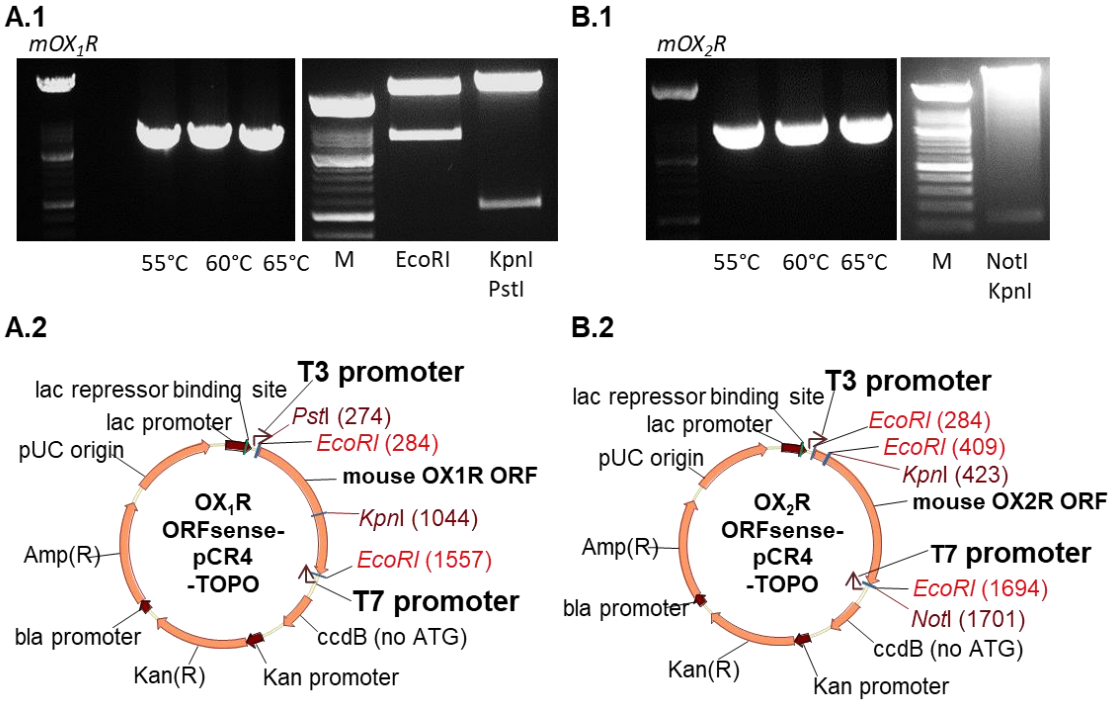

Figure 3.3.20.: Cloning of OX_1R and OX_2R RNA-probes for FISH. (**A.1**) OX_1R or (**B.1**) OX_2R sequences were amplified by PCR and the product cloned into the (**A.2/B.2**) pCR4-TOPO vector. (**A.1.**) A test restriction with *EcoR*I or *Kpn*I and *Pst*I gave information about the cloning success and gene orientation within the plasmid. (**B.1.**) A test restriction with *Not*I and *Kpn*I gave information about the cloning success and gene orientation within the plasmid.

The DNA for mouse OX_1R (Figure 3.3.20 A.1) and mouse OX_2R (Figure 3.3.20 B.1) were amplified via PCR using pCMV-OX_1R and pCMV-OX_2R plasmids as templates. The PCR products were separated via 1.5 % agarose gel electrophoresis and bands at the OX_1R and OX_2R size of 1316 and 1270 bp respectively purified and cloned into the pCR4-TOPO vector for *in vitro* transcription (Figure 3.3.20 A.1 and B.1).

For the pCR4-TOPO vector containing the *OX_1R* sequence, a test restriction with *Eco*RI at the restriction sides at 284 bp and 1557 bp was performed to test for PCR product insertion and *Kpn*I and *Pst*I digesting the plasmid DNA at 1044 bp or 787 bp and 274 bp determined the orientation of the PCR product within the plasmid. If the DNA was inserted in sense orientation when transcribed from the promoter specific for the bacteriophage T3 RNA polymerases the digestion resulted in fragments of 1,273 and 3,939 bp for *Eco*RI and 770 and 4,442 bp for *Kpn*I and *Pst*I restriction (Figure 3.3.20 A.1).

The orientation of *OX_2R* in pCR4-TOPO vector was determined via restriction with *Not*I and *Kpn*I at 1,701 bp and 423 or 1,555 bp, depending on the orientation (Figure 3.3.20 B.1). If *OX_2R* was inserted in sense orientation when transcribed from the T3 promoter restriction resulted in fragments of 4,071 and 1,278 bp, if it has antisense orientation the fragments were 138 and 5211 bp, as seen in Figure 3.3.20 B.1. *OX_1R* and *OX_2R* RNA probes were produced using the vectors tested in Figure 3.3.20 A.1 and B.1, taking the orientation of the sequence within the plasmid into account by *in vitro* transcription with the MAXIscript®T7/T3 Transcription Kit (Ambion).

The overview of the hypothalamic area of LepRb-ZsGreen mice brain sections after *OX_1R* FISH did not reveal distinct Cy5 (red) signals under the confocal microscope that were different from the hybridisation with sense probes (Figure 3.3.22), while ZsGreen cells were detected as usually in brain sections of these mice (Figure 3.3.21 A.1).

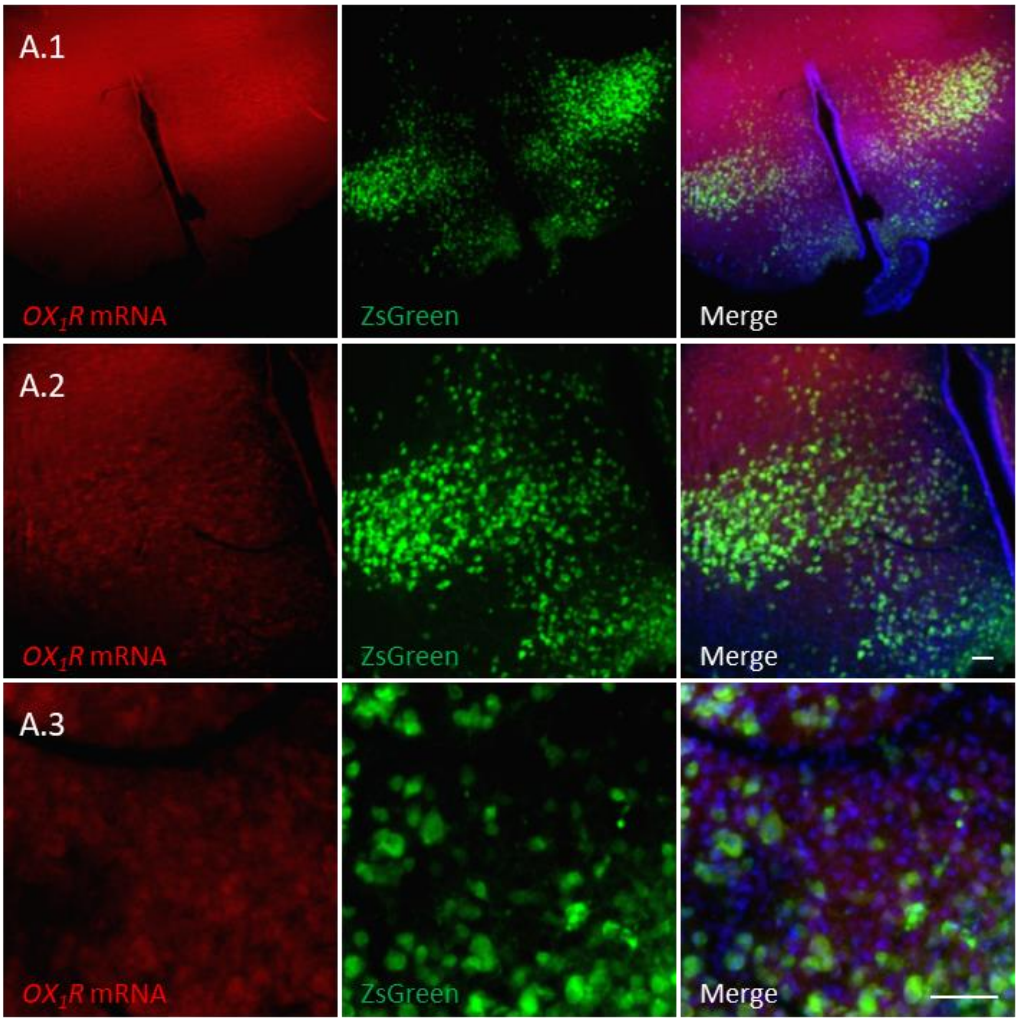

Figure 3.3.21.: *OX_1R* FISH in LepRb-ZsGreen mice brain sections. Hybridised anti-sense RNA-probes of *OX_1R* are labelled with Cy5 (Red) and ZsGreen expressing cells (green). Both Channels were merged with each other and DAPI (blue) to investigate possible co-localisations in (**A.1**) an overview of the brain sections hypothalamic area (**A.2**) 20-fold and (**A.3**.) 63-fold magnification. Bars are indicating 50 µm.

In higher magnifications of 20x (Figure 3.3.21 A.2) or 63x (Figure 3.3.21 A.3) there were also no explicit Cy5 signals, that indicated hybridised and labelled *OX_1R* probes, detectable. Results for *OX_2R* FISH resembled the results of *OX_1*R FISH with no specific hybridisation signals when incubated with antisense RNA probes.

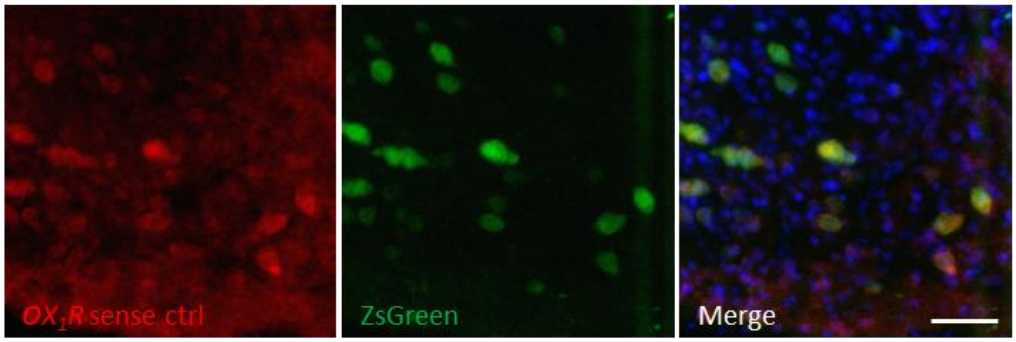

Figure 3.3.22.: Negative control for *OX_1R* FISH in LepRb-ZsGreen mice brain sections. FISH with RNA-probes of *OX_1R* in sense orientation were used as negative control for and compared to *OX_1R* FISH. The figure shows confocal microscope pictures in 63-fold magnification of the Cy5 and ZsGreen channel alone and merged with DAPI. Bar indicates 50 µm.

3.3.3.2 Fluorescent activated cell sorting of cells dissociated from LepRb-ZsGreen *mouse hypothalami*

In addition to experiments using hypothalamic cell lines, LepRb receptor expressing neurons were isolated using fluorescence-activated cell sorting (FACS) in a first attempt.

Dissociated cells of LepRb-ZsGreen mouse hypothalami were sorted into ZsGreen positive (+) and ZsGreen negative (-) cells by fluorescent activated cell sorting (FACS). The comparison of mRNA expression profiles of the two samples could reveal co-expression of orexin receptors and LepR and therefore possible shared target neurons for leptin and orexin.

The sorting success was determined via fluorescent microscopy after FACS. Many cells in ZsGreen(+) samples were fluorescent (Figure 3.3.23 B.) while in ZsGreen(-) samples no fluorescent cell could be detected (Figure 3.3.23 A.). In general, ZsGreen(-) samples contained a higher number of cells then ZsGreen(+) samples that showed a rounded phenotype yet were still intact after the cell dissociation protocol and FACS.

The sorted cells were pelleted, and RNA extracted for cDNA synthesis and PCR. PCR for the housekeeping gene *ß-actin* served as control for RNA content of the samples and *LepR* PCR served as a second assessment of the sorting result. PCR products were separated via 1.5 % agarose gel electrophoresis and screened for DNA fragments of 239 bp for *ß-actin* and 126 bp for *LepRb (1)* (Figure 3.3.23 C.). The figure shows one of various FACS experiments with similar outcome, as an example.

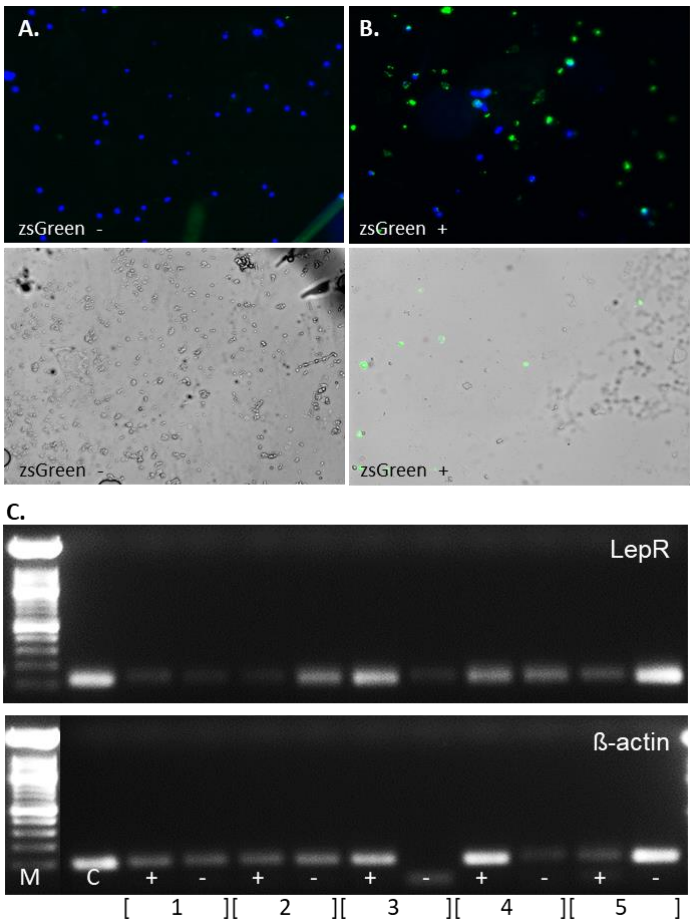

Figure 3.3.23.: Fluorescent activated cell sorting (FACS) success was determined via fluorescent microscopy after FACS of (A.) ZsGreen negative (-) and (B.) ZsGreen positive (+) samples. (C.) The gel pictures show a second assessment of sorting results by *LepRb* and *ß-actin* PCR in ZsGreen(-) and ZsGreen(+) samples compared to cDNA prepared from whole hypothalamus RNA. Numbers indicated sorting event and (+) and (-) ZsGreen(+) and (-) samples.

The control was positive for *ß-actin* and *LepR*. Furthermore *ß-actin* was determined in the ZsGreen(+) and - sample from sorting 1, 2, 4 and 5 and the ZsGreen(+) sample of sorting 3. Bands for *ß-actin* in 3+, 4+ and 5- show a similar intensity as the control, 4- is barely detectable, while all others show lesser intensity then control. *LepRb* bands were most intense in control, 2-, 3+, 4+ and 4- and 5- but also, albeit weakly, detected for all other samples. Summarising all FACS experiments, no clear results could be obtained mainly due to poor RNA recovery after extraction.

4 Discussion

In this thesis, possible interactions of orexins and leptin were systematically investigated by using LepRb-ZsGreen mice for co-localisation studies of either prepro-orexin and the LepRb for direct effects of leptin on orexin neurons or orexin receptors and LepRb to find possible shared target neurons of leptin and orexin. Furthermore intracellular pathways which might be regulated by leptin and/or orexin treatment were analysed using immortalised hypothalamic cell lines as *in vitro* model.

4.1 ZsGreen is eutopically expressed in LepRb positive cells of LepRb-ZsGreen mice.

An early *in situ* hybridisation study already showed high LepRb expression in the arcuate nucleus, that was expected due to known effects of leptin on metabolism and food regulation, but the receptor was additionally detected in a vast number of further brain regions in the mouse brain (Mercer et al., 1996). LepR-like immunoreactivity is also widely distributed in the rat brain including the choroid plexus, cerebral cortex, hippocampus, thalamus, and hypothalamus (Hakansson et al., 1998; Horvath et al., 1999), which can also be seen in brain sections of LepRb-ZsGreen mice. The functionality of expressed LepRb in the mouse brain was proven by signal transducer and activator of transduction 3 (STAT3) *in situ* hybridisation labelling after different durations of leptin treatment compared to treatment with NaCl (Mütze et al., 2006).

The expression of ZsGreen in vibratome sections of LepRb-ZsGreen mice was compared to the literature on LepRb mRNA in rat, adult and postnatal wild-type mouse brains (Elmquist et al., 1998; Scott et al., 2009; Caron et al., 2010) and EYFP distribution in LepRb-Cre/EYFP reporter mouse brains (Scott et al., 2009) . ZsGreen expression in LepRb-ZsGreen mice was similar to the distribution of *LepRb mRNA* and activated neurons by leptin as indicated by Stat3 phosphorylation (Table 4.1.1). In addition, the ZsGreen expression in LepRb-ZsGreen mice showed high consistency with previously published data on EYFP expression in Leprb neurons (Scott et al., 2009). The detection of fluorescence was further improved in the LepRb-ZsGreen mice presented here when compared to LepRb-EYFP mice since in LepRb-ZsGreen fluorescence can be easily detected whereas in LepRb-EYFP mice an additional step applying immunohistochemical staining of EYFP was nessessary (Scott et al., 2009).

Table 4.1.1: Comparison of literature on LepRb to ZsGreen distribution in LepRb-ZsGreen mice (exemplary on hypothalamic areas)

Brain region	LepRb mRNA, rat brain [1]	LepRb mRNA in WT mouse brain [2]	Leptin sensitive cells adult mouse (Stat3) [3]	Leptin sensitive cells postnatal mouse (Stat3) [3]	ZsGreen in LepRb-ZsGreen mouse brain
Medial preoptic area		xxx			
Median preoptic nucleus		xx	xxx(x)	xxx	
Retrochiasmatic area		xxxx	x	xx	
Arcuate nucleus	xxx	xxxx	xx	xxx	xxxx
Ventromedial nucleus, central		xx	-	xxx	
Ventromedial nucleus, dorsomedial	xxx	xxx	-	xxx	xxx
Lateral hypothalamic area	xx	xx	x	xx(x)	xx
Dorsomedial nucleus, dorsal		xxx			
Dorsomedial nucleus, ventral		xxx	x	xxx	xxxx
Ventral premammillary nucleus	xx	xxx	xxx(x)	xxxx	xxx
Posterior hypothalamic area	xx	xx	-	-	xxx
Posterior periventricular nucleus	xxx		xx	xx	x
Dorsomedial nucleus, caudal	xxx		x	x	
Dorsomedial nucleus, anterior	xx		x	xx	
Medial mammillary nucleus	xx		-	-	

x, xx, xxx, and xxxx indicate low, medium, strong, and very strong expression/activation. – indicates the absence of expression/activation. Fields were left empty if no data were available.

1 (Elmquist et al., 1998)

2 (Scott et al., 2009)

3 (Caron et al., 2010)

All LepRb mRNA expressing areas found in rats (Elmquist et al., 1998) or wild-type mice (Caron et al., 2010) via *in situ* hybridisation were also found and even expanded in *LepRb* mRNA, EYFP and STAT3 labelling studies of LepRb-Cre EYFP reporter mice (Scott et al.,

2009). The only exception is the choroid plexus, that was only investigated in rat brains where it showed very high *leptin receptor* mRNA expression, although the hybridisation probe specific to *LepRb* did not detect the corresponding mRNA (Elmquist et al., 1998). However, co-expression of long and short leptin receptor isoforms and the functionality of LepRb in STAT3 signalling was shown in cell lines derived from choroid plexus epithelial cells (Merino et al., 2006).

Genetically labelled cells in reporter mouse lines are usually easier to detect than immunohistochemically labelled targets or targets detected by *in situ* hybridisation, because once the floxed reporter gene is activated by cre, its expression is not regulated, whereas labelling efficacy with probes or antibodies can be restricted by their specificity, the amount of target mRNA/protein, the quality of brain sections and variables in the experimental procedure. Differences in the detection of EGFP labelled EYFP or EYFP itself in LepRb-Cre-EYFP reporter mice and ZsGreen expression in LepRb-ZsGreen reporter mice could be attributed to the highly efficient fluorescence of ZsGreen compared to EGFP or EYFP (Scott et al., 2009; Nakamura et al., 2013).

As mentioned earlier, ZsGreen expression in some LepRb-ZsGreen mice of the colony was ectopic and found throughout the whole brain and body. These mice could not be distinguished by geno- but phenotype. Their eyes, tale and paws showed a slight yellow colour change compared to their littermates and organs like the brain or fat tissue had a strong, bright yellow colour. This ectopic ZsGreen expression could originate from a single animal that was not detected before being used for breeding, since this colony derives from a single pair of LepRb-ZsGreen mice. Possibly this mouse had a mutation in LepRb expression and once the *LepRb* gene was expressed in a cell, cre is active and leads to ZsGreen expression regardless of the current state of LepRb expression

4.2 LepRb is not expressed in orexin neurons indicating an indirect effect of leptin on orexin neurons.

For a direct effect of leptin on orexin neurons, the LepRb must be expressed in the orexin neurons in the lateral hypothalamic area (LH). This expression of LepR in orexin neurons as well as STAT3 activation in these has been previously suggested in multiple labelling studies, that used different orexin or hypocretin and LepR antisera (Hakansson et al., 1999; Horvath et al., 1999). In the ovine brain immunohistochemical labelling indicated that 100 % of orexin expressing neurons also contain the LepRb (Iqbal et al., 2001). Furthermore,

leptin has been shown to directly inhibit primary orexin neurons that were isolated from mouse hypothalami (Yamanaka et al., 2003b)

While LepRb expressing cells in LepRb-ZsGreen mice are already labelled by ZsGreen, orexin cells had to be labelled via *in situ* hybridisation to investigate a possible co-localisation of the two proteins.

The antisense RNA probes used to label orexin neurons were against the mouse orexin A and B precursor protein prepro-orexin (PPO) mRNA. The respective DNA sequence was amplified from a PPO-pCMV plasmid via PCR, purified from the electrophoresis gel and cloned into the pCR4-TOPO vector, which contains T3 and T7 promoter for *in vitro* transcription of plasmid DNA into labelled sense and antisense RNA probes, using the MAXIscript®T7/T3 Transcription Kit (Ambion). The cloning success and orientation of the gene within the plasmid was proven by test restriction. The specificity of the final probe was shown by control FISH with PPO sense probe, which showed no distinct signal in contrast to FISH with PPO antisense probe. Furthermore, the Cy5 signal after FISH with *PPO* antisense probe was accurately limited to the LH, where orexin is produced (de Lecea et al., 1998; Sakurai et al., 1998). Therefore, it can be concluded that PPO antisense probes strictly hybridise to PPO within the brain sections and Cy5 fluorescence is equivalent to PPO expression.

The brain sections were analysed computationally with the plugin JACoP (**J**ust **A**nother **Co**-localisation **P**lugin) for ImageJ software. The initial pixel-based co-localisation analysis came out positive for up to 4 % of the PPO labelled pixels also showing fluorescence for ZsGreen. Pearson's and Manders split coefficients were therefore slightly above zero. Consequently, the results were re-analysed based on whole objects/cells. The object-based analysis came out positive for a comparably low fraction of all cells. Visual examination of these positive co-localisation results revealed, that these results accounted to cells in close proximity to each other, each showing the fluorescent signal of only one fluorescent channel. Thus, all the detected co-localisations by JACoP of PPO mRNA and the LepRb can be regarded as false-positives.

In conclusion, after visual and computational analysis of FISH on sections of three whole mouse hypothalami, no cell co-localising PPO and LepRb was found. To make sure that the strong fluorescent signal of ZsGreen in LepRb positive cells did not quench or cover a co-localised Cy5 signal, a control FISH was performed with labelled anti proopiomelanocortin (POMC) oligonucleotides. POMC neurons are known to be directly

regulated by leptin and therefore express the LepRb (Balthasar et al., 2004; van de Wall et al., 2008; Rahmouni, 2012). The visual and computational analysis of POMC FISH showed that Cy5 fluorescence, which visualised hybridised POMC probes, was distinctly detected in the arcuate nucleus and 17.2 % of POMC labelled cells also expressed the LepRb. Thus, co-localisation is detectable after FISH in ZsGreen expressing cells. The fraction of POMC expressing LepRb is consistent with results of a single cell mRNA expressing study via droplet-sequencing (Drop-seq), where three subpopulations of POMC neurons were distinguished, of which only one expressed *LepR* mRNA (Campbell et al., 2017). The results of the present FISH study show no expression of LepRb in orexin neurons and therefore no possibility of direct regulation of orexin neurons by leptin. While contradicting results of various studies showing co-localisation by immunohistochemical labelling (Hakansson et al., 1999; Horvath et al., 1999; Iqbal et al., 2001) or direct inhibitory effects of leptin on isolated orexin neurons (Yamanaka et al., 2003a), the results of the present study confirm more recent studies on a rather indirect effect of leptin on orexin neurons through neurotensin expressing neurons in the LH (Goforth et al., 2014; Gjerde, 2015). The inconsistency with the multiple labelling studies may result from non-specific binding of antisera against orexin and/or LepR or the difficulty of immunohistochemistry of receptors, due to their very low and membrane bound protein expression within the brain tissue.

4.3 Orexin and leptin interaction merges at the same target cells

Orexin and leptin effects may also merge at shared target cells, which express orexin receptors and LepRb. The ERK1/2 pathway is activated by orexins and leptin, therefore serves as a possible molecular interaction side of the two peptides (Ammoun et al., 2006a; Johansson et al., 2007; Tang et al., 2008; Rahmouni, 2012; Leonard, 2014). It has been shown that NPY and POMC expressing cells, that also contain the LepRb are innervated by orexin neurons (Horvath et al., 1999; Funahashi et al., 2000; Guan et al., 2001; Muroya et al., 2004a), are responsive to orexin A (Rauch et al., 2000) and show immunoreactivity for OX_1R (Funahashi et al., 2003). Furthermore, Ca^{2+} influx is increased by direct stimulation with orexin A in NPY neurons and decreased in POMC neurons of the arcuate nucleus in which leptin shows an opposite effect compared to orexin A (Muroya et al., 2004b).

4.3.1 Immortalised hypothalamic cell lines mHypoE N25/2 and mHypoE N41 as *in vitro* model neurons

To study the activity of leptin and orexins on shared target neurons the murine, immortalised, embryonic, hypothalamic cell lines mHypoE N25/2 and mHypoE N41 were purchased from CELLutions Biosystems (Ontario, Canada), based on their profile that claimed they would express LepRb, OX_1R, OX_2R, NPY and POMC (Belsham et al., 2004; CellutionsBiosystemsInc., 2009). Before conducting further experiments, the expression of all three receptors was confirmed in both cell lines via qPCR. The first experiment on NPY regulation by orexin A or B and/or leptin treatment was conducted for 6 different time points to screen for a timeframe in which the treatments show an effect since the regulation of mRNA could occur very quickly within 15 min but also slowly and may take up to multiple hours. In an initial experiment, the strongest NPY regulation in mHypoE N41 cells was found after orexin B treatment for 30 min, 1 h and 3h, which was attenuated when co-treated with leptin and orexin A treatment for 3 h. In mHypoE N25/2 cells, orexin A and B treatment for 3 h let to the strongest increase in NPY. Therefore, these three timepoints of 30 min, 1 h and 3 h treatment were repeated to confirm the initial results. However, the regulation of NPY was very inconsistent and had high deviations throughout the three experiments in both cell lines. The investigation of POMC regulation resulted in comparably irregular outcomes. Orexins activate the mitogen-activated protein kinase (MAPK) pathway (Wenzel et al., 2009). However, in mHypoE N41, mHypoE N25/2 and mHypoA 2/23 cells orexin A treatment exhibited no phosphorylation of the MAPK downstream protein extracellular signal-regulated kinase (ERK1/2) indicating that these cell lines are not responsive to orexins. Although other immortalised murine hypothalamic cell lines from CELLutions Biosystems (Ontario, Canada) were successfully used as *in vitro* models to study endocrine systems of the hypothalamus, for instance leptin and insulin driven regulation in POMC expressing cells (Cai et al., 2007), inhibition of agouti-related peptide (AgRP) expression by glycolysis (Cheng et al., 2008), leptin effects in neurotensin expressing cells (Cui et al., 2005, 2006) and even NPY positive neurons (Dhillon and Belsham, 2011), the results of experiments presented here lead to the conclusion that mHypoE N41, mHypoE N25/2 and mHypoA 2/23 cells are not suitable for conclusive *in vitro* experiments of leptin-orexin interactions in the hypothalamus. Recently, the expression of OX_1R and a Ca^{2+} response to orexin A as well as the phosphorylation of ERK1/2 by orexin A was described in mHypoE N41 cells (Imperatore et al., 2016). With the present experiments these data cannot be confirmed. The reason for this discrepancy remains unclear. Clear responses to orexins

were obtained in the present study when mHypoE N41 cells stably transfected with human OX_1R or OX_2R were used indicating the functionality of the methods used here.

When mHypoE N41, mHypoE N25/2 or mHypoA 2/23 cells were treated with medium without antibiotics or serum, that was usually used for experiments with mHypoE/A cells, but now primed by cultured adipocytes for 48 h, ERK1/2 was significantly phosphorylated after 5 or 30 min of incubation. This effect indicated that cultured adipocytes may secrete a compound with MAPK pathway activating abilities in these hypothalamic cell lines into the medium.

4.3.2 mHypoE-N41-OX_1R and mHypoE-N41-OX_2R cells as *in vitro* model for orexin receptor expressing neurons

There was no effect of orexins detected in mHypoE N41, mHypoE N25/2 or mHypoA 2/23 cells, possibly due to low and/or not functional expression of OX_1R and OX_2R in these cell lines. For conclusive orexin experiments in hypothalamic cells, mHypoE N41 cells were stably transfected with human OX_1R or OX_2R, which led to the two new cell lines mHypoE-N41-OX_1R and mHypoE-N41-OX_2R (Wang et al., 2014b). The high expression of human OX_1R and human OX_2R in mHypoE-N41-OX_1R and mHypoE-N41-OX_2R cells respectively compared to mHypoE N41 cells was verified via qPCR before conducting further experiments. Orexin A and B application induced Ca^{2+} influx in both stably transfected but not in normal mHypoE N41 cells, which proves the functionality of the transfected orexin receptors. The differing intensity of Ca^{2+} influx in mHypoE-N41-OX_1R cells after orexin A and B treatment reflects the higher affinity of orexin A then orexin B to OX_1R, while the similar affinity for both orexins to the OX_2R is also represented in the Ca^{2+} influx experiments with mHypoE-N41-OX_2R cells (Sakurai et al., 1998).

A possible interaction of the adipocyte-primed medium and orexin was studied at ERK1/2 phosphorylation levels. Orexin A and adipocyte-primed medium alone both increased pERK1/2 amount in mHypoE-N41-OX_1R and mHypoE-N41-OX_2R, but this effect was only altered by slight but not significant further elevation of pERK1/2, when mHypoE-N41-OX_1R cells were co-treated with orexin A and adipocyte-primed medium for 10 min. Overall, orexin A or adipocyte-primed medium had a stronger effect on mHypoE-N41-OX_2R cells. Thus, adipocytes may secrete compounds that activate the MAPK pathway in the hypothalamic cell lines and orexin A and B also enable MAPK activity in these hypothalamic cell lines containing human orexin receptors, but their effect on ERK1/2 phosphorylation is not altered

by co-treatment of the two cell lines. Therefore, it can be concluded that orexin A or B don't interact with adipocyte-primed medium at the level of ERK1/2 phosphorylation. To better characterise the effect of adipocyte-primed medium on the hypothalamic cell lines it must be determined what compound is secreted by adipocytes into the medium.

To achieve a higher throughput of samples than obtained by the Western-blot analyses, a dual luciferase reporter gene assays was used investigating reporter gene activation by co-expression of firefly luciferase under the control of an Elk-1-sensitive promoter that is normalised to the expression of renilla luciferase under the control of a constantly active promoter, like the herpes simplex virus thymidine kinase (TK). In mHypoE-N41-OX_1R and mHypoE-N41-OX_2R cells, the activity of Elk-1, a transcription factor that is among others activated by the MAPK/ERK1/2 pathway, was measured. In this assay Elk-1 activates a promoter that is cloned upstream of the luciferase reporter gene (Lhoták V, 1991; Janknecht R, 1992; Jantti et al., 2013). Cells from the two cell lines were transfected with the plasmids pSG-GalElk-1 (Kortenjann M, 1994; Jantti et al., 2013), pGL3 G5 E4 D38 (Jantti et al., 2013) and pRL-TK (Promega) and treated with different concentrations of orexin A or B or adipocyte-primed medium to investigate their effect on Elk-1 activity. Orexin A and B increased the activity of Elk-1 in a doses dependent manner in mHypoE-N41-OX_1R and mHypoE-N41-OX_2R but not in mHypoE N41 cells, which also demonstrates the functionality of the human orexin receptors in these cell lines. Adipocyte-primed medium also led to elevated Elk-1 activity, but in all three cell lines, which indicates an effect of the medium that is not dependent on orexin receptor signalling.

When mHypoE-N41-OX_2R cells were treated with orexin A and adipocyte-primed medium together Elk-1 activity was increased but still showed dose dependency to orexin A. mHypoE-N41-OX_1R and mHypoE N41 control cells showed very strong Elk-1 activation, when adipocyte primed medium was co-applied, but no doses dependend reaction to orexin A. Possibly, these cell lines are more sensitive to the compounds secreted by adipocytes and, therefore, MAPKs are already fully activated. Diluting the medium with unprimed control medium and testing different dilutions on mHypoE-N41-OX_1R cells could reveal if its effect on Elk-1 activation can be reduced, so that the cells still show a dose dependency to orexin A. OX_1R antagonism has been shown to have anti-obese and anti-diabetic effects in rats and ob/ob mice (Haynes et al., 2000; Haynes et al., 2002), while for OX_2R an increase in signalling has been proven to prevent diet induced obesity (Funato et al., 2009). These contrarious functions of the two orexin receptors could be reflected in their sensitivity to the adipocyte primed medium. In any case, these results need to be confirmed in further

independent experiments, since they derive from multiple samples but within the same transfection experiment.

Elimination of orexin A effects through pre-incubation with the dual orexin receptor antagonist TCS1102 shows that orexin receptors play a key role in the activation of the MAPK pathway in mHypoE-N41-OX_1R and mHypoE-N41-OX_2R cells, via orexin A. TCS1102 showed only an effect at high concentration of 100 nM or above on Elk-1 activation stimulated by adipocyte-primed medium. This result suggests that the MAPK pathway is activated by adipocyte-primed medium in an orexin receptor independent manner. Hence, an increase in Elk-1 activity was also observed in mHypoE N41 cells, which did not show a reaction to orexin A or B.

Testing increasing concentrations of TCS1102 on the inhibition of Elk-1 activation showed that the antagonist is more potent in mHypoE-N41-OX_2R cells, where a dose as small as 1 nM reduces orexin A-induced Elk-1 activity by 50 % already. In mHypoE-N41-OX1R cells the same reduction was reached by a pre-incubation with 10 nM TCS1102. The higher potency of TCS1102 was already reported with inhibitory constants (Ki) of 3 nM and 0.2 nM for OX_1R and OX_2R respectively and is therefore in accordance to literature (Bergman et al., 2008; Winrow et al., 2010). When the cells were pre-incubated with a high concentration of 100 nM TCS1102 though, Elk-1 activity was also strongly reduced after treatment with adipocyte primed medium in all three cell lines. High doses of TCS1102 may show unspecific effects and/or might have a toxic effect on the cells resulting in cell death. The reporter gene assay measures a ratio of firefly luciferase, that indicates the expression of the tested gene and renilla luciferase, that serves as internal control for slightly varying cell numbers and transfection efficacy. Total renilla luciferase values should be within a similar range within a transfection experiment but were clearly reduced by 100 nM TCS1102, for example from 341 to 22.5 in mHypoE-N41-OX_1R cells treated with adipocyte-primed medium. The other two cell lines showed a similar decline of renilla luciferase activity after pre-incubation with 100 nM TCS1102, which could indicate a dramatic reduction of cells in these samples, which is not detectable in the analysed ratio of the two luciferases.

The effects of orexin A and adipocyte-primed medium were completely abolished by incubation with UO126 or PD98059, inhibitors of the upstream activator of ERK1/2, MAPK/ERK kinase 1 (MEK1), prior treatment, thus the reporter gene assay specifically indicates Elk-1 activation (phosphorylation) resulting from activation of the MAPK/ERK pathway.

Next to the most prominent STAT3 pathway, Leptin has been shown to also activate the MAPK/ERK pathway through SHP-2 (Poeggeler et al., 2010; Rahmouni, 2012). Orexin receptors have also been reported to activate SHP-2, through immunoreceptor tyrosine-based inhibitory motif ITIM of the receptor (Firar et al., 2009; Leonard, 2014). These findings suggested that SHP-2 was a promising target to merge leptin and orexin signalling. Therefore, SHP-2 influence on Elk-1 activation was investigated using the inhibitor of SHP-1 and SHP-2 protein tyrosine phosphatases, NSC-87877 (Chen et al., 2006). However, inhibiting SHP-1 and SHP-2 did neither reduce Elk-1 expression induced by orexin A nor by adipocyte-primed medium, indicating that their effect is independent of SHP-2.

4.3.3 LepRb-ZsGreen mice as in vivo model to analyse leptin – orexin interactions

Neurons that express LepRb are labelled by ZsGreen expression in LepRb-ZsGreen mice and FISH with antisense OX_1R or OX_2R probes provides a possibility to identify neurons that co-express OX_1R or OX_2R and LepRb and therefore might serve as shared target neurons for orexin with leptin interaction. Double labelling studies only determined OX_1R immunoreactivity in NPY and POMC neurons in the arcuate nucleus but did not investigate co-expression of LebRb in these cells (Funahashi et al., 2003). Other studies showed that the same cells were responsive to leptin and directly activated via orexin A application (Rauch et al., 2000) and that orexin neurons innervate LepRb expressing NPY and POMC neurons, where they induced Ca^{2+} influx (Horvath et al., 1999; Funahashi et al., 2000; Guan et al., 2001; Muroya et al., 2004b). All these results indirectly show that some cells must express OX_1R or OX_2R and LepRb, without labelling the receptor expression itself.

For orexin receptor FISH OX_1R or OX_2R DNA was amplified from plasmids via PCR and cloned into the pCR4-TOPO vector, like for PPO. The correct size and orientation of the sequence within the plasmid was proven via restriction analysis before using the probes for FISH experiments on brain sections of LepRb-ZsGreen mice. Under the fluorescent and confocal microscope no distinct signal for Cy5, that labelled hybridised antisense probes, was detected. Other than cytoplasmic proteins, receptors are usually lowly expressed and even tyrosine signal amplification (TSA™ Plus Cyanine 5 System, PerkinElmer™) of the hybridisation signal did not reveal explicit Cy5 fluorescent. It could be possible that the probe was too large for successful hybridisation, but even hydrolysis of the probes into smaller fragments did not improve the fluorescent signal after FISH. Because FISH experiments with antisense orexin receptor mRNA probes did not result in distinct signals, cells that express orexin receptors and LepRb could not be identified via FISH.

Separating LepRb expressing ZsGreen(+) cells from ZsGreen(-) cells, that do not express LepRb, by fluorescent activated cell sorting (FACS) provides another possibility to identify and characterise co-expression of LepRb with one or both orexin receptors. Cells from LepRb-ZsGreen mouse hypothalami were isolated and sorted according to ZsGreen fluorescence. The sorting success and cell viability after FACS was microscopically verified in ZsGreen(+) and ZsGreen(-) samples. The overall number of cells in ZsGreen(+) samples was lower than in the respective ZsGreen(-) sample because only a fraction of all hypothalamic cells expresses LepRb (Merino et al., 2006; Scott et al., 2009; Caron et al., 2010; Campbell et al., 2017). The sorted cells were meant to be characterised via RNA extraction and qPCR for orexin receptors and peptides like NPY and POMC, but RNA extraction turned out to be difficult, since most column based RNA isolation kits, that are provided by companies are designed for specific cell numbers and none in the range combining numbers of ZsGreen(+) and ZsGreen(-) samples. To get comparable results for ZsGreen(+) and ZsGreen(-) samples the RNA should be extracted with the same protocol. Different protocols were tested and cell lysis with Trizol® Reagent (ambion® life technologies™) followed by phenol-chloroform-isoamyl precipitation provided the most promising results.

PCR performed on samples from FACS and control samples derived from whole LepRb-ZsGreen mouse hypothalamus RNA revealed very low housekeeping gene *ß-actin* expression and therefore even much lower expression *of LebRb*. Although microscopic monitoring of sorting success revealed a clear division of ZsGreen(+) and ZsGreen(-) cells these results were not reflected in *LebRb* mRNA levels. The low quality and quantity of harvested RNA from FACS samples could not lead to conclusive PCR results. Possibly, FACS stressed the neurons to a point, where cells were still intact but already in a pre-apoptotic state, that does not allow the cell to maintain normal protein levels and focuses on cell survival or death instead.

4.4 Conclusion and future perspectives

Regarding possible interaction sites for orexin and leptin, the results of this study lead to the conclusion, that orexin neurons do not express LepRb and therefore cannot be regulated by leptin directly. The proximity of LebRb and orexin expressing cells in the lateral hypothalamus as revealed by fluorescent *in situ* hybridisation supports previous findings on an indirect leptin effect on orexin neurons through interneurons, which do express LepRb.

Although literature strongly suggest an interaction of orexins and leptin in shared target neurons, like NPY or POMC expressing neurons in the arcuate nucleus it turned out to be very difficult to find an appropriate *in vitro* or *in vivo* model for conclusive interaction studies. The immortalised hypothalamic cell lines mHypoE N25/2, mHypoE N41 and mHypoA 2/23 were advertised by their distributor as expressing the respective proteins, like OX_1R, OX_2R, LepR, NPY and POMC. However, the analyses of the regulation of NPY and POMC mRNA expression after orexin or leptin stimulation in this work reveal that these cell lines do not respond appropriately to orexins and leptin and thus are not suitable for coherent leptin-orexin interaction investigations. On the other hand, these cell lines showed significant responses on MAPK phosphorylation when they were treated with medium that was primed by adipocyte secretion for 48 h. In contrast, when mHypoE N41 cells were stably transfected with human OX_1R or OX_2R they showed significant and specific reactivity to orexin A and B. Together with the effect of adipocyte primed medium on the immortalised hypothalamic cell lines, the new mHypoE-N41-OX_1R and mHypoE-N41-OX_2R cell lines serve as promising *in vitro* models for further studies. First initial experiments already indicated that the effect of adipocyte-primed medium seems to be independent of orexin signalling and both orexin and adipocyte-primed medium effect were independent of the SHP1/2 pathway. Other pathways, for example STAT3 activation after treatment with adipocyte-primed medium must be investigated to identify adipocyte-primed medium and orexin signalling. Future project might be able to determine the compound secreted by adipocytes into the medium that leads to the activation of the MAPK/ERK1/2 pathway in hypothalamic cells.

Finally, mouse lines developed recently with LoxP flanked orexin receptor genes could be utilised, together with the LebRb-Cre/ZsGreen mice, to generate a new mouse line with conditional orexin receptor knock-out in LebRb expressing cells. Such a mouse line might reveal phenotypic and behavioural conclusions on the interaction of orexin and leptin in shared target cells as *in vivo* model. Moreover, possible molecular changes, for example altered NPY or POMC expression, in the hypothalamus of these mice would insinuate a link between leptin and orexin signalling in mutual target neurons.

5 References

Acuna-Goycolea C, van den Pol AN (2009) Neuroendocrine proopiomelanocortin neurons are excited by hypocretin/orexin. J Neurosci 29:1503-1513.

Akiyama M, Yuasa T, Hayasaka N, Horikawa K, Sakurai T, Shibata S (2004) Reduced food anticipatory activity in genetically orexin (hypocretin) neuron-ablated mice. Eur J Neurosci 20:3054-3062.

Ammoun S, Johansson L, Ekholm ME, Holmqvist T, Danis AS, Korhonen L, Sergeeva OA, Haas HL, Akerman KE, Kukkonen JP (2006a) OX1 orexin receptors activate extracellular signal-regulated kinase in Chinese hamster ovary cells via multiple mechanisms: the role of Ca2+ influx in OX1 receptor signaling. Molecular endocrinology 20:80-99.

Ammoun S, Johansson L, Ekholm ME, Holmqvist T, Danis AS, Korhonen L, Sergeeva OA, Haas HL, Akerman KE, Kukkonen JP (2006b) OX1 orexin receptors activate extracellular signal-regulated kinase in Chinese hamster ovary cells via multiple mechanisms: the role of Ca2+ influx in OX1 receptor signaling. Mol Endocrinol 20:80-99.

Anand BK, Brobeck JR (1951) Localization of a "feeding center" in the hypothalamus of the rat. Proc Soc Exp Biol Med 77:323-324.

Antunes VR, Brailoiu GC, Kwok EH, Scruggs P, Dun NJ (2001) Orexins/hypocretins excite rat sympathetic preganglionic neurons in vivo and in vitro. Am J Physiol Regul Integr Comp Physiol 281:R1801-R1807.

Arias-Carrión O, Herrera-Solís A, Poot-Aké A, Jiménez-Moreno R, Murillo-Rodríguez E (2015) Hypocretin (Orexin) Cell Transplantation as a New Therapeutic Approach in Narcolepsy.

Balthasar N, Coppari R, McMinn J, Liu SM, Lee CE, Tang V, Kenny CD, McGovern RA, Chua SC, Elmquist JK, Lowell BB (2004) Leptin Receptor Signaling in POMC Neurons Is Required for Normal Body Weight Homeostasis. Neuron 42:983-991.

Beck B, Richy S, Dimitrov T, Stricker-Krongrad A (2001) Opposite regulation of hypothalamic orexin and neuropeptide Y receptors and peptide expressions in obese Zucker rats. Biochem Biophys Res Commun 286:518-523.

Belsham DD, Cai F, Cui H, Smukler SR, Salapatek AM, Shkreta L (2004) Generation of a phenotypic array of hypothalamic neuronal cell models to study complex neuroendocrine disorders. Endocrinology 145:393-400.

Bergman JM, Roecker AJ, Mercer SP, Bednar RA, Reiss DR, Ransom RW, Meacham Harrell C, Pettibone DJ, Lemaire W, Murphy KL, Li C, Prueksaritanont T, Winrow CJ, Renger JJ, Koblan KS, Hartman GD, Coleman PJ (2008) Proline bis-amides as

potent dual orexin receptor antagonists. Bioorganic & Medicinal Chemistry Letters 18:1425-1430.

Boutrel B, Kenny PJ, Specio SE, Martin-Fardon R, Markou A, Koob GF, de Lecea L (2005) Role for hypocretin in mediating stress-induced reinstatement of cocaine-seeking behavior. Proc Natl Acad Sci U S A 102:19168-19173.

Bray GA (1991) Treatment for Obesity: A Nutrient Balance/Nutrient Partition Approach. Nutrition Reviews 49:33-45.

Bray GA (2004) Medical consequences of obesity. The Journal of clinical endocrinology and metabolism 89:2583-2589.

Buckingham JC (1977) The endocrine function of the hypothalamus. j Pharm Pharmac 29:649-656.

Caballero B (2007) The global epidemic of obesity: an overview. Epidemiologic reviews 29:1-5.

Cai F, Gyulkhandanyan AV, Wheeler MB, Belsham DD (2007) Glucose regulates AMP-activated protein kinase activity and gene expression in clonal, hypothalamic neurons expressing proopiomelanocortin: additive effects of leptin or insulin. The Journal of endocrinology 192:605-614.

Cai XJ, Evans ML, Lister CA, Leslie RA, Arch JR, Wilson S, Williams G (2001) Hypoglycemia activates orexin neurons and selectively increases hypothalamic orexin-B levels: responses inhibited by feeding and possibly mediated by the nucleus of the solitary tract. Diabetes 50:105-112.

Campbell JN, Macosko EZ, Fenselau H, Pers TH, Lyubetskaya A, Tenen D, Goldman M, Verstegen AM, Resch JM, McCarroll SA, Rosen ED, Lowell BB, Tsai LT (2017) A molecular census of arcuate hypothalamus and median eminence cell types. Nature neuroscience 20:484-496.

Campfield L, Smith F, Guisez Y, Devos R, Burn P (1995) Recombinant mouse OB protein: evidence for a peripheral signal linking adiposity and central neural networks. Science 269:546-549.

Caron E, Sachot C, Prevot V, Bouret SG (2010) Distribution of leptin-sensitive cells in the postnatal and adult mouse brain. J Comp Neurol 518:459-476.

CellutionsBiosystemsInc. (2009) Neuronal Cell Lines - Easy to Cilture/Stable Rat and Mouse Hypothalamic Cell Lines (And Other Cell Lines).

Chemelli RM, Willie JT, Sinton CM, Elmquist JK, Scammell T, Lee C, Richardson JA, Williams SC, Xiong Y, Kisanuki Y, Fitch TE, Nakazato M, Hammer RE, Saper CB, Yanagisawa M (1999) Narcolepsy in orexin knockout mice: molecular genetics of sleep regulation. Cell 98:437-451.

Chen L, Sung S-S, Yip MLR, Lawrence HR, Ren Y, Guida WC, Sebti SM, Lawrence NJ, Wu J (2006) Discovery of a Novel Shp2 Protein Tyrosine Phosphatase Inhibitor. Molecular pharmacology 70:562-570.

Cheng H, Isoda F, Belsham DD, Mobbs CV (2008) Inhibition of agouti-related peptide expression by glucose in a clonal hypothalamic neuronal cell line is mediated by glycolysis, not oxidative phosphorylation. Endocrinology 149:703-710.

Coleman DJ (1978) Obese and Diabetes: Two Mutant Genes Causing Diabetes-Obesity Syndroms in Mice. Diabetologia 14:141-148.

Cui H, Cai F, Belsham DD (2005) Anorexigenic hormones leptin, insulin, and alpha-melanocyte-stimulating hormone directly induce neurotensin (NT) gene expression in novel NT-expressing cell models. J Neurosci 25:9497-9506.

Cui H, Cai F, Belsham DD (2006) Leptin signaling in neurotensin neurons involves STAT, MAP kinases ERK1/2, and p38 through c-Fos and ATF1. FASEB J 20:2654-2656.

Cui H, Sohn JW, Gautron L, Funahashi H, Williams KW, Elmquist JK, Lutter M (2012) Neuroanatomy of melanocortin-4 receptor pathway in the lateral hypothalamic area. J Comp Neurol 520:4168-4183.

Dahmen N, Bierbrauer J, Kasten M (2001) Increased prevalence of obesity in narcoleptic patients and relatives. Eur Arch Psychiatry Clin Neurosci 251:85-89.

Date Y, Ueta Y, Yamashita H, Yamaguchi H, Matsukura S, Kangawa K, Sakurai T, Yanagisawa M, Nakazato M (1999) Orexins, orexigenic hypothalamic peptides, interact with autonomic, neuroendocrine and neuroregulatory systems. Proc Natl Acad Sci U S A 96:748-753.

de Lecea L, Kilduff TS, Peyron C, Gao X, Foye PE, Danielson PE, Fukuhara C, Battenberg EL, Gautvik VT, Bartlett FS, Frankel WN, van den Pol AN, Bloom FE, Gautvik KM, Sutcliffe JG (1998) The hypocretins: hypothalamus-specific peptides with neuroexcitatory activity. Proc Natl Acad Sci U S A 95:322-327.

Dhillon SS, Belsham DD (2011) Leptin differentially regulates NPY secretion in hypothalamic cell lines through distinct intracellular signal transduction pathways. Regulatory peptides 167:192-200.

Diano S, Horvath B, Urbanski HF, Sotonyi P, Horvath TL (2003) Fasting activates the nonhuman primate hypocretin (orexin) system and its postsynaptic targets. Endocrinology 144:3774-3778.

Dube MG, Kalra SP, Kalra PS (1999) Food intake elicited by central administration of orexins/hypocretins: identification of hypothalamic sites of action1This study was presented in part at the 28th Annual Meeting of the Society for Neuroscience, Los Angeles, CA, in November 1998.1. Brain Research 842:473-477.

Elmquist JK, Bjorbaek C, Ahima RS, Flier JS, Saper CB (1998) Distributions of leptin receptor mRNA isoforms in the rat brain. The Journal of comparative neurology 395:535-547.

Estabrooke IV, McCarthy MT, Ko E, Chou TC, Chemelli RM, Yanagisawa M, Saper CB, Scammell TE (2001) Fos expression in orexin neurons varies with behavioral state. J Neurosci 21:1656-1662.

Firar AE, Voisin T, Rouyer-Fessard C, Ostuni MA, Couvineau A, Laburthe M (2009) Discovery of a functional immunoreceptor tyrosine-based switch motif in a 7-transmembrane-spanning receptor: role in the orexin receptor OX1R-driven apoptosis. The FASEB Journal 23:4069-4080.

Frederich RC, Hamann A, Anderson S, Löllmann B, Lowell BB, Flier JS (1995) Leptin levels reflect body lipid content in mice: Evidence for diet-induced resistance to leptin action. Nature Medicine 1:1311-1314.

Funahashi H, Yamada S, Kageyama H, Takenoya F, Guan JL, Shioda S (2003) Co-existence of leptin- and orexin-receptors in feeding-regulating neurons in the hypothalamic arcuate nucleus-a triple labeling study. Peptides 24:687-694.

Funahashi H, Hori T, Shimoda Y, Mizushima H, Ryushi T, Katoh S, Shioda S (2000) Morphological evidence for neural interactions between leptin and orexin in the hypothalamus. Regul Pept 92:31-35.

Funato H, Tsai AL, Willie JT, Kisanuki Y, Williams SC, Sakurai T, Yanagisawa M (2009) Enhanced orexin receptor-2 signaling prevents diet-induced obesity and improves leptin sensitivity. Cell Metab 7:64-76.

Gautvik KM, de Lecea L, Gautvik VT, Danielson PE, Tranque P, Dopazo A, Bloom FE, Sutcliffe JG (1996) Overview of the most prevalent hypothalamus-specific mRNAs, as identified by directional tag PCR subtraction. Proc Natl Acad Sci U S A 93:8733-8738.

Girault EM, Yi CX, Fliers E, Kalsbeek A (2012) Orexins, feeding, and energy balance. Progress in brain research 198:47-64.

Gjerde E (2015) Developmental Responses of the Lateral Hypothalamus to Leptin and Ghrelin in Neonatal Rats: McGill University Libraries.

Goforth PB, Leinninger GM, Patterson CM, Satin LS, Myers MG, Jr. (2014) Leptin acts via lateral hypothalamic area neurotensin neurons to inhibit orexin neurons by multiple GABA-independent mechanisms. J Neurosci 34:11405-11415.

Gonzalez-Muniesa P, Martinez-Gonzalez MA, Hu FB, Despres JP, Matsuzawa Y, Loos RJF, Moreno LA, Bray GA, Martinez JA (2017) Obesity. Nature reviews Disease primers 3:17034.

Griffond B, Risold PY, Jacquemard C, Colard C, Fellmann D (1999) Insulin-induced hypoglycemia increases preprohypocretin (orexin) mRNA in the rat lateral hypothalamic area. Neurosci Lett 262:77-80.

Guan JL, Saotome T, Wang QP, Funahashi H, Hori T, Tanaka S, Shioda S (2001) Orexinergic innervation of POMC-containing neurons in the rat arcuate nucleus. Neuroreport 12:547-551.

Hagan JJ et al. (1999) Orexin A activates locus coeruleus cell firing and increases arousal in the rat. Proc Natl Acad Sci U S A 96:10911-10916.

Hakansson M, de Lecea L, Sutcliffe JG, Yanagisawa M, Meister B (1999) Leptin receptor- and STAT3-immunoreactivities in hypocretin/orexin neurones of the lateral hypothalamus. J Neuroendocrinol 11:653-663.

Hakansson ML, Brown H, Ghilardi N, Skoda RC, Meister B (1998) Leptin receptor immunoreactivity in chemically defined target neurons of the hypothalamus. J Neurosci 18:559-572.

Hara J, Beuckmann CT, Nambu T, Willie JT, Chemelli RM, Sinton CM, Sugiyama F, Yagami K, Goto K, Yanagisawa M, Sakurai T (2001) Genetic ablation of orexin neurons in mice results in narcolepsy, hypophagia, and obesity. Neuron 30:345-354.

Harris GC, Wimmer M, Aston-Jones G (2005) A role for lateral hypothalamic orexin neurons in reward seeking. Nature 437:556-559.

Haslam DW, James WPT (2005) Obesity. The Lancet 366:1197-1209.

Haynes AC, Jackson B, Chapman H, Tadayyon M, Johns A, Porter RA, Arch JR (2000) A selective orexin-1 receptor antagonist reduces food consumption in male and female rats. Regul Pept 96:45-51.

Haynes AC, Chapman H, Taylor C, Moore GB, Cawthorne MA, Tadayyon M, Clapham JC, Arch JR (2002) Anorectic, thermogenic and anti-obesity activity of a selective orexin-1 receptor antagonist in ob/ob mice. Regul Pept 104:153-159.

Heymsfield SB, Greenberg AS, Fujioka K, et al. (1999) Recombinant leptin for weight loss in obese and lean adults: A randomized, controlled, dose-escalation trial. JAMA 282:1568-1575.

Hiroaki Masuzaki YO, Naohi Isse, Noriko Satoh, Taku Okazaki, Michika Shigemoto, Kiyoshi Mori, Naohisa Tamura, Kiminori Hosoda, Yasunao Yoshimasa, Hisato Jingami, Teruo Kawada, and Kazuwa Nakao (1995) Human Obese Gene Expression Adipocyte-Specific Expression and Regional Differences in the Adipose Tissue Diabetes 44:855-858.

Horn CC, AA, aMIF (1999) Neural substrate for an intergrated metabolic control of feeding behaviour. Am J Physiol 276:R113-119.

Horvath TL, Diano S, van den Pol AN (1999) Synaptic interaction between hypocretin (orexin) and neuropeptide Y cells in the rodent and primate hypothalamus: a novel circuit implicated in metabolic and endocrine regulations. J Neurosci 19:1072-1087.

Ida T, Nakahara K, Katayama T, Murakami N, Nakazato M (1999) Effect of lateral cerebroventricular injection of the appetite-stimulating neuropeptide, orexin and neuropeptide Y, on the various behavioral activities of rats. Brain Res 821:526-529.

Image J, Category: Colocalization in: https://imagej.net/Colocalization_Analysis (2017-11-14)

Imperatore R, Palomba L, Morello G, Spiezio AD, Piscitelli F, Marzo VD, Cristino L (2016) Formation of OX-1R/CB1R heteromeric complexes in embryonic mouse hypothalamic cells: Effect on intracellular calcium, 2-arachidonoyl-glycerol biosynthesis and ERK phosphorylation. Pharmacological research : the official journal of the Italian Pharmacological Society 111:600-609.

Ingalls AM, Dickie MM, Snell GD (1950) Obese, a new mutation in the house mouse. J Hered 41:317-318.

Iqbal J, Pompolo S, Murakami T, Grouzmann E, Sakurai T, Meister B, Clarke IJ (2001) Immunohistochemical characterization of localization of long-form leptin receptor (OB-Rb) in neurochemically defined cells in the ovine hypothalamus. Brain Res 920:55-64.

Janknecht R NA (1992) Elk-1 protein domains required for direct and SRF-assisted DNA-binding. . Nucleic Acids Research 20:3317-3324.

Jantti MH, Putula J, Somerharju P, Frohman MA, Kukkonen JP (2012) OX1 orexin/hypocretin receptor activation of phospholipase D. Br J Pharmacol 165:1109-1123.

Jantti MH, Putula J, Turunen PM, Nasman J, Reijonen S, Lindqvist C, Kukkonen JP (2013) Autocrine endocannabinoid signaling through CB1 receptors potentiates OX1 orexin receptor signaling. Molecular pharmacology 83:621-632.

Jeff DeFalco MT, Hongyan Liu, Connie Zhao, XiaoLi Cai, Jamey D. Marth, Lynn Enquist, Jeffrey M. Friedman (2001) Virus-Assisted Mapping of Neural Inputs to a Feeding Center in the Hypothalamus Science 291:2608-2613.

Jeffrey M. Friedman JLH (1995) Leptin and the regulation of body weight in mammals. Nature 395:763-770.

Johansson L, Ekholm ME, Kukkonen JP (2007) Regulation of OX1 orexin/hypocretin receptor-coupling to phospholipase C by Ca2+ influx. Br J Pharmacol 150:97-104.

Jöhren O, Brüggemann N, Dominiak P (2004) Orexins (hypocretins) and adrenal function. Horm Metab Res 36:370-375.

Jöhren O, Neidert SJ, Kummer M, Dendorfer A, Dominiak P (2001) Prepro-orexin and orexin receptor mRNAs are differentially expressed in peripheral tissues of male and female rats. Endocrinology 142:3324-3331.

Juel K. Elmquist CB, Rexford S. Ahima, Jeffrey S. Flier, and Clifford B. Saper (1998) Distributions of Leptin Receptor mRNA Isoforms in the Rat Brain. The Journal of Comparative Neurology 395:535-547.

Kennedy GC (1953) The Role of Depot Fat in the Hypothalamic Control of Food Intake in the Rat.

Klein J, Fasshauer M, Benito M, Kahn CR (2000) Insulin and the β3-Adrenoceptor Differentially Regulate Uncoupling Protein-1 Expression. Molecular endocrinology 14:764-773.

Kong SKaL, C. Y. (1995) The Use if Fura 2 for Measurement of Free Calcium Concentration. Biochemical Education 23.

Kortenjann M TO, Shaw PE. (1994) Inhibition of v-raf-dependent c-fos expression and transformation by a kinase-defective mutant of the mitogen-activated protein kinase Erk2. . Molecular and Cellular Biology 14:4815-4824.

Kotz CM, Teske JA, Levine JA, Wang C (2002) Feeding and activity induced by orexin A in the lateral hypothalamus in rats. Regul Pept 104:27-32.

Lee MG, Hassani OK, Jones BE (2005) Discharge of identified orexin/hypocretin neurons across the sleep-waking cycle. J Neurosci 25:6716-6720.

Leinninger GM, Opland DM, Jo YH, Faouzi M, Christensen L, Cappellucci LA, Rhodes CJ, Gnegy ME, Becker JB, Pothos EN, Seasholtz AF, Thompson RC, Myers MG, Jr. (2011) Leptin action via neurotensin neurons controls orexin, the mesolimbic dopamine system and energy balance. Cell Metab 14:313-323.

Leinninger GM, Jo YH, Leshan RL, Louis GW, Yang H, Barrera JG, Wilson H, Opland DM, Faouzi MA, Gong Y, Jones JC, Rhodes CJ, Chua S, Jr., Diano S, Horvath TL, Seeley RJ, Becker JB, Munzberg H, Myers MG, Jr. (2009) Leptin acts via leptin receptor-expressing lateral hypothalamic neurons to modulate the mesolimbic dopamine system and suppress feeding. Cell Metab 10:89-98.

Leonard JPKaCS (2014) Orexin/hypocretin receptor signalling cascades. British Journal of Pharmacology 171.

Lhoták V GP, Letwin K, Pawson T. (1991) Characterization of elk, a brain-specific receptor tyrosine kinase. . Molecular and Cellular Biology 11:2469-2502.

Lin L, Faraco J, Li R, Kadotani H, Rogers W, Lin X, Qiu X, de Jong PJ, Nishino S, Mignot E (1999) The sleep disorder canine narcolepsy is caused by a mutation in the hypocretin (orexin) receptor 2 gene. Cell 98:365-376.

Lopez M, Seoane L, Garcia MC, Lago F, Casanueva FF, Senaris R, Dieguez C (2000) Leptin regulation of prepro-orexin and orexin receptor mRNA levels in the hypothalamus. Biochem Biophys Res Commun 269:41-45.

Louis A. Tartaglia MD, Xun Weng, Nanhua Deng, Janice Culpepper, Rene Devos, Grayson J. Richards, L. Arthur Campfield, Frederick T. Clark, Jim Deeds, Craig Muir, Sean Sanker, Ann Moriarty, Karen J. Moore, John S. Smutko, Gail G. Mays, Elizabeth A. Woolf, Cheryl A. Monroe, and Robert I. Tepper (1995) Identification and Expression Cloning of a Leptin Receptor, OB-R Cell 83.

Louis GW, Leinninger GM, Rhodes CJ, Myers MG, Jr. (2010) Direct innervation and modulation of orexin neurons by lateral hypothalamic LepRb neurons. J Neurosci 30:11278-11287.

Lowry OH, Rosebrough NJ, Farr AL, Randall RJ (1951) PROTEIN MEASUREMENT WITH THE FOLIN PHENOL REAGENT. Journal of Biological Chemistry 193:265-275.

Lubkin M, Stricker-Krongrad A (1998) Independent feeding and metabolic actions of orexins in mice. Biochem Biophys Res Commun 253:241-245.

Lund PE, Shariatmadari R, Uustare A, Detheux M, Parmentier M, Kukkonen JP, Akerman KE (2000) The orexin OX1 receptor activates a novel Ca2+ influx pathway necessary for coupling to phospholipase C. The Journal of biological chemistry 275:30806-30812.

Ma X, Zubcevic L, Bruning JC, Ashcroft FM, Burdakov D (2007) Electrical inhibition of identified anorexigenic POMC neurons by orexin/hypocretin. J Neurosci 27:1529-1533.

Madisen L, Zwingman TA, Sunkin SM, Oh SW, Zariwala HA, Gu H, Ng LL, Palmiter RD, Hawrylycz MJ, Jones AR, Lein ES, Zeng H (2010) A robust and high-throughput Cre reporting and characterization system for the whole mouse brain. Nature neuroscience 13:133-140.

Manders EM, Stap J, Brakenhoff GJ, van Driel R, Aten JA (1992) Dynamics of three-dimensional replication patterns during the S-phase, analysed by double labelling of DNA and confocal microscopy. J Cell Sci 103 (Pt 3):857-862.

Manders EMM, Verbeek FJ, Aten JA (1993) Measurement of co-localization of objects in dual-colour confocal images. Journal of Microscopy 169:375-382.

Marcus JN, Aschkenasi CJ, Lee CE, Chemelli RM, Saper CB, Yanagisawa M, Elmquist JK (2001) Differential expression of orexin receptors 1 and 2 in the rat brain. J Comp Neurol 435:6-25.

Martinez-Gonzalez MA, Martinez JA, Hu FB, Gibney MJ, Kearney J (1999) Physical inactivity, sedentary lifestyle and obesity in the European Union. International journal

of obesity and related metabolic disorders : journal of the International Association for the Study of Obesity 23:1192-1201.

Martinez JA (2007) Body-weight regulation: causes of obesity. Proceedings of the Nutrition Society 59:337-345.

Mercer JG, Hoggard N, Williams LM, Lawrence CB, Hannah LT, Trayhurn P (1996) Localization of leptin receptor mRNA and the long form splice variant (Ob-Rb) in mouse hypothalamus and adjacent brain regions by in situ hybridization. FEBS Letters 387:113-116.

Merino B, Díez-Fernández C, Ruiz-Gayo M, Somoza B (2006) Choroid plexus epithelial cells co-express the long and short form of the leptin receptor. Neuroscience Letters 393:269-272.

Mondal MS, Nakazato M, Matsukura S (2002) Characterization of orexins (hypocretins) and melanin-concentrating hormone in genetically obese mice. Regul Pept 104:21-25.

Mondal MS, Nakazato M, Date Y, Murakami N, Hanada R, Sakata T, Matsukura S (1999) Characterization of orexin-A and orexin-B in the microdissected rat brain nuclei and their contents in two obese rat models. Neuroscience Letters 273:45-48.

Moriguchi T, Sakurai T, Nambu T, Yanagisawa M, Goto K (1999) Neurons containing orexin in the lateral hypothalamic area of the adult rat brain are activated by insulin-induced acute hypoglycemia. Neurosci Lett 264:101-104.

Morton GJ, Cummings DE, Baskin DG, Barsh GS, Schwartz MW (2006) Central nervous system control of food intake and body weight. Nature 443:289-295.

Muroya S, Uramura K, Sakurai T, Takigawa M, Yada T (2001) Lowering glucose concentrations increases cytosolic Ca2+ in orexin neurons of the rat lateral hypothalamus. Neurosci Lett 309:165-168.

Muroya S, Funahashi H, Yamanaka A, Kohno D, Uramura K, Nambu T, Shibahara M, Kuramochi M, Takigawa M, Yanagisawa M, Sakurai T, Shioda S, Yada T (2004a) Orexins (hypocretins) directly interact with neuropeptide Y, POMC and glucose-responsive neurons to regulate Ca 2+ signaling in a reciprocal manner to leptin: orexigenic neuronal pathways in the mediobasal hypothalamus. The European journal of neuroscience 19:1524-1534.

Muroya S, Funahashi H, Yamanaka A, Kohno D, Uramura K, Nambu T, Shibahara M, Kuramochi M, Takigawa M, Yanagisawa M, Sakurai T, Shioda S, Yada T (2004b) Orexins (hypocretins) directly interact with neuropeptide Y, POMC and glucose-responsive neurons to regulate Ca 2+ signaling in a reciprocal manner to leptin: orexigenic neuronal pathways in the mediobasal hypothalamus. Eur J Neurosci 19:1524-1534.

Mütze J, Roth J, Gerstberger R, Matsumura K, Hübschle T (2006) Immunohistochemical evidence of functional leptin receptor expression in neuronal and endothelial cells of the rat brain. Neuroscience Letters 394:105-110.

Nakamura Y, Ishii J, Kondo A (2013) Bright fluorescence monitoring system utilizing Zoanthus sp. green fluorescent protein (ZsGreen) for human G-protein-coupled receptor signaling in microbial yeast cells. PloS one 8:e82237.

Nambu T, Sakurai T, Mizukami K, Hosoya Y, Yanagisawa M, Goto K (1999) Distribution of orexin neurons in the adult rat brain. Brain Res 827:243-260.

Narita M, Nagumo Y, Hashimoto S, Narita M, Khotib J, Miyatake M, Sakurai T, Yanagisawa M, Nakamachi T, Shioda S, Suzuki T (2006) Direct involvement of orexinergic systems in the activation of the mesolimbic dopamine pathway and related behaviors induced by morphine. J Neurosci 26:398-405.

Nishino S, Ripley B, Overeem S, Nevsimalova S, Lammers GJ, Vankova J, Okun M, Rogers W, Brooks S, Mignot E (2001) Low cerebrospinal fluid hypocretin (orexin) and altered energy homeostasis in human narcolepsy. Annals of Neurology 50:381-388.

Perez CA, Stanley SA, Wysocki RW, Havranova J, Ahrens-Nicklas R, Onyimba F, Friedman JM (2011) Molecular annotation of integrative feeding neural circuits. Cell Metab 13:222-232.

Peyron C, Tighe DK, van den Pol AN, de Lecea L, Heller HC, Sutcliffe JG, Kilduff TS (1998) Neurons containing hypocretin (orexin) project to multiple neuronal systems. The Journal of neuroscience : the official journal of the Society for Neuroscience 18:9996-10015.

Peyron C et al. (2000) A mutation in a case of early onset narcolepsy and a generalized absence of hypocretin peptides in human narcoleptic brains. Nat Med 6:991-997.

Poeggeler B, Schulz C, Pappolla MA, Bodó E, Tiede S, Lehnert H, Paus R (2010) Leptin and the skin: a new frontier. Experimental Dermatology 19:12-18.

Rahmouni K (2012) Chapter 27 - Leptin Signaling and Energy Homeostasis A2 - Robertson, David. In: Primer on the Autonomic Nervous System (Third Edition) (Biaggioni I, Burnstock G, Low PA, Paton JFR, eds), pp 131-134. San Diego: Academic Press.

Ramanjaneya M, Conner AC, Chen J, Kumar P, Brown JE, Johren O, Lehnert H, Stanfield PR, Randeva HS (2009) Orexin-stimulated MAP kinase cascades are activated through multiple G-protein signalling pathways in human H295R adrenocortical cells: diverse roles for orexins A and B. The Journal of endocrinology 202:249-261.

Rauch M, Riediger T, Schmid HA, Simon E (2000) Orexin A activates leptin-responsive neurons in the arcuate nucleus. Pflugers Arch 440:699-703.

Rodgers RJ, Halford JC, Nunes de Souza RL, Canto de Souza AL, Piper DC, Arch JR, Upton N, Porter RA, Johns A, Blundell JE (2001) SB-334867, a selective orexin-1 receptor antagonist, enhances behavioural satiety and blocks the hyperphagic effect of orexin-A in rats. Eur J Neurosci 13:1444-1452.

Sakurai T, Nagata R, Yamanaka A, Kawamura H, Tsujino N, Muraki Y, Kageyama H, Kunita S, Takahashi S, Goto K, Koyama Y, Shioda S, Yanagisawa M (2005) Input of orexin/hypocretin neurons revealed by a genetically encoded tracer in mice. Neuron 46:297-308.

Sakurai T et al. (1998) Orexins and orexin receptors: a family of hypothalamic neuropeptides and G protein-coupled receptors that regulate feeding behavior. Cell 92:573-585.

Saxena A, Wagatsuma A, Noro Y, Kuji T, Asaka-Oba A, Watahiki A, Gurnot C, Fagiolini M, Hensch TK, Carninci P (2012) Trehalose-enhanced isolation of neuronal sub-types from adult mouse brain. Biotechniques 52:381-385.

Schwartz MW, Peskind E, Raskind M, Boyko EJ, Porte Jr D (1996) Cerebrospinal fluid leptin levels: Relationship to plasma levels and to adiposity in humans. Nature Medicine 2:589-593.

Scott MM, Lachey JL, Sternson SM, Lee CE, Elias CF, Friedman JM, Elmquist JK (2009) Leptin targets in the mouse brain. The Journal of Comparative Neurology 514:518-532.

Seeley RvD, G.; Campfield, L.; Smith, F.; Burn, P.; Nelligan, J.; Bell, S.; Baskin, D.; Woods, S.; Schwartz, M (1996) Intraventricular Leptin Reduces Food Intake and Body Weight of Lean Rats but Not Obese Zucker Rats. Hormone and Metabolic Research 28:664-668.

Shiuchi T, Haque MS, Okamoto S, Inoue T, Kageyama H, Lee S, Toda C, Suzuki A, Bachman ES, Kim YB, Sakurai T, Yanagisawa M, Shioda S, Imoto K, Minokoshi Y (2009) Hypothalamic orexin stimulates feeding-associated glucose utilization in skeletal muscle via sympathetic nervous system. Cell Metab 10:466-480.

Stanley S, Pinto S, Segal J, Pérez CA, Viale A, DeFalco J, Cai X, Heisler LK, Friedman JM (2010) Identification of neuronal subpopulations that project from hypothalamus to both liver and adipose tissue polysynaptically. Proceedings of the National Academy of Sciences 107:7024-7029.

Streamson C. Chua J, Iakovos K. Koutras, Lily Han, Shun-Mei Liu, Joy Kay, Sun J. Young, Wendy K. Chung, and Rudolph L. Leibel (1997) Fine Structure of the Murine Leptin Receptor Gene: Splice Site Suppression Is Required to Form Two Alternatively Spliced Transcripts. Genomics 45:264-270.

Stricker-Krongrad A, Richy S, Beck B (2002) Orexins/hypocretins in the ob/ob mouse: hypothalamic gene expression, peptide content and metabolic effects. Regul Pept 104:11-20.

Stunkard AJ (1996) Current views on Obesity. The American Journal of Medicine 100:230-236.

Szekely M, Petervari E, Balasko M, Hernadi I, Uzsoki B (2002) Effects of orexins on energy balance and thermoregulation. Regul Pept 104:47-53.

Tadataka Tsuji TY, Susumu Tanaka, Sanam Bakhshishayan and Mikihiko Kogo (2011) Analyses of the facilitatory effect of orexin on eating and masticatory muscle activity in rats. J Neurophysiol 106:3129-3135.

Taheri S, Mahmoodi M, Opacka-Juffry J, Ghatei MA, Bloom SR (1999) Distribution and quantification of immunoreactive orexin A in rat tissues. FEBS Letters 457:157-161.

Taheri S, Gardiner J, Hafizi S, Murphy K, Dakin C, Seal L, Small C, Ghatei M, Bloom S (2001) Orexin A immunoreactivity and preproorexin mRNA in the brain of Zucker and WKY rats. Neuroreport 12:459-464.

Tang J, Chen J, Ramanjaneya M, Punn A, Conner AC, Randeva HS (2008) The signalling profile of recombinant human orexin-2 receptor. Cell Signal 20:1651-1661.

Thannickal TC, Moore RY, Nienhuis R, Ramanathan L, Gulyani S, Aldrich M, Cornford M, Siegel JM (2000) Reduced number of hypocretin neurons in human narcolepsy. Neuron 27:469-474.

Thorpe AJ, Teske JA, Kotz CM (2005) Orexin A-induced feeding is augmented by caloric challenge. American Journal of Physiology-Regulatory, Integrative and Comparative Physiology 289:R367-R372.

Thorpe AJ, Mullett MA, Wang C, Kotz CM (2003) Peptides that regulate food intake: regional, metabolic, and circadian specificity of lateral hypothalamic orexin A feeding stimulation. American Journal of Physiology-Regulatory, Integrative and Comparative Physiology 284:R1409-R1417.

Trepel M (2015) Neuroanatomie Struktur und Funktion.

Tritos NA, Mastaitis JW, Kokkotou E, Maratos-Flier E (2001) Characterization of melanin concentrating hormone and preproorexin expression in the murine hypothalamus. Brain Res 895:160-166.

Trivedi P, Yu H, MacNeil DJ, Van der Ploeg LH, Guan XM (1998) Distribution of orexin receptor mRNA in the rat brain. FEBS Lett 438:71-75.

Tsuneki H, Wada T, Sasaoka T (2010) Role of orexin in the regulation of glucose homeostasis. Acta physiologica 198:335-348.

van de Wall E, Leshan R, Xu AW, Balthasar N, Coppari R, Liu SM, Jo YH, MacKenzie RG, Allison DB, Dun NJ, Elmquist J, Lowell BB, Barsh GS, de Luca C, Myers MG, Jr., Schwartz GJ, Chua SC, Jr. (2008) Collective and individual functions of leptin receptor modulated neurons controlling metabolism and ingestion. Endocrinology 149:1773-1785.

van den Top M, Lee K, Whyment AD, Blanks AM, Spanswick D (2004) Orexigen-sensitive NPY/AgRP pacemaker neurons in the hypothalamic arcuate nucleus. Nat Neurosci 7:493-494.

van den Top M, Nolan MF, Lee K, Richardson PJ, Buijs RM, Davies CH, Spanswick D (2003) Orexins induce increased excitability and synchronisation of rat sympathetic preganglionic neurones. J Physiol 549:809-821.

Venner A, Karnani MM, Gonzalez JA, Jensen LT, Fugger L, Burdakov D (2011) Orexin neurons as conditional glucosensors: paradoxical regulation of sugar sensing by intracellular fuels. J Physiol 589:5701-5708.

Wang B, Chandrasekera PC, Pippin JJ (2014a) Leptin- and Leptin Receptor-Deficient Rodent Models: Relevance for Human Type 2 Diabetes Current Diabetes Reviews 10:131-145.

Wang J, Osaka T, Inoue S (2001) Energy expenditure by intracerebroventricular administration of orexin to anesthetized rats. Neurosci Lett 315:49-52.

Wang J, Osaka T, Inoue S (2003) Orexin-A-sensitive site for energy expenditure localized in the arcuate nucleus of the hypothalamus. Brain Res 971:128-134.

Wang Z, Liu S, Kakizaki M, Hirose Y, Ishikawa Y, Funato H, Yanagisawa M, Yu Y, Liu Q (2014b) Orexin/hypocretin activates mTOR complex 1 (mTORC1) via an Erk/Akt-independent and calcium-stimulated lysosome v-ATPase pathway. The Journal of biological chemistry 289:31950-31959.

Wenzel J, Grabinski N, Knopp CA, Dendorfer A, Ramanjaneya M, Randeva HS, Ehrhart-Bornstein M, Dominiak P, Jöhren O (2009) Hypocretin/orexin increases the expression of steroidogenic enzymes in human adrenocortical NCI H295R cells. American journal of physiology Regulatory, integrative and comparative physiology 297:R1601-1609.

WHO (2017) Obesity and Overweight. In: http://www.who.int/mediacentre/factsheets/fs311/en/.

Williams EP, Mesidor M, Winters K, Dubbert PM, Wyatt SB (2015) Overweight and Obesity: Prevalence, Consequences, and Causes of a Growing Public Health Problem. Current obesity reports 4:363-370.

Williams G, Harrold JA, Cutler DJ (2000) The hypothalamus and the regulation of energy homeostasis: lifting the lid on a black box. Proc Nutr Soc 59:385-396.

Willie JT, Chemelli RM, Sinton CM, Yanagisawa M (2001) To eat or to sleep? Orexin in the regulation of feeding and wakefulness. Annu Rev Neurosci 24:429-458.

Winrow CJ, Tanis KQ, Reiss DR, Rigby AM, Uslaner JM, Uebele VN, Doran SM, Fox SV, Garson SL, Gotter AL, Levine DM, Roecker AJ, Coleman PJ, Koblan KS, Renger JJ (2010) Orexin receptor antagonism prevents transcriptional and behavioral plasticity resulting from stimulant exposure. Neuropharmacology 58:185-194.

Yamada H, Okumura T, Motomura W, Kobayashi Y, Kohgo Y (2000) Inhibition of food intake by central injection of anti-orexin antibody in fasted rats. Biochem Biophys Res Commun 267:527-531.

Yamamoto Y, Ueta Y, Yamashita H, Asayama K, Shirahata A (2002) Expressions of the prepro-orexin and orexin type 2 receptor genes in obese rat. Peptides 23:1689-1696.

Yamamoto Y, Ueta Y, Serino R, Nomura M, Shibuya I, Yamashita H (2000) Effects of food restriction on the hypothalamic prepro-orexin gene expression in genetically obese mice. Brain Res Bull 51:515-521.

Yamamoto Y, Ueta Y, Date Y, Nakazato M, Hara Y, Serino R, Nomura M, Shibuya I, Matsukura S, Yamashita H (1999) Down regulation of the prepro-orexin gene expression in genetically obese mice. Brain Res Mol Brain Res 65:14-22.

Yamanaka A, Sakurai T, Katsumoto T, Yanagisawa M, Goto K (1999) Chronic intracerebroventricular administration of orexin-A to rats increases food intake in daytime, but has no effect on body weight. Brain Res 849:248-252.

Yamanaka A, Beuckmann CT, Willie JT, Hara J, Tsujino N, Mieda M, Tominaga M, Yagami K, Sugiyama F, Goto K, Yanagisawa M, Sakurai T (2003a) Hypothalamic orexin neurons regulate arousal according to energy balance in mice. Neuron 38:701-713.

Yamanaka A, Beuckmann CT, Willie JT, Hara J, Tsujino N, Mieda M, Tominaga M, Yagami K, Sugiyama F, Goto K, Yanagisawa M, Sakurai T (2003b) Hypothalamic orexin neurons regulate arousal according to energy balance in mice. Neuron 38:701-713.

Yoshida K, McCormack S, Espana RA, Crocker A, Scammell TE (2006) Afferents to the orexin neurons of the rat brain. J Comp Neurol 494:845-861.

Zhang Y, Proenca R, Maffei M, Barone M, Leopold L, Friedman JM (1994) Positional cloning of the mouse obese gene and its human homologue. Nature 372:425-432.

Zucker FDSaI (1972) Circadian Rythms in Drinking Behavior and Locomotor Activity of Rats Are Eliminated by Hothalamic Lesions. Proc Natl Acad Sci U S A 69:1583-1586.

6 Appendix

6.1 Material

Table 6.1: Utilised equipment

Name	Manufacturer
ABI PRISM® 7000 Sequence Detection System	Thermo Fisher Scientific (Waltham, USA)
Analytical balance ABT 100-5M	Kern & Sohn (Balingen, Germany)
Autoclave VX-65	Systec (Linden, Germany)
Bag sealer	Folio Severin (Sundern, Germany)
Biological safety cabinet safe 2020	Thermo Fisher Scientific (Waltham, USA)
CCD-Camera CellCam	Phase (Lübeck, Germany)
Centrifuge 5415D	Eppendorf (Hamburg, Germany)
Centrifuge 5415R	Eppendorf (Hamburg, Germany)
Centrifuge GR412	Jouan (Unterhaching, Germany)
Centrifuge Universal 320 R	Hettich (Tuttlingen, Germany)
Chemiluminescence system Fusion Solo S	Vilber Lourmat Deutschland GmbH (Eberhardzell, Germany)
Chemistry balance seca	Sartorius (Göttingen, Germany)
CO_2-Incubator	Memmert (Schwabach, Germany)
CO_2-Incubator Galaxy® 170S	Eppendorf (Hamburg, Germany)
Confocal microscope TCS SP5	Leica Microsystems (Wetzlar Germany)
Counting Chamber Fuchs-Rosenthal	Bioanalytic GmbH (Umkirch/Freiburg, Germany)
Cryostat CM3050	Leica Biosystems (Nussloch, Germany)
Disperser Ultra-Turrax® T 18	IKA®-Werke GmbH & CO. KG (Staufen, Germany

Electrophoresis cell Sub-Cell GT	Bio-Rad Laboratories GmbH (München, Germany)
Electrophoresis power supply Power Pac 300	Bio-Rad Laboratories GmbH (München, Germany)
Electroporator 2510	Eppendorf (Hamburg, Germany)
Fluorescence microscope DMI 6000B	Leica Microsystems (Wetzlar, Germany)
Freezer -20 °C	Liebherr Medline (Bulle, Switzerland)
Fridge 4 °C	Liebherr Medline (Bulle, Switzerland)
Fully automated vibrating blade microtome VT1200s	Leica Biosystems (Nussloch, Germany)
Gel documentation system	Phase (Lübeck, Germany)
Hot Air Sterilisers UT 6060	Heraeus (Hanau, Germany)
Heating block QBT 2	Grant Instruments (Cambridge, UK)
Hoefer® SemiPhorTM Electophoresis Blotter TE-70	Amersham Biosciences (Little Chalfont, UK)
Ice machine	Ziegra (Isernhagen, Germany)
Incubation Shaker Multitron Standard	Infors AG (Bottmingen Switzerland)
Lab scale MC1 LC220S	Sartorius (Göttingen, Germany)
Micro Scissors	Fine Science Tools (Heidelberg, Germany)
Microscope, invers IM35	Zeiss (Feldbach, Germany)
Micro centrifuge 200R / 220R	Hettich (Tuttlingen, Germany)
Mini-Tumbling Table WT17	Biometra (Göttingen, Germany)
MoFlo Legacy Cell Sorter	Beckman Coulter (Krefeld, Germany)
Multipette® plus	Eppendorf (Hamburg, Germany)
pH-Meter 531	WTW (Weilheim, Germany)
Pipette (10, 100, 200 und 1000 µl)	Eppendorf (Hamburg, Germany)
Pipetus® pipetting filler	Hirschmann Laborgeräte (Eberstadt, Germany)
Power supply PowerEaseTM 500 (Westernblot)	Thermo Fisher Scientific (Waltham, USA)

Scissors	Fine Science Tools (Heidelberg, Germany)
Shaker DRS-12	NeoLab (Heidelberg, Germany)
Sterilisator Steri 250	Swiss Made (Simon Keller AG) (Burgdorf, Switzerland)
Thermocycler T Gradient	Biometra (Göttingen, Germany)
Thermomixer block heater compact	Thermo Fisher Scientific (Waltham, USA)
Thread Scissors, Pointed-Pointed straight	Fine Science Tools (Heidelberg, Germany)
Ultra-Low Temperature Freezer (-80 °C) HERAfreezeTM HFU T-series	Thermo Fisher Scientific (Waltham, USA)
UV-Vis Spektrophotometer NanoDrop 2000	Thermo Fisher Scientific (Waltham, USA)
UV-Vis Spektrophotometer Novaspec II	Amersham Biosciences (Little Chalfont, UK)
Vortex REAX 2000	Heidolph Instruments (Schwabach, Germany)
Water jet pump SUE300Q	Heto-Holten A/S (Alleröd, Denmark)
Water Purification Milli-Q® Integral System	Merck Millipore (Billerica, USA)
Wasserbad Typ 850 022	Lauda (Lauda-Königshofen, Germany)
XCell IITM-Blotmodul	Thermo Fisher Scientific (Waltham, USA)
XCell SureLockTM-chamber	Thermo Fisher Scientific (Waltham, USA)

Table 6.2: Consumables

Name	**Manufacturer**
Beaker (div.)	Schott Duran (Wertheim, Germany)
Canula (20G, 21G, 25G)	BD (Franklin Lakes, USA)
Cell culture flask Cellstar® T75	Greiner Bio-One (Kremsmünster, Austria)
Cell Culture Microplate, µClear® (96-Well)	Greiner Bio-One (Kremsmünster, Austria)
Cell culture plates Cellstar® (6-, 24-, 96-Well)	Greiner Bio-One (Kremsmünster, Austria)
Conical Centrifuge Tubes (Falcon™ 15 ml, 50 ml)	Thermo Fisher Scientific (Waltham, USA)

Cover slip	Carl Roth (Karlsruhe, Germany)
Electroporation Cuvettes, Gene Pulser/MicroPulser	Bio-Rad Laboratories GmbH (München, Germany)
Feather™ disposable scalpel No 10, 11	Electron Microscopy Sciences (Hatfield, USA)
Immobilon™ PVDF transfer membrane, pore size 0.45 µm	Merck Millipore (Billerica, USA)
Minisart® NML Syringe, 0.2 µm	Sartorius (Göttingen, Germany)
Pipettes (5 ml, 10 ml, 25 ml, 50 ml)	Greiner bio-one (Kremsmünster, Austria)
Parafilm	Pechiney Plastic Packaging (Akron, USA)
Pasteur pipette (150 mm)	TH.Geyer – Labsolute (Renningen, Germany)
Pasteur pipette (230 mm)	Glaswarenfabrik Karl Hecht (Sondheim/Rhön, Germany)
PCR-Plate (96-Well)	Sarstedt (Nümbrecht, Germany)
Petri dish (35 mm, 10 cm)	Greiner Bio-One (Kremsmünster, Austria)
Pipet tip (10 µl, 200 µl, 1000 µl)	Sarstedt (Nümbrecht, Germany)
Pipet tip combitips advanced (0.5 ml, 5 ml)	Eppendorf (Hamburg, Germany)
Reaction tube (0.2 ml, 0.5 ml, 1.5 ml, 2 ml)	Eppendorf (Hamburg, Germany)
Reaction tube (0.2 ml, 0.5 ml, 1.5 ml, 2 ml)	Sarstedt (Nümbrecht, Germany)
Sealing Tape (optically clear)	Sarstedt (Nümbrecht, Germany)
Serological Pipettes Cellstar® (5 ml, 10 ml, 25 ml, 50 ml)	Greiner Bio-One (Kremsmünster, Austria)
sterile nylon-mesh filter, 70 µm	Sysmex Partec GmbH (Görlitz, Germany)
Syringe (5 ml)	BD (Franklin Lakes, USA)
Vis Cuvettes	Eppendorf (Hamburg, Germany)
Whatman-Paper	GE Healthcare (Little Chalfont, UK)

Table 6.3.: Kits

Name	Manufacturer
Cloned AMV First-Strand cDNA Synthesis Kit (Invitrogen)	Thermo Fisher Scientific (Waltham, USA)
DIG Oligonucleotide Tailing Kit	Roche (Basel, Switzerland)
DyNAzyme II DNA Polymerase	Thermo Fisher Scientific (Waltham, USA)
MAXIscript®T7/T3 Transcription Kit (Ambion)	Thermo Fisher Scientific (Waltham, USA)
NucleoBond® Xtra Midi/Maxi Kit	Macherey-Nagel (Düren, Germany)
NucleoSpin® Gel and PCR clean up Kit	Macherey-Nagel (Düren, Germany)
NucleoSpin® Plasmid QuickPure Kit	Macherey-Nagel (Düren, Germany)
NucleoSpin® RNA purification Kit	Macherey-Nagel (Düren, Germany)
Papain dissociation Kit	Worthington
Platinum™ SYBR™ Green qPCR SuperMix-Kit (Invitrogen)	Thermo Fisher Scientific (Waltham, USA)
Platinum™ Taq DNA Polymerase High Fidelity (Invitrogen)	Thermo Fisher Scientific (Waltham, USA)
RNA Nanoprep Kit	Stratagene (La Jolla, California)
TOPO® TA Cloning® Kit for Sequencing (Invitrogen)	Thermo Fisher Scientific (Waltham, USA)
TSA™ Plus Cyanine 5 System	PerkinElmer™ (Waltham, USA)

Table 6.4.: Chemicals

Name	Manufacturer
Acrylamide	Sigma-Aldrich (St. Louis, USA)
Agarose	Carl Roth (Karlsruhe, Germany)
Ammonium acetate	Sigma-Aldrich (St. Louis, USA)
Ammonium Persulphate (APS)	Sigma-Aldrich (St. Louis, USA)
AP-V	Tocris Bioscience (Bristol, UK)
ß-Mercapto-ethanol (ß-ME)	Merck Millipore (Billerica, USA)

Bovine Serum Albumin (BSA)	Sigma-Aldrich (St. Louis, USA)
Bromophenol blue	Thermo Fisher Scientific (Waltham, USA)
Calcium chloride ($CaCl_2$ (50nM))	Merck Millipore (Billerica, USA)
Chloroform	Carl Roth (Karlsruhe, Germany)
Copper(II)-sulphate Pentahydrate ($CuSO_4 \cdot 5\ H_2O$)	Carl Roth (Karlsruhe, Germany)
Fetal Bovine Serum (FCS)	Merck Millipore (Billerica, USA)
DAPI (4',6-diamidino-2-phenylindole)	Thermo Fisher Scientific (Waltham, USA)
Dexamethasone	Abcam (Cambridge, UK)
Dextran sulphate	Merck Millipore (Billerica, USA)
Diethyl pyrocarbonate (DEPC)	Sigma-Aldrich (St. Louis, USA)
Dimethyl sulfoxide (DMSO)	Sigma-Aldrich (St. Louis, USA)
Dithiotrol (DTT)	GE Healthcare (Little Chalfont, UK)
D-Trehalose	Sigma-Aldrich (St. Louis, USA)
EDTA	Thermo Fisher Scientific (Waltham, USA)
Ethanol	Merck Millipore (Billerica, USA)
Ethidiumbromid (EtBr, 1 %)	Carl Roth (Karlsruhe, Germany)
Folin's phenol reagent	Merck Millipore (Billerica, USA)
Formamid	Sigma-Aldrich (St. Louis, USA)
Fura-2AM	Thermo Fisher Scientific (Waltham, USA)
Glucose	Sigma-Aldrich (St. Louis, USA)
Glycerol	AplliChem (Darmstadt, Germany)
Glycine	Carl Roth (Karlsruhe, Germany)
HEPES	Thermo Fisher Scientific (Waltham, USA)
Hydrogen peroxide (H_2O_2, 30 %)	Merck Millipore (Billerica, USA)
Horseradish peroxidase (HRP)	Thermo Fisher Scientific (Waltham, USA)
Indomethacin	Sigma-Aldrich (St. Louis, USA)
Isobotylmethylxanthin (IBMX)	Sigma-Aldrich (St. Louis, USA)
Isoflurane	Baxter (Deerfield, USA)

Isopropanol	Sigma-Aldrich (St. Louis, USA)
Kynureic acid	Sigma-Aldrich (St. Louis, USA)
Methanol (MeOH)	TH Geyer-Chemsolute (Renningen, Germany)
Paraformaldehyde (PFA)	Sigma-Aldrich (St. Louis, USA)
PD98059	Tocris Bioscience (Bristol, UK)
Phenol-chloroform	Sigma-Aldrich (St. Louis, USA)
Phenol-chloroform-isoamyl	Sigma-Aldrich (St. Louis, USA)
Phenylmethylsulfonylfluorid (PMSF)	Carl Roth (Karlsruhe, Germany)
Potassium chloride (KCl)	Sigma-Aldrich (St.Louis, USA)
Potassium sodium tartrate-Tetrahydrat (K-Na-Tartrat · 4 H_2O)	Merck Millipore (Billerica, USA)
Pluronic F127	Thermo Fisher Scientific (Waltham, USA)
Probenecid	Thermo Fisher Scientific (Waltham, USA)
TCS 1102	Tocris Bioscience (Bristol, UK)
Tris	Carl Roth (Karlsruhe, Germany)
Tris Base	Carl Roth (Karlsruhe, Germany)
Tris-HCL pH 6.5 (0.5 M)	Bio-Rad Laboratories GmbH (München, Germany)
Tris-HCL pH 8.8 (1.5 M)	Bio-Rad Laboratories GmbH (München, Germany)
Triton-x 100	Promega (Madison, USA)
Sodium dodecyl sulphate (SDS)	Sigma-Aldrich (St. Louis, USA)
Sodium acetate (3M)	Sigma-Aldrich (St. Louis, USA)
Sodium azide	Sigma-Aldrich (St. Louis, USA)
Sodium chloride (NaCl)	Sigma-Aldrich (St. Louis, USA)
Sodium carbonate (Na_2CO_3 (1 M))	Honeywell Specialty Chemicals (Seelze, Germany)
Sodium dihydrogen phosphate monohydrate ($NaH_2PO_4 \cdot H_2O$)	Merck Millipore (Billerica, USA)

Sodium hydroxide (NaOH)	Thermo Fisher Scientific (Waltham, USA)
Sodium phosphate dibasic heptahydrate ($Na_2HPO_4 \cdot 2H_2O$)	Sigma-Aldrich (St. Louis, USA)
Temed	Carl Roth (Karlsruhe, Germany)
Trypsin	Biochrom (Berlin, Germany)
Tween 20	PanReac AppliChem (Darmstadt)
UO126	Tocris Bioscience (Bristol, UK)

Table 6.5.: Enzymes

Name	**Manufacturer**
EcoRI	New England BioLabs (Ipswich, USA)
NotI	New England BioLabs (Ipswich, USA)
RNase A (Invitrogen)	Thermo Fisher Scientific (Waltham, USA)
SpeI	New England BioLabs (Ipswich, USA)

Table 6.6.: Antibodies

Name	**Manufacturer**
Anti-Digoxigenin-POD Fab-fragment from sheep	Roche (Basel, Switzerland)
Goat anti-Rabbit IgG Secondary Antibody, HRP	Thermo Fisher Scientific (Waltham, USA)
rabbit anti-Phospho-p44/42 MAPK (Thr202/Tyr204)	Cell Signaling Technology® (Danvers, USA)

Table 6.7.: Antibiotics

Name	**Manufacturer**
Ampicillin	Sigma-Aldrich (St. Louis, USA)
Penicillin / Streptomycin	Biochrom (Berlin, Germany)

Table 6.8.: Commercial buffer and solutions

Name	Manufacturer
Dako Fluorescent Mounting Medium	Agilent Technologies (Santa Clara, USA)
Dulbecco`s Phosphate Buffered Saline, PBS	Biowest (Nuaille, Frankreich)
SuperSignal® West Femto Maximum Sensitivity Substrate	Thermo Fisher Scientific (Waltham, USA)
Trizol Reagent	Thermo Fisher Scientific (Waltham, USA)
UltraPure™ SSC, 20X	Thermo Fisher Scientific (Waltham, USA)

Table 6.9.: Self-produced buffers and solutions

Buffer/Solution	Composition
DEPC-H_2O (0,1 %)	500 µl DEPC in 500 ml deionised H_2O, incubated over night, with opened cap under a fume hood, autoclaved for 15 min at 100 ° C
Electrophoresis buffer	3 g Tris Base, 14.5 g Glycine, 1 g SDS to 1 L with deionised H_2O
Hybridisation buffer	1 ml Formamid, 0.4 ml Dextran sulphate, 196 µl DEPC-H_2O, 120 µl 5 M NaCl, 40 µl Denhardt's solution, 40 µl 1 M Tris (pH 7.5), 4 µl 0.5 M EDTA
Lowry Mix	1 mM K-Na-Tartrat · 4 H_2O and 400 µM $CuSO_4$ · 5 H_2O solved in 2 % Na_2CO_3 in 0.1 N NaOH
NTE buffer	100 ml 5 M NaCl, 10 ml 1 M Tris (pH 8.0), 2 ml 0.5 M EDTA in 1 L autoclaved deionised H_2O
PBS-T washing buffer	65 mM Na_2HPO_4 · 2 H_2O with 25 mM NaH_2PO_4 · H_2O, 100 mM NaCl, 0.1 % Tween 20, pH to 7.5 using NaOH
TE Buffer	10 mM Tris-HCl, 1 mM EDTA, in DEPC-H_2O
TNT washing buffer	0.1 M Tris-HCl, 0.15 M NaCl, 0.1 % Tween-20 ad 1 L with deionised H_2O
Towbin Blot buffer	3 g Tris Base, 14.4 g Glycine, 1 g SDS ad 800 ml with deionised H_2O, pH 8.2-8.4 and then 200 ml MeOH

SDS-PAGE buffer (4x)	5 ml Tris-HCL (pH 6.8), 0.8 g SDS, 4 ml Glycerol, 4 mg Bromophenol blue, 0.6 g DTT with deionised H_2O ad 10 ml

Table 6.10.: Cell lines and bacteria

Cell line	**Manufacturer**
Immortalized cells from the epididymal WAT from male C57BL/6 wild type mice	Prof. Klein (University zu Lübeck, Germany)
mHypoA 2/23	Cedarlane Laboratories (Bourlington, Canada)
mHypoE N25/2	CELLutions Biosystems (Ontario, Canada)
mHypoE N41	CELLutions Biosystems (Ontario, Canada)
mHypoE-N41-OX_1R	Wang et al., 2014 based on CELLutions Biosystems (Ontario, Canada)
mHypoE-N41-OX_2R	Wang et al., 2014 based on CELLutions Biosystems (Ontario, Canada)
One Shot™ TOP10 Electrocomp™ *E. coli*	Thermo Fisher Scientific (Waltham, USA)

Table 6.11.: Cell culture media (were stored at 4 °C)

Cell line	**Composition**	**Manufacturer**
Basic culture medium for preadipocytes	DMEM (4.5 g/L glucose; + glutamine; - pyruvat), FCS 20%, Pen/Strep100 µg/mL	Thermo Fisher Scientific (Waltham, USA)
Differentiation medium for adipocytes (mDM)	DMEM (4.5 g/L glucose; + glutamine; - pyruvat), FCS 20%, T3 1 nM, Insulin 20 nM	Thermo Fisher Scientific (Waltham, USA)
Induction medium for adipocytes	mDM, 500 µM IBMX, 250 µM Indomethacine, 2 µg/mL Dexamethason	Thermo Fisher Scientific (Waltham, USA)
mHypoE/A culture medium	DMEM high (glucose 4.5 g/L), 10 % FCS, 100 µg/ml Pen/Strep	Thermo Fisher Scientific (Waltham, USA)

Table 6.12.: Mouse line

Name	Genetic background	Company
LepRb-ZsGreen	$LepRb^{IRES\text{-}Cre}$ x $ROSA26^{LoxP\text{-}STOP\text{-}LoxP\text{-}ZsGreen1}$ on a C57BL/6 wild type mice background	Jackson Laboratory (Bar Harbour, USA)

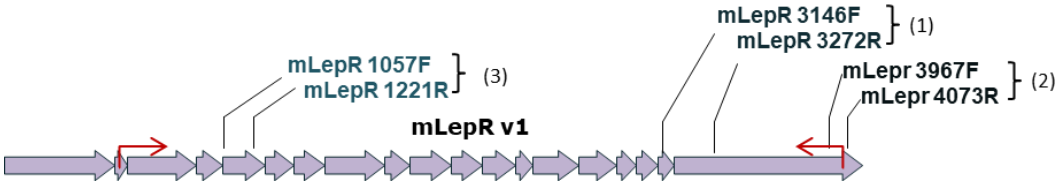

Figure 6.1.1.: LepR primer tested for PCR after fluorescent activated cell sorting (FACS) experiments. 3 different primer pairs were tested for LebR PCR, (1) is specific for the long version of the LebR (LebRb) and exon spanning, (2) is also specific for LepRb but is not able to bind in LepRb-ZsGreen mice due to cre knock in and (3) is able to detect all versions of LebR.

Table 6.13.: Primer Pairs

Primer pair	Orientation	Sequence	Amplicon (bp)
ß-actin	*forward*	5'- ATG GAA TCC TGT GGC ATC CAT -3'	
	reverse	5'- TTC TGC ATC CTG TCA GCA ATG -3'	239
LepR (1)	*forward*	5'- TGA AAA AGT TGT TTT GGG ACG ATG T -3'	
	reverse	5'- CCA AAT ATC ACT GAT TCT GCA TGC T -3'	126
LepR (2)	*forward*	5'- ATG CCC CAA TTT CAA ACC TG -3'	
	reverse	5'- TGG AAT GGA ACC TTC AGG CTT -3'	106
LepR (3)	*forward*	5'- ATA GAT GAT TCG CCT CTG CCC -3'	
	reverse	5'- TGA CTG AAA ACT CAC ACC GGC -3'	164
NPY	*forward*	5'- CGC TCT GCG ACA CTA CAT CAA -3'	
	reverse	5'- GGC GTT TTC TGT GCT TTC CTT -3'	108
OX_1R (mouse)	*forward*	5'- TTG GTG CGG AAC TGG AAA C -3'	
	reverse	5'- CCA TCA GCA TCT TAG CCG TCT -3'	144
OX_1R (human)	*forward*	5'- CAT CAG CGT CCT CAA TGT CCT -3'	
	reverse	5'- CCT TAA ACT GCT CCC GGA ATT -3'	172

OX_1R ORF	*forward*	5'- ATG GAA CCC TCG GCC ACT CC -3'	
(FISH)	*reverse*	5'- GCG TTC AGG ACA GCA CGG TA-3'	1316
OX_2R	*forward*	5'- TTC CCG GAA CTT CTT CTG TGG -3'	
(mouse)	*reverse*	5'- TCA GCA GCA ACA GCG CTA ATC -3'	111
OX_2R	*forward*	5'- TCC TGG TTT GTG TGG CAG TGT -3'	
(human)	*reverse*	5'- AGG TGA TGG TCA CGA GCA CAT -3'	101
OX_2R ORF	*forward*	5'- CCA TGT CCA GCA CCA AAC TG -3'	
(FISH)	*reverse*	5'- TAC GCG TTC AGA CCT CCA GC -3'	1270
POMC	*forward*	5'- AGC GTT ACG GTG GCT TCA TGA -3'	
	reverse	5'- TGG AAT GAG AAG ACC CCT GCA -3'	124
PPO	*forward*	5'- CAT GAA CTT TCC TTC TAC AA -3'	
(FISH)	*reverse*	5'- ATA GAA GAT GGG TTC AGA CT-3'	406

Table 6.14.: Standards

Name	**Manufacturer**
1 kb DNA Ladder	New England BioLabs (Ipswich, USA)
Precision Plus Protein Standards	Bio-Rad Laboratories GmbH (München, Germany)
Lambda DNA / Sty I marker	Genaxxon bioscience (Ulm, Germany)

Table 6.15.: Software

Name	**Manufacturer**
EvolutionCapt Solo 6 Version 17.01	Vilber Lourmat (Eberhardzell, Germany)
GraphPad Prism Version 5/7	GraphPad Software (La Jolla, USA)
ImageJ Version 1.49v	Free Software
Leica Application Suite Advanced Fluorescence Version 2.5.0.6735	Leica Microsystems (Wetzlar)
Microsoft Excel 2016	Microsoft (Redmond, USA)
Microsoft PowerPoint 2016	Microsoft (Redmond, USA)

NanoDrop 2000/2000c Version 1.5	Thermo Fisher Scientific (Waltham, USA)
Primer Express® Software Version 2.0	Thermo Fisher Scientific (Waltham, USA)
Sequence Detection Software Version 1.2.3	Thermo Fisher Scientific (Waltham, USA)

6.2 Curriculum Vitae

Personal details:

Name	Eva Frevel
Place & date of birth	October 30st 1985 in Recklinghausen, Germany
Nationality	German
Contact	frevel.eva@gmail.com

Education:

Since 06/2014	**PhD studies in Neurobiology** Thesis: *Interaction of adipokines, especially leptin, with orexin signalling* DFG Research Training Group 1957 “Adipocyte-Brain Crosstalk”, University of Lübeck
03/2010 to 02/2013	**Master of Science, Biology** Focus: Neurobiology Thesis: *Electrophysiological analysis of the interaction between calcium activated potassium-channels with the C-terminus of the P/Q-type calciumchannel* Ruhr-University Bochum
10/2006 to 02/2010	**Bachelor of Science, Biology** Thesis (experiments were performed at the institute of molecular biology of the university hospital Essen, Germany): *Recombinant human, epidermal growth factor (rhEGF) induces differential expression of cellular genes in EGF receptor tyrosine kinase inhibitor sensitive human bronchial carcinoma cells compared to control cell”* Ruhr-University Bochum

06/2005	**General higher education entrance qualification (Abitur: German equivalent of A levels)**
	Marie Curie Gymnasium, Recklinghausen

Working and teaching experience:

08/2017 to 09/2017	Visiting researcher at the Department of Veterinary Biosciences, Veterinary Biochemistry and Cell Biology at the Faculty of Veterinary Medicine of the
	University of Helsinki
06/2017 to 11/2017	Scholarschip from the DFG Research Training Group 1957 "Adipocyte-Brain Crosstalk"
	University of Lübeck
06/2014 to 05/2017	Research Assistant at the Institute of Experimental and Clinical Pharmacology and Toxicology
	University of Lübeck
2010 to 2013	Teaching assistant at the Department of General Zoology and Neurobiology
	Ruhr University Bochum, Germany
2016 to 2017	Co-organisation of the ABC Symposium 2017

Participation in conferences and congresses:

- Poster presentation at the first international CBBM Symposium 2016, Energy Metabolism Between Reward and Revenge, February 26-27, 2016, Lübeck, Germany
- Poster presentation at the first Adipocyte-Brain Crosstalk Symposium 2017, March 3-4, 2017, Lübeck, Germany
- Poster presentation at the ENDO 2017, The Endocrines Society's 99th annual Meeting and Expo, April 1-4, 2017, Orlando Florida

Manuscript

- Frevel E. and Jöhren O. "LepRb distribution in lepRb-zsGreen reporter mice reveals no expression of LepRb on orexin neurons", *in preparation*

6.3 Acknowledgement

I want to take this opportunity to thank my supervisor Prof. Dr. Olaf Jöhren for the opportunity to work with him on this interesting topic and to become part of the GRK1957 ‘Adipocyte Brain Crosstalk’ program. I wish to especially emphasise his guidance and persistent support, as well as helping advice, not only regarding the scientific work but also on how to handle stress- and doubtful periods.

I would also like to thank Prof. Dr. Markus Schwaninger, for letting me work in the Institute for Pharmacology and Toxicology. The good atmosphere there was always shaped by respect, encouragement and support.

Furthermore, I am thankful to Prof. Dr. Henrik Oster, from the Institute for Neurobiology – Chronobiology at the University of Lübeck for his wliingness to be my secondary supervisor and for providing the original animals for my experiments. I also want to thank Prof. Dr. Jyrki Kukkonen at the Department of Veterinary Biosciences, Veterinary Biochemistry and Cell Biology at the Faculty of Veterinary Medicine of the University of Helsinki for opening his lab for me as a visiting researcher,

Special thanks go out to my co-workers and fellow students from the Pharmacology and GRK for personal and work support whenever needed, entertaining lunch breaks and a vast number of cakes. I am especially thankful to Christine Eichholz, who taught me numerous techniques and always helped dynamically. I am also particularly grateful to Lisa, for countless Franzbrötchen and her listening ear, Ellie for her insight, that helped me to change perspective many times, Julica for her dedication and loyalty, Gianna for her inner child that never failed to cheer me up, Alisa for the exquisite poetic communication, Marius for being an incredibly altruistic and helpful person and Ale for being my confidant. In addition, Landia, Ping, Sebastian, Siva and Wiebke also contributed in a unique manner to an exceptionally positive work climate for me.

I am eternally grateful to my family for their immense love and support, not only during my PhD but throughout life and to my longtime friends and companions Hannah, Kathrin and Mina, Milena and the Madels-Group, who I can always count on.